Max Planck Institute
of Colloids and Interfaces

Population Dynamics of Bacterial Persistence

Kumulative Dissertation
zur Erlangung des akademischen Grades
"doctor rerum naturalium"
(Dr. rer. nat.)
in der Wissenschaftsdisziplin "Theoretische Biologische Physik"

eingereicht an der
Mathematisch-Naturwissenschaftlichen Fakultät
der Universität Potsdam

angefertigt in der
Abteilung Theorie und Bio-Systeme
des Max-Planck-Institut für Kolloid- und Grenzflächenforschung

von
Pintu Patra

Potsdam, September 2013

Published online at the
Institutional Repository of the University of Potsdam:
URL http://opus.kobv.de/ubp/volltexte/2014/6925/
URN urn:nbn:de:kobv:517-opus-69253
http://nbn-resolving.de/urn:nbn:de:kobv:517-opus-69253

Abstract

The life of microorganisms is characterized by two main tasks, rapid growth under conditions permitting growth and survival under stressful conditions. The environments, in which microorganisms dwell, vary in space and time. The microorganisms innovate diverse strategies to readily adapt to the regularly fluctuating environments. Phenotypic heterogeneity is one such strategy, where an isogenic population splits into subpopulations that respond differently under identical environments. Bacterial persistence is a prime example of such phenotypic heterogeneity, whereby a population survives under an antibiotic attack, by keeping a fraction of population in a drug tolerant state, the persister state. Specifically, persister cells grow more slowly than normal cells under growth conditions, but survive longer under stress conditions such as the antibiotic administrations.

Bacterial persistence is identified experimentally by examining the population survival upon an antibiotic treatment and the population resuscitation in a growth medium. The underlying population dynamics is explained with a two state model for reversible phenotype switching in a cell within the population. We study this existing model with a new theoretical approach and present analytical expressions for the time scale observed in population growth and resuscitation, that can be easily used to extract underlying model parameters of bacterial persistence. In addition, we recapitulate previously known results on the evolution of such structured population under periodically fluctuating environment using our simple approximation method. Using our analysis, we determine model parameters for *Staphylococcus aureus* population under several antibiotics and interpret the outcome of cross-drug treatment.

Next, we consider the expansion of a population exhibiting phenotype switching in a spatially structured environment consisting of two growth permitting patches separated by an antibiotic patch. The dynamic interplay of growth, death and migration of cells in different patches leads to distinct regimes in population propagation speed as a function of migration rate. We map out the region in parameter space of phenotype switching and migration rate to observe the condition under which persistence is beneficial.

Furthermore, we present an extended model that allows mutation from the two phenotypic states to a resistant state. We find that the presence of persister cells may enhance the probability of resistant mutation in a population. Using this model, we explain the experimental results showing the emergence of antibiotic resistance in a *Staphylococcus aureus* population upon tobramycin treatment.

In summary, we identify several roles of bacterial persistence, such as help in spatial expansion, development of multidrug tolerance and emergence of antibiotic resistance. Our study provides a theoretical perspective on the dynamics of bacterial persistence in different environmental conditions. These results can be utilized to design further experiments, and to develop novel strategies to eradicate persistent infections.

Zusammenfassung

Das Leben von Mikroorganismen kann in zwei charakteristische Phasen unterteilt werde, schnelles Wachstum unter Wachstumsbedingungen und Überleben unter schwierigen Bedingungen. Die Bedingungen, in denen sich die Mikroorganismen aufhalten, verändern sich in Raum und Zeit. Um sich schnell an die ständig wechselnden Bedingungen anzupassen entwickeln die Mikroorganismen diverse Strategien. Phänotypische Heterogenität ist eine solche Strategie, bei der sich eine isogene Population in Untergruppen aufteilt, die unter identischen Bedingungen verschieden reagieren. Bakterielle Persistenz ist ein Paradebeispiel einer solchen phänotypischen Heterogenität. Hierbei überlebt eine Population die Behandlung mit einem Antibiotikum, indem sie einen Teil der Bevölkerung in einem, dem Antibiotikum gegenüber tolerant Zustand lässt, der sogenannte "persister Zustand". Persister-Zellen wachsen unter Wachstumsbedingungen langsamer als normale Zellen, jedoch überleben sie länger in Stress-Bedingungen, wie bei Antibiotikaapplikation.

Bakterielle Persistenz wird experimentell erkannt indem man überprüft ob die Population eine Behandlung mit Antibiotika überlebt und sich in einem Wachstumsmedium reaktiviert. Die zugrunde liegende Populationsdynamik kann mit einem Zwei-Zustands-Modell für reversibles Wechseln des Phänotyps einer Zelle in der Bevölkerung erklärt werden. Wir untersuchen das bestehende Modell mit einem neuen theoretischen Ansatz und präsentieren analytische Ausdrücke für die Zeitskalen die für das Bevölkerungswachstums und die Reaktivierung beobachtet werden. Diese können dann einfach benutzt werden um die Parameter des zugrunde liegenden bakteriellen Persistenz-Modells zu bestimmen. Darüber hinaus rekapitulieren wir bisher bekannten Ergebnisse über die Entwicklung solch strukturierter Bevölkerungen unter periodisch schwankenden Bedingungen mithilfe unseres einfachen Näherungsverfahrens. Mit unserer Analysemethode bestimmen wir Modellparameter für eine emphStaphylococcus aureus-Population unter dem Einfluss mehrerer Antibiotika und interpretieren die Ergebnisse der Behandlung mit zwei Antibiotika in Folge.

Als nächstes betrachten wir die Ausbreitung einer Population mit Phänotypen-Wechsel in einer räumlich strukturierten Umgebung. Diese besteht aus zwei Bereichen, in denen Wachstum möglich ist und einem Bereich mit Antibiotikum der die beiden trennt. Das dynamische Zusammenspiel von Wachstum, Tod und Migration von Zellen in den verschiedenen Bereichen führt zu unterschiedlichen Regimen der Populationsausbreitungsgeschwindigkeit als Funktion der Migrationsrate. Wir bestimmen die Region im Parameterraum der Phänotyp Schalt-und Migrationsraten, in der die Bedingungen Persistenz begünstigen.

Darüber hinaus präsentieren wir ein erweitertes Modell, das Mutation aus den beiden phänotypischen Zuständen zu einem resistenten Zustand erlaubt. Wir stellen fest, dass die Anwesenheit persistenter Zellen die Wahrscheinlichkeit von resistenten Mutationen in einer Population erhöht. Mit diesem Modell, erklären wir die experimentell beobachtete Entstehung von Antibiotika- Resistenz in einer *Staphylococcus aureus* Population infolge einer Tobramycin Behandlung.

Wir finden also verschiedene Funktionen bakterieller Persistenz. Sie unterstützt die räumliche Ausbreitung der Bakterien, die Entwicklung von Toleranz gegenüber mehreren Medikamenten und Entwicklung von Resistenz gegenüber Antibiotika. Unsere Beschreibung liefert eine theoretische Betrachtungsweise der Dynamik bakterieller Persistenz bei verschiedenen Bedingungen. Die Resultate könnten als Grundlage neuer Experimente und der Entwicklung neuer Strategien zur Ausmerzung persistenter Infekte dienen.

Contents

Chapter 1

Introduction

Organisms find numerous ways to survive, as well as to flourish, in the surrounding environment. For example, organisms adapt to the daily light cycles by using internal circadian clocks, echolocating animals, such as bats and dolphins, use sonic response for navigation and for foraging, chameleon camouflage to blend with the surroundings to hide from predators as well as to target their prey. Understanding how organisms adapt, in the presence of various interactions with their environments, is often complex and challenging. Microbes, the most abundant form of life on earth that have adapted to survive under diverse environments, provide model systems for qualitative understanding of the general principles of evolution [66]. Short replication time, small genome size and the possibility of genetic manipulation of these microorganisms make them convenient for the quantitative studies of evolution within laboratory experiments. For example, several ecological interactions such as competition, cooperation, predator prey dynamics, etc., have been realized in microbial populations [5, 36, 44, 85]. Additionally, the arrival of modern techniques such as single cell genome sequencing and microfluidic devices, allow to integrate and inspect multiple aspects of evolution in cellular dimensions, for example, controlling microenvironments, measuring single cell dynamics, analyzing signaling pathways, etc [13, 86, 136]. The study of evolution in microorganisms can boost the understanding of the development of antibiotic resistance, which is emerging as a serious problem in medicine [94, 117].

An important feature of microbial life is population heterogeneity that affects the response of a population to heterogeneous environments [69, 74, 121]. Population heterogeneity, where cells within a population display a wide range of physiological properties, can occur in the form of monomodal (Fig. 1.1(a)) or bimodal (Fig. 1.1(b)) or even multimodal distribution in physiological traits [13, 19]. Heterogeneity in cellular traits

within an isogenic population, i.e., phenotypic heterogeneity, has been observed experimentally in several cases, for example, the lactose utilization network in *Escherichia coli*, the competence switch for genetic transformation in *Bacillus subtilis*, and the lysis or lysogeny decision switch in *Bacteriophage lambda* [25, 128]. Stochastic phenotype switching in bacterial persistence is another example of bistability which has been well studied in recent years due to its relevance in antibiotic treatment failures [19, 53].

In this thesis, we consider the example of bacterial persistence to understand the response dynamics and evolution of a population under the influence of different environmental conditions. In this mechanism an individual cell can acquire different phenotypes (physiological states) and switches stochastically between these different phenotypic states, for example, normal and persister phenotypes in *E.coli* [4]. The persister phenotype generated from normal phenotype is less responsive to the growth medium, i.e., persister cells divide slowly in the presence of nutrients and exhibit a reduced death rate in the presence of bactericidal substances. A population exhibiting phenotype switching mechanism shows drug-tolerance in the form of differential antibiotic response, achieved through phenotypic heterogeneity [55, 75], this property is referred to "bacterial persistence"[67] (Figure 1.2). Persistence has been described in parasites, fungi and bacteria (both pathogenic and non-pathogenic) and, poses a great challenge to the proficiency of drug treatments. To describe the importance and current state of research on bacterial persistence, we will discuss briefly the historical events which shaped the study of this particular phenomenon. Then, moving into the mechanistic description of the phenotype switching in model organism *E.coli*, we will discuss the results from previous theoretical studies and, the prospect of further studies in this field. In the following section, we will start with some basic concepts in population dynamics and evolutionary theory, which are the important tools for modeling evolution in a population.

1.1 Population dynamics and Evolution

Population dynamics is a central aspect in the field of ecology which focus on the study of time evolution of the number of individuals, which could be in interaction with other individuals or the surrounding environment. On the other hand, the evolutionary theory focus on changes over generations in the frequency or relative proportion of various traits that affect the dynamics of a population. These two different approaches are used together to study evolution in biological entities.

The first model for the time evolution of a population was proposed by Malthus, which describes population growth in the absence of any kind of interaction (Eq. 1.1) as an exponential function of time [80]. Later, this model was modified by Verhulst to

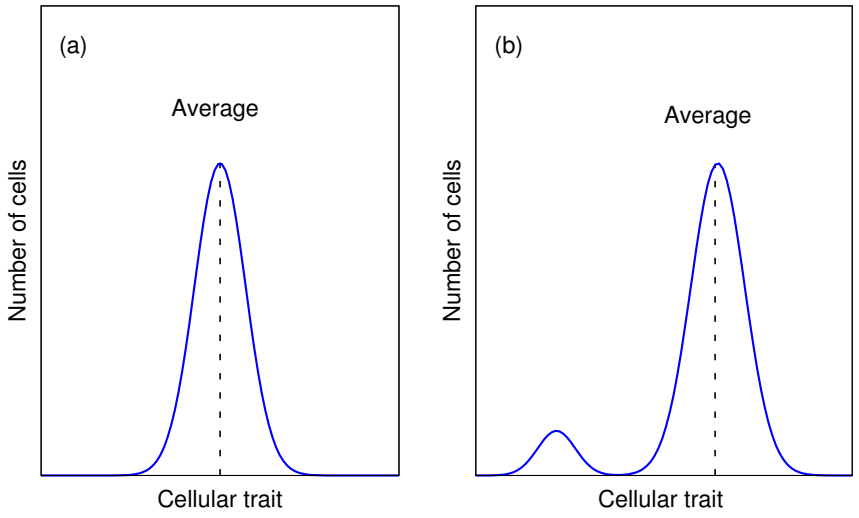

FIGURE 1.1: Heterogeneity in a population : (a) Monomodal Gaussian distribution. Cellular traits of the cells in a population can vary around an average value. (b) Multimodal distribution comprising subpopulations of unequal sizes. A subpopulation of cells can have cellular traits far from the population mean.

describe population growth in resource limited or bounded environments [129]. In the modified model, the population growth is defined by the equation of logistic growth which accounts for the density dependent effects on growth imposed by the environmental constraints (Eq. 1.2). The improved models include the effect of competitions and environmental factors, such as nutrients, temperature, toxic materials, etc., that can change the dynamics of populations in an alternative fashion, as an additional input to these two basic equations (Eq. 1.1, Eq. 1.2).

$$\frac{d\,n}{dt} = \mu\, n \qquad \text{Unbounded growth} \tag{1.1}$$

$$\frac{d\,n}{dt} = \mu \left(1 - \frac{n}{K}\right) n \qquad \text{Bounded growth} \tag{1.2}$$

The rate (μ) at which an individual duplicates itself is defined as the growth rate of the individual. In case of bounded growth, the population size (n) is limited by the maximum capacity (K) of the medium.

In evolution theory, the measure of reproductive success and survival chance of an individual in the population is defined by a single quantity, the 'fitness' f of an individual. The evolutionary forces act as a selection agent on the variations in fitness of different type of individuals or species, which are characterized by different traits, in a population. The evolution of a trait is well described by the replicator equation [108], which is

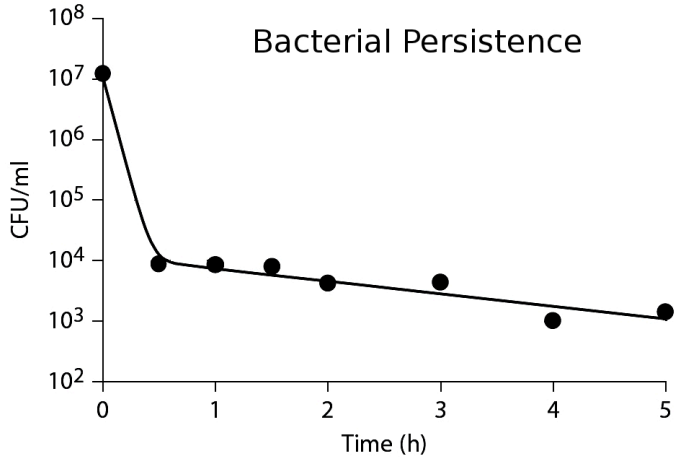

FIGURE 1.2: Bacterial Persistence. A bacterial population of treated with an antibiotic displays a biphasic decay or two-time scale decay. Most of the cells are killed in the fast decay phase, whereas a tiny fraction ($10^{-3} - 10^{-5}$) survives even after a couple of hours of antibiotic administration. These surviving cells are named Persisters. (Note: Colony forming unit (CFU) is a count of viable bacterial numbers)

shown below,

$$\frac{d\,x_i}{dt} = x_i(f_i - \langle f_i \rangle). \tag{1.3}$$

The equation defines the rate of change of a particular trait (i) within a population as a function of the fitness difference between the fraction (x_i) of population exhibiting this trait (f_i) and the total population ($\langle f_i \rangle$). In the simplest case, when individuals in a population duplicates with variable growth rates, the individuals with higher growth rate ($\equiv$ fitness) will be selected against the others and eventually will spread over the whole population. The evolutionary selection can act on various levels from genes to individuals as the fitness of an individual is the sum of all physical traits (phenotype) which is specified by the genomic information (genotype) in the DNA sequence of the individual [122]. The growth or duplication rate (μ) is determined by genetic contents [60] and taken as the measure of fitness of an individual [84]. Therefore, growth dynamics together with evolutionary selection completes the mathematical description of an evolving population [83].

1.2 Bacterial persistence

The phenomenon of bacterial persistence against antibiotics was first observed by Joseph W. Bigger in 1944 while studying the failure of antibiotic penicillin to sterilize a staphylococcal infection [7]. He found that a fraction of cells always survives the killing by penicillin. He named these cells "persisters". He proposed that persisters are in dormant

or non-dividing phase, and survive because penicillin inhibits cell wall formation only in growing cells. He found that these cells were pre-existing as persisters in the population, but could be induced to normal state when in contact with a new environment. The offspring produced by the surviving persisters consisted only a small fraction of population that could once again survive the treatment with penicillin. Hence, the persisters were very different from traditionally observed resistant cells, those can even grow in the presence of antibiotics and generate offspring which are permanently immune to the treated antibiotic. The surviving population fraction during antibiotic treatment, being very small, did not get much attention by the researchers because the discovery of antibiotics was of prime importance in that era. Thus, the physiological role and molecular mechanism of bacterial persistence against antibiotics remained undiscovered for about four decades.

In 1980s, Harris Moyed started to look again into the problem of persistence [88]. He selected for mutants with high level of persisters, the hip (high persister) mutants, by repeatedly exposing growing *E.coli* cultures with ampicillin. He found the fraction of surviving cells upon antibiotic treatment in hip mutants was about 100-1000 fold larger than the wild type population. He looked for the mutations in hip mutants, and identified a new gene *hipA*, causing the increase in persister frequency. This experiment gave the first evidence that persistence has a genetic basis.

The next breakthrough came in the form of a single cell microfluidics experiment showing microscopic images of pre-existing persister cells in a growing culture of *E. coli* wild type and hip mutants [4]. The experiment showed that bacterial persistence or persister formation is an outcome of the phenotype switching mechanism of a single cell. Phenotype switching generates a mixed population containing normal and persister cells, which upon addition of an antibiotic, decays with different time scales leading to a biphasic killing curve as observed in several previous studies. Once the antibiotic is removed, surviving persister cells can switch back to the normal phenotype, which again generates a new population that is genetically identical and susceptible as the original culture. They found that the persisters are either in a non-growing state or slow growing state and generated with very small switching rates from normal cells, such that they always represent a small fraction in the population. The generation of persisters in the absence of any stress (i.e. during growth) suggests that the mechanism of phenotype switching might have evolved as a regulatory mechanism for responding to inappropriate environmental conditions. Numerous studies have shown that persistence is not only limited to *E. coli* and *Staphylococcus aureus* cells, but most bacteria exhibit the persister phenotype [58].

The molecular mechanism and the control of persistence has become a prime target of experimental studies in the last few years [33, 78]. Several studies were performed addressing basic questions like, whether the persister formation is solely controlled by molecular reaction within the cell, can persistence be induced or enhanced by environmental factors, etc. Several studies found that persister numbers are regulated or induced in many conditions that lead to growth reduction, such as amino acid deprivation, biofilm formation, stress induction, and entry into stationary phase [21, 63, 79, 105]. The generation of persister cells is shown to be growth dependent in *E. coli* and *Pseudomonas aeruginosa* [9, 53, 114]. In the lag phase or early exponential phase, where cells adapt to their growth medium and are unable to divide, there is no persisters generation. In the exponential growing phase, where the cells begin to divide and the population grows exponentially, persisters are generated in constant proportions. The fraction of persisters reaches maximum in the stationary phase, where all the essential nutrients are depleted.

Another important aspect of bacterial persistence, the physiological state of persister cells, has been investigated by several researchers. These studies indicated that persisters are non-growing cells having reduced rates of DNA replication, translation, cell-wall synthesis and metabolism, and thereby are insensitive to antibiotics relying on these growth dependent processes. Further, gene sequence analysis also supported the dormant state hypothesis as several genes involved in intracellular metabolism were downregulated in persisters [63]. On the contrary, a few recent studies reported that persistence may not always be associated with the dormant or the slow growing fraction of the population and, moreover, the cells growing normally prior to the antibiotic treatment could behave as persisters upon antibiotic treatment [95, 131].

1.2.1 Persistence: a cause of antibiotic failures

Persistence has been characterized in several pathogenic microbes such as *Mycobacterium tuberculosis, Staphylococcus aureus, Candida albicans, Pseudomonas aeruginosa* and *E. coli* [19]. These pathogens are the known cause of various chronic infections, such as tuberculosis and cystic fibrosis, which often recur in spite of proper antibiotic treatments. However, these pathogens do not show any sign of genetic resistance when observed under controlled laboratory experiments. This indicates that the drug tolerant persister cells are the main culprit behind such recalcitrance to antibiotic treatments [115]. For instance, patients suffering from Cystic fibrosis (CF), a genetic disorder characterized by an imbalance in chloride and sodium levels in epithelial tissues in the lungs and intestines, are highly susceptible to emphPseudomonas aeruginosa infections, which is the leading cause of many deaths. The cause of the inadequacy in curing a *P. aeruginosa* infection

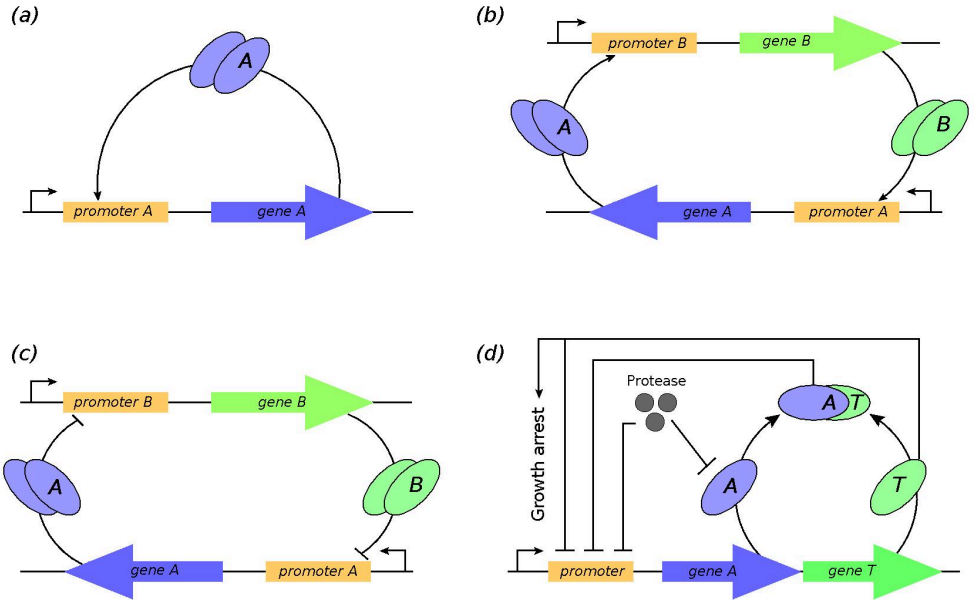

FIGURE 1.3: Examples of bistable gene circuits: Genes (indicated by thick arrows) produces proteins (indicated by ellipse) which regulate negatively (thin blunt arrow) or positively (thin point arrow) the activity of either its own promoter (thick rectangles) or promoter of other genes. (a) Bistable switch with single positive feedback loop. (b) Bistable switch with double-positive feedback loop. (c) Bistable switch with double-negative feedback loop. (d) Toxin Antitoxin network in E. coli.

is again the presence of drug-tolerant persister cells [28, 75]. A direct correspondence between persister cells and recurrence of chronic infection has been observed in clinical isolates from CF patients [91]. In this study, the fraction of drug tolerant persister cells in a clinical isolate from the lungs of a patient in the late stage of infection (96 months) is found to be 100-fold more than the clinical isolates at the onset of chronic infection. This observation suggests that the high persister mutant has been selected by the periodic administration of antibiotics. The association of persisters with antibiotic treatment failure has also been recognized in several other studies [19, 75].

1.2.2 Molecular mechanism of persistence

The first experiment showing that persistence has a genetic basis was performed by Moyed et al. [88]. In this experiment, they isolated a mutant of *E. coli* K-12 strain that displays 100 fold increase in persistence against several antibiotics (phosphomycin, cycloserine, and ampicillin). The genetic analysis of high persister (hip) mutant revealed a mutation in a new gene, named '*hip A*' gene. Further studies found that *hipA* locus belong to a class of loci in the genome, the toxin-antitoxin (TA) locus. Several studies have shown the direct connection between TA loci and persistence formation [79, 105]. The TA locus codes for two proteins, a toxin and antitoxin protein, where a toxin is a stable protein that inhibits cell growth and an antitoxin is an unstable protein [135].

The antitoxin regulates the toxin by forming a tight complex with it [107], which repress the gene expression (Figure 1.3 (d)). The overproduction of toxin inhibits important cellular processes which are potential targets for many antibiotics, thereby may produce antibiotic tolerant persister [63]. Therefore, the variation of toxin antitoxin ratio in a cell defines the phenotypic state [105]. In the absence of any stress, such variation could be induced by the intrinsic stochasticity in biomolecular reactions at transcription and translation level [25]. Furthermore, during stress conditions or in the presence of bactericidal substances, the uneven balance of toxin and antitoxin may also induce persistence. Recent experiments [21, 22] have shown active generation of persisters (i.e. increase in persister fractions) in *E. coli* cells when treated with antibiotics that trigger SOS response (a global response to DNA damage) such as ciprofloxacin. The SOS response induced persistence was shown to be dependent on the production of tisB toxin. The mutants lacking the SOS response or tisB deleted strains displayed significantly reduced level of persisters when treated with DNA-damaging antibiotics. Thus, clearly the production of toxins could drive a cell from a normal growing state into a persister state. In *E. coli*, there are about 36 TA loci and, in the pathogenic bacterium *Mycobacterium tuberculosis* about 100 TA locus [76, 135]. The deletion of several TA loci reduced the level of persisters in a biofilm [76] and the induced persistence during SOS response [22]. The toxin-Antitoxins (TA) loci are divided into three classes. In Type I TA loci, the antitoxins are anti-sense RNAs that repress the translation of the toxin encoding mRNA, whereas in type II TA loci, an antitoxin protein neutralizes the activity of encoding gene as well as the toxin proteins. Type III TA loci code for small RNA antitoxins that neutralizes the toxin proteins by establishing a direct protein-RNA contact. A recent study showed that the deletion of Type II TA loci (in *E. coli* K-12 strain consisting 10 TA loci) progressively reduced the levels of persisters, while the growth rate and minimum inhibitory concentrations (MICs) of the antibiotics (ciprofloxacin and ampicillin) were unaffected [79]. This result confirms the direct proportionality between TA loci and persister fractions. However, the deletion of all 10 TA loci did not lead to zero persistence, suggesting that TA loci is not the sole key to persistence, there could be other unknown genes which have not been characterized yet.

1.2.3 Persistence against multiple drugs

Persister generation does not follow a universal single scheme. There are multiple pathways through which persister formation can be achieved and modulated. Some of these pathways are inherently present in the genome and some are regulated or induced through various environmental interactions. Several pathways were identified in genetic screening of persister cells in *E. coli* [76]. However, the complete knockout of

these identified candidate genes never achieved zero persistence, although reduced significantly the level of persisters. Similarly, in another independent experiment, deletion of multiple toxin-antitoxin loci could not lead to zero persistence [79]. This suggests that there are several redundant pathways, some of them still to be identified, through which persistence can be achieved. Antibiotics of differing action mechanism target different processes and pathways in the cell, which might lead to variable levels of persistence in a population. The variability in persistence against different antibiotic is termed as multidrug tolerance. Multidrug tolerance has been observed in *E. coli* and *S. aureus* cells against several antibiotics [45, 71, 72, 133]. This is another important area of research where several labs have worked on recently.

1.2.4 Other examples of phenotypic heterogeneity

Phenotypic heterogeneity, specifically bistability, in populations has been observed in numerous bacterial species and eukaryotes under diverse conditions. Phenotype diversity is found to be a direct consequence of multistability of the gene expression in a cell, which arises due to feedback and nonlinear responses within a gene regulatory network of the cell. In a regulatory network, the smallest unit, i.e., the gene expresses specific proteins which either regulate itself or other genes, and are continuously degraded. As the protein level passes a certain threshold value the gene expression is driven towards one of the stable states, this property is called multistability of the regulated gene. Such regulatory networks or motifs has been identified in several species, furthermore their underlying properties have been realized using synthetic networks [30, 40, 57]. For example, a simple genetic circuit composed of a positively autoregulated gene or two mutually auto activating genes (double positive feedback) or two mutually repressing genes (double negative feedback) [60] can demonstrate a bistable output (Figure 1.3). A population exhibiting bistability bifurcates into subpopulation of cells having one of the two stable states of gene expression, which is typically observed as a bimodal distribution in the population gene expression (as shown in figure 1.1(b)). For example, sporulation and competence in *B. subtilis* cells, lac operon network in *E. coli* and lysis-lysogeny switch in *phage* λ [25, 128], etc., are well studied cases of such bistability. The fate of a single cell ending in one of the two stable phenotypic states has also been linked with the stochastic fluctuations or noises in cellular components in several stages during a cell cycle [124]. Noise can be generated by the inherent stochasticity in biochemical reactions maintaining gene expression (intrinsic noise) or due to the fluctuations in other regulating factors that influence gene expression (extrinsic noise). It has been shown, in *E. coli*, that both intrinsic and extrinsic noise contribute to phenotype variability [27, 118].

1.3 Overview of theoretical work

The population dynamics of bacterial persistence or the reversible phenotype switching mechanism is proposed and well studied in the last decade by several independent research groups [4, 67–69, 121]. These studies focus on the measurement of the phenotypic switching and its evolution in different environments. The inheritablilty of phenotype switching, i.e., transmission to newer generations raise questions about the evolutionary adaptation or selection of this trait.

The basic idea is that phenotype switching allow cells to generate different phenotypes, which are maladapted to the present conditions, but when the condition changes, one of the maladapted phenotype becomes best suited to the new condition and hence, provides a benefit to the population. This phenomenon is termed as a bet-hedging strategy in the field of ecology, where the population allocates some individual in a protective state as its insurance policy to survive under adverse environmental conditions [67]. In a fluctuating environment, the interplay between insurance cost and benefit determine the circumstances under which phenotype switching is advantageous. Lachmann et al. [69] found that inheritance of a phenotype switching is advantageous in a periodically fluctuating environment with cycle length much longer than the replication time of the organism. The best strategy or the optimal phenotype transition rate under such cyclic environment is inversely proportional to the length of the environmental cycle. Therefore, it was suggested that the environmental conditions may act as selective agent that can select the organisms having an optimal transition rate or allow a directional process by which a population can achieve the optimal transition rate.

Balaban et al. showed that the biexponential decay of a bacterial population observed during the antibiotic killing is a signature of phenotype switching [4]. The normally growing cells generate persister cells through phenotype switching, which leads to a mixed population during growth. This mixed population decays, upon antibiotic treatment, with two time scales as the persister subpopulation is not killed as fast as the normal subpopulation. The surviving persister subpopulation on reinoculation grows as fast as the normal cells after an initial lag period (associated with slow growth of persisters), which leads to a biexponential population growth. They proposed a two-state model to describe the biexponential kinetics of the population and, evaluated phenotype switching rates by fitting the model with experimental data [4]. The two state model was further used to study the temporal evolution of a population in a fluctuating environment [67]. This analysis showed that in slow varying periodic environments, there exist an optimal phenotype switching rate between the two phenotypes which maximizes the long-term growth rate of the population. The optimal switching rate is given by the frequency of environmental variation, specifically, the duration of growth and stress determines the

optimal switching from normal to persister and persister to normal state, respectively [67]. Using experimentally measured phenotype switching rates for two different strains, they showed that in a periodically fluctuating environment with characteristic growth and stress duration, one bacterial strain can overtake the other strain if its phenotype switching is tuned close to the optimal phenotype switching rates.

A more general description was put forward by E. Kussell et al.[68] describing phenotype switching as a macroscopic information processing mechanism in fluctuating environments. The underlying idea is that a population can carry information about an environment through its internal state (using subpopulation allocation) that is determined by the current environmental conditions and phenotype switching rates. This subpopulation allocation can then be optimized for maximum growth in repetitive environmental conditions by regulating phenotype switching rates in accordance to environmental fluctuations. They found that in slowly fluctuating environments, the optimal switching rate from a given phenotype (X) to another phenotype (Y) is directly proportional to the probability that the environment changes from the state favoring phenotype (X) to the state favoring phenotype (Y) and, inversely proportional to the average duration of environmental state favoring phenotype (X). In simple words, this means that the switching to a phenotype will be favored if the environmental state favoring this phenotype occurs more frequently and the switching back from this phenotype will be favored if the mean residence time of environmental state favoring this phenotype is smaller than in the other states.

1.4 Motivation

The experimental study of bacterial persistence focus on two main objectives, namely, the description of molecular mechanism of phenotype switching in single cells and the understanding of antibiotic tolerance in populations. On the other hand, theoretical studies develop a mechanistic understanding of the molecular mechanism as well as the population dynamics and evolution of bacterial persistence. These approaches help in understanding the properties of drug tolerant persisters and in developing new therapeutics designs to prevent antibiotic failures. The present work focus on the population dynamics and evolution of bacterial persistence in spatially and temporally varying environments. The main objective of this thesis is to integrate results and obtain model parameters from experimental observations and, to develop theoretical framework to analyze the dynamics in realistic scenarios under which population evolves.

1.4.1 Temporal dynamics of bacterial persistence

Previous theoretical studies on the evolutionary dynamics of bacterial persistence or phenotype switching are based on numerical simulation and rigorous theoretical analysis within certain limits. A common assumption in previous theories is that the environmental duration is large or that the environment fluctuates very slowly. This assumption has been used to predict the evolutionary dynamics of phenotype switching in fluctuating environments [29, 67–69]. If an environment occurs rarely or has a short duration, this approach cannot predict the evolutionary behavior or the long term growth rate. Although it is expected that in a short environmental period phenotype switching, being harmful to the population, might not evolve. However, a simple analytical approach that can explain the evolutionary dynamics in both short and long environmental duration, even in the simple case of two state population model, is missing. The relation between experimental observations and the model parameters of persistence mechanism has been overlooked because most studies focus on the long term evolutionary dynamics rather than short term transient dynamics. Therefore, a simple theoretical approach is necessary which can connect experimental observables with the model parameters and explain the transient as well as the evolutionary dynamics in both short and long environmental duration.

1.4.2 Spatial dynamics of bacterial persistence

Most theoretical and experimental studies exploit temporally changing environments to understand the role of bacterial persistence. Spatially structured environments are also used to study evolution in bacterial populations [41, 56, 70, 102–104, 137], but have not been considered in the study of persistence. In the human body antibiotic distribution is usually uneven due to complex flow patterns inside the body, such as different diffusion rates into tissues, local binding, inactivation of antibiotics, etc. The spatial heterogeneity in drug concentration is shown to have direct consequences in the emergence of antibiotic resistance [35, 42, 43, 137]. On the other hand, in the human body, bacterial population form biofilms, a protected region or compartment where antibiotics cannot penetrate and bacteria can remain viable. These cells have to migrate through a region of high antibiotic concentrations or other stressful environments to find a region of low antibiotic concentration to form another biofilm or to infect other organs in the body [51, 65] or to infect an untreated individual [20, 77]. Therefore, the antibiotic tolerant persister cells might help a population to propagate between growth permitting regions by minimizing the chance of extinction while crossing a region of high antibiotic concentration. Therefore, the dynamics of bacterial persistence under

such spatial environments might help in understanding its role in antibiotic resistance and designing experiments to study spatial evolution.

1.4.3 Population dynamics of multidrug tolerance

Bacterial persistence was first reported in *S. aureus* populations [7]. Since then it has been an important model organism other than *E. coli* to understand the relevance of persister cells in antibiotic treatment failures. *E. coli* cells have shown partial drug tolerance or persistence to several drugs such as ciprofloxacin, amplicin and streptomycin [8, 45, 53]. Likewise, *S. aureus* cells, over a long time, have developed resistance against several antibiotics with differing killing mechanism. Several studies found that failure in antibiotic treatment against staphylococcal infection is associated with the persistence mechanism [31, 49]. Hence, a systematic study of characterizing persistence of *S. aureus* against different antibiotics is necessary for the development of new drugs and multidrug therapies to eliminate persisters [71]. An important question with respect to multidrug therapy is whether persisters selected by different antibiotics are identical or different in their physiology and numbers. The efficacy of cross drug treatment relies on whether or not the surviving population from one antibiotic treatment can be killed by the addition of another antibiotic with dissimilar mechanism. These intriguing questions must be answered at least for the very first organisms that displayed persistence. Such study will also provide model parameter such as switching rates and growth rates for *S. aureus* that can be compared with other model organisms like *E. coli*, *P. aeruginosa*, etc.

1.4.4 Role of persisters in the emergence of antibiotic resistance

Another important feature of bacterial evolution is antibiotic resistance, whereby bacteria become resistant and continue to multiply in the presence of antibiotics designed to kill them [61, 94, 117]. Childhood diseases such as pneumonia and dysentery are no longer curable by earlier discovered drugs because the responsible pathogens have developed resistance against them. A large percentage of deaths in hospital are caused by infections from highly resistant bacteria such as methicillin-resistant *Staphylococcus aureus* (MRSA) and vancomycin-resistant *Enterococci*. Antibiotic resistance is a serious issue that is undermining the health care industry and threatens to become worse in the absence of serious concerns. Therefore, the understanding of the role of persister cells in the emergence of antibiotic resistance is crucial to cultivate therapeutic strategies to prevent treatment failures. Several studies speculated that persister cells surviving longer upon antibiotic treatment might provide a pool from which antibiotic resistant

cells can emerge [23, 61, 116, 117]. However, common antibiotics those targets growth maintaining processes, allow survival of non-dividing cells [10], which can undergo mutations in limited ways. However, a recent study shows that persistence may not always be incompatible with cellular growth [95, 131]. They found that the *Mycobacterium segmentis* persisters prior to antibiotic (isoniazid) treatment were dividing as fast as the normal cells. The heterogeneous response came through the variation in drug activation process between persisters and normal cells, specifically persister cells expressed low-level of KatG, a catalase peroxidase required for activation of antibiotics. The surviving subpopulation of persister cells remained stationary due to the balance of growth with antibiotic death [131]. The ongoing division in the presence of antibiotics may lead to the emergence of resistant mutants in such cases. The stress response programs such as SOS, stringent, oxidative stress response, etc. which regulates persistence are also shown to increase rates of genome-wide mutagenesis and horizontal gene transfer in *E. coli*, *S. aureus*, and *P. aeruginosa* [16, 37, 72, 81, 100]. Therefore, a systematic study considering the stochastic effects of mutation and extinction processes must be performed. Such a theoretical analysis might help in designing and understanding future experimental studies identifying the role of persisters in antibiotic resistance.

In this thesis, we will address the above discussed interesting problems and intriguing questions to provide a better understanding of bacterial persistence mechanism.

Thesis organization

The thesis is organized as a "cumulative thesis" and consists of six chapters. Chapter 2-4 consist of three manuscripts, out of which two manuscripts (chapter 2 and 4) have been published, one is submitted (chapter 3). Chapter 5 contains additional unpublished results. A list of published and submitted manuscripts are provided below. Chapter 2 focuses on the temporal dynamics of bacterial persistence mechanism in several typical experimental scenarios. Chapter 3 studies the expansion of a phenotypically heterogeneous population in spatially heterogeneous environments. Chapter 4 presents an application of the theoretical results obtained in chapter 2 by analyzing experimental results on multidrug tolerance, whereas Chapter 5 explain the role of bacterial persistence in the emergence of antibiotic resistance. The thesis in total (chapter 2-5) explores the role of bacterial persistence in spatially and temporally fluctuating environments.

1.5 List of publications

- Population Dynamics of Bacterial Persistence. P Patra and S Klumpp, PloS ONE **8**, e62814 (2013).
- Phenotypically heterogeneous populations in spatially heterogeneous environments. P Patra and S Klumpp, **under review at Phys Rev Letters**.
- Interplay between population dynamics and drug tolerance of *Staphylococcus aureus* persister cells. S Lechner, P Patra, S Klumpp, and R Bertram, J. Mol. Microbiol. Biotechnol. **22**, 381 (2012).

1.6 Author contributions

1. Population Dynamics of Bacterial Persistence.
2. Phenotypically heterogeneous populations in spatially heterogeneous environments.

   These are two theory papers. The projects were planned by P Patra and S Klumpp. The theoretical analysis was carried out by PP. The papers were written by PP and SK.

3. Interplay between population dynamics and drug tolerance of *Staphylococcus aureus* persister cells.

   This is a joint experimental/theoretical study. The experiments were planned and done by S Lechner and R Bertram, the theoretical analysis was done by PP and SK. The paper was written by SL, RB with contributions from PP and SK. Additional unpublished results from the theoretical analysis are included in Appendix A.2 of the thesis.

Chapter 2

Population dynamics of bacterial persistence

A version of this chapter is published as: P. Patra and S. Klumpp, Population dynamics of bacterial persistence, PLoS One **8**, e62814 (2013).

Online version: `http://dx.doi.org/10.1371/journal.pone.0062814`

Abstract

Persistence is a prime example of phenotypic heterogeneity, where a microbial population splits into two distinct subpopulations with different growth and survival properties as a result of reversible phenotype switching. Specifically, persister cells grow more slowly than normal cells under unstressed growth conditions, but survive longer under stress conditions such as the treatment with bactericidal antibiotics. We analyze the population dynamics of such a population for several typical experimental scenarios, namely a constant environment, shifts between growth and stress conditions, and periodically switching environments. We use an approximation scheme that allows us to map the dynamics to a logistic equation for the subpopulation ratio and derive explicit analytical expressions for observable quantities that can be used to extract underlying dynamic parameters from experimental data. Our results provide a theoretical underpinning for the study of phenotypic switching, in particular for organisms where detailed mechanistic knowledge is scarce.

2.1 Introduction

The life of microorganisms is characterized by two main tasks, rapid growth and proliferation under conditions permitting growth and survival under stressful conditions [93]. One strategy to cope with such varying environmental conditions is phenotypic heterogeneity, the splitting of a genetically homogeneous population into subpopulations that execute different strategies for survival [19, 25, 113]. Phenotypic tolerance to antibiotics (persistence) is a prime example of such phenotypic heterogeneity: When a bacterial culture is treated with an antibiotic, typically a small fraction of the population, the persisters, survives and allows the culture to grow back once the antibiotic has been removed (Fig. 2.1), thus making it difficult to eradicate the population [7, 73, 75]. The re-grown culture remains susceptible to the antibiotic with the exception of yet again a small fraction of persisters, indicating that, in contrast to resistance, persistence is a phenotypic effect. Indeed observations at a single cell level have shown that cell switch in a stochastic fashion between the persister state and the normal state [4]. Moreover these experiments have shown that persistence is not an adaptive response to the antibiotics, but rather that persisters are present in the population before the antibiotic treatment [4] (there is however evidence that adaptive responses also play a role in some situations [21, 22]). The persister cells present in the population before treatment were shown to grow much more slowly than normal cells [4, 110], indicating that persistence while providing a fitness benefit (survival advantage) under stress conditions also invokes a fitness cost under unstressed conditions. Persistence is thus based on the coexistence of subpopulations growing with different growth rates. Mechanistically, the formation of persisters has been linked to the expression of chromosomal toxin-antitoxin systems [62, 79, 88, 89], which are believed to give rise to a genetic circuit that exhibits bistable behavior resulting in subpopulations with different phenotypes characterized by different growth rates [15, 60, 78, 105]. Indeed, experimental and theoretical studies of the coupling of gene expression and cell growth indicate that such growth bistability should be considered a rather generic phenomenon that can arise when gene circuits modulate cell growth [60, 119].

The molecular mechanisms for the generation of persisters are currently a topic of very active research. Persistence has been observed in a wide range of bacterial species [73, 75, 115], but on the mechanistic level, so far relatively little is known for bacteria other than the model organism *E. coli*. In the absence of detailed mechanistic knowledge, the main window into persistence is the study of the population dynamics upon antibiotic treatment, in particular, the survival upon administration of the drug and the re-growth of the population upon removal of the drug. Here we study a theoretical model for this dynamics that was originally proposed by Balaban et al. [4]. We make

use of an excellent approximation (based on the assumption that the rates of phenotype switching are small, which is typically the case) to derive explicit analytical expression for a number of observable quantities for several typical experimental scenarios: constant environment, shift from growth to stress conditions or vice versa and periodically switching environments. Our analysis is similar to previous theoretical studies on phenotype switching [67, 68]. A small but important difference to the systematic perturbative approach used in Ref. [68] is that our theory is based on the approximation of small phenotype switching rates (as compared to the growth and death rates), while the approximation of Ref. [68] is based on long durations of environmental durations, such that populations structures reach their steady state before the environment changes. The latter is not required in our approximation and our approach thus allows us to study both short and long environmental durations (while long durations are expected to be typical for the natural environment, and thus appropriate for an evolutionary comparison of different modes of phenotype switching, such as stochastic and adaptive [68], short durations may be of importance for some experimental situations, such as resuscitation experiments after short periods of antibiotic treatment). We also note that while the mathematics of ours and the previous study are closely related, the scope of the studies is different. Rather than aiming at a general theoretical framework for phenotype switching phenomena, our goal here is to obtain simple explicit expression for measurable quantities. These expressions can be used to analyze experimental data for population growth and decay to provide insights into the mechanism of persistence based on simple population-scale experiments.

2.2 Phenotype switching

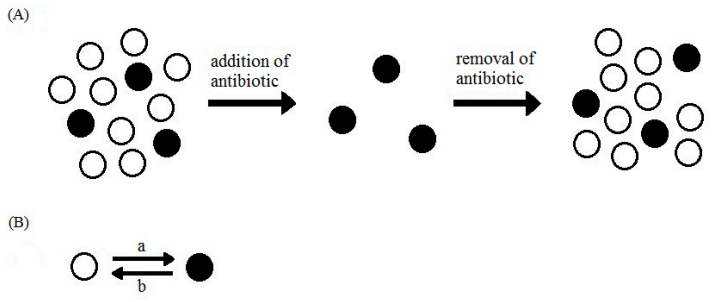

FIGURE 2.1: **(A) Dynamics of heterogeneous population consisting of normal (white) and persister (black) cells**: The persisters survive the addition of an antibiotic, and allow the population to grow back after the removal of the antibiotic. (B) Phenotype switching: Cells stochastically switch between the normal and persister state with rates a and b

We consider a bacterial population where an individual cell can have two distinct phenotypic states (Fig. 2.1) which are characterized by different sensitivities to given environmental conditions. The environmental sensitivity is reflected in growth and decay rates of the subpopulation in the given environment. For instance, in the case of persister cell on which we focus, normal cells are more sensitive to various stresses, i.e. they decay faster under various stress conditions such as antibiotic treatment [4] and phage attack [99], but also grow faster in unstressed conditions.

A cell in the normal state can switch to the persister state with rate a and a cell in the persister state can switch back to the normal state with rate b. The instantaneous switching between phenotypic states leads to distinct subpopulation of normal and persister cells which compose the total population. We denote the growth rate of normal cells (n) and persister cells (p) by μ_n^m and μ_p^m respectively, where m indicates the growth medium or, more generally the growth conditions. Below we will use indices 'g' and 's' to denote unstressed growth and stress conditions, respectively (e.g., growth medium not containing or containing an antibiotic). The resulting population dynamics can be described by the following system of equations [4],

$$\begin{aligned} \frac{dn}{dt} &= \mu_n^m n - an + bp \\ \frac{dp}{dt} &= \mu_p^m p + an - bp. \end{aligned} \tag{2.1}$$

In order to determine the steady state of these dynamical equations, we consider the time evolution of the subpopulation ratio $f = n/p$, which is given by

$$\frac{df}{dt} = b - af^2 + \Delta_m f = -a(f - f^{'})(f - f^*), \tag{2.2}$$

where

$$\begin{aligned} f^* &= \frac{\Delta_m + \sqrt{(\Delta_m)^2 + 4ab}}{2a}, \\ f^{'} &= \frac{\Delta_m - \sqrt{(\Delta_m)^2 + 4ab}}{2a} \end{aligned} \tag{2.3}$$

and $\Delta_m = (\mu_n^m - a) - (\mu_p^m - b)$.

f^* and f' are fixed points of Eq. (2.2): f' is an unstable fixed point (which moreover can be negative) and f^* is a stable fixed point and always positive. Thus, the steady state population ratio is given by f^*.

In conditions of unstressed growth, Δ_m is positive. When the switching rates are small compared to the growth rates, as it is typically the case (Table 2.1), the steady state

ratio can be approximated by $f^* \approx \Delta_m/a$ or

$$\frac{n^*}{p^*} \approx \frac{(\mu_n^m - \mu_p^m)}{a}. \tag{2.4}$$

The last equation has a simple, but instructive interpretation: the steady state population structure with a certain ratio of normal and persister cells in conditions of unstressed growth is determined by a balance of two processes: The fast-growing normal cells outgrow the slow-growing persisters (with $\Delta_m \approx \mu_n^m - \mu_p^m$), but they also replenish the persister population via switching to the persistent state (with rate a). We linearize Eq. (2.2) around the fixed point f^* to determine the time scale in which the steady state is approached,

$$\frac{df}{dt} \approx -\sqrt{\Delta_m^2 + 4ab}\,(f - f^*). \tag{2.5}$$

This equation shows that the subpopulation ratio f approaches the steady state f^* with rate $([(\mu_n^m - a) - (\mu_p^m - b)]^2 + 4ab)^{1/2}$, which, for small switching rates a and b, is approximately equal to the growth rate difference between the two subpopulations.

Likewise, the same approximation applied to stress condition (with $\Delta_m < 0$), leads to the steady state $f^* \approx -b/\Delta_m$ or

$$\frac{p^*}{n^*} \approx \frac{(\mu_p^m - \mu_n^m)}{b}. \tag{2.6}$$

In this case, the steady state population structure is determined by the balance of persisters outlasting the normal population (with $-\Delta_m \approx \mu_p^m - \mu_n^m$) and reproducing it through phenotype switching (with rate b).

The existence of a finite steady state in the subpopulation ratio indicates a stable coexistence of the two cells types that grow (or decay) with different rates. It is worth noting that such coexistence is an effect of phenotype switching, as normally a faster growing subpopulation will outgrow a slow-growing one, so that the subpopulation ratio will approach either zero or infinity. Here however, switching of cells between the two phenotypes that correspond to the two subpopulations can replenish the slower-growing (or faster-decaying) subpopulation and balance the outgrowth effect.

So far we have only considered the subpopulation ratio or the fractions of total population that belong to the two phenotypes. Within the model of Eqs. (2.1), these fractions approach a steady state, while the overall population always grows or decays exponentially on long time scales. Thus, both subpopulations grow or decay with the same average rate in the steady state, which corresponds to the effective growth rate (or decay rate) of the total population. The steady state growth rate of the total population

(μ_{st}) is obtained from Eqs. (2.1) by substituting Eq. (2.3) and is given by

$$\mu_{st} = \frac{(\mu_n^m - a) + (\mu_p^m - b) + \sqrt{\Delta_m^2 + 4ab}}{2}. \tag{2.7}$$

We use again an approximation of small switching rates and neglect terms of quadratic order in the switching rates (terms proportional to ab). With this approximation the steady state growth rate is simplified to

$$\mu_{st} \simeq \mu_n^g - a \tag{2.8}$$

in unstressed growth ($\mu_n^g > \mu_p^g > 0$) and to

$$\mu_{st} \simeq \mu_n^s - b \tag{2.9}$$

under stress conditions ($\mu_n^s < \mu_p^s < 0$).

The comparison of these two approximate expressions shows that the presence of persister cells causes a small reduction in the steady state growth rate under unstressed conditions (of order a), but leads to a significant reduction in the steady state death rate of the total population under stress conditions as compared to a population without any persister cells. Therefore one can expect the presence of persister cells to be beneficial provided that stress conditions do regularly occur.

TABLE 2.1: **Rates for switching between the normal and persister phenotype.**

organism	switching rate a ($n \to p$) [hr^{-1}]	switching rate b ($p \to n$) [hr^{-1}]	reference
E. coli	$10^{-6} - 10^{-3}$	$10^{-6} - 10^{-1}$	[4]
S. aureus	$10^{-5} - 10^{-3}$	$10^{-2} - 10^{-1}$	[72]

The balance between phenotype switching and outgrowing of one subpopulation by the other that we have discussed above is intricately linked to the exponential growth or decay of the total population. While exponential growth phase is the main focus of our study, we want to briefly address the case where the population reaches a stationary phase due to a finite carrying capacity (K) of the growth environment, a typical situation in both natural habitats and in the test tube. To this end, we modify the growth terms in Eq. (2.1) by multiplying them with $[1 - (n + p)/K]$. In a growth environment (with positive growth rates), the total population will then reach a steady-state value of $n + p = K$ for long times. The ratio between persisters and normal cells is then determined not by a balance of one-way phenotype switching and growth, but by a balance between switching in both directions, given by $an - bp = 0$. As a consequence, the ratio f is given by $f = n/p \approx b/a$ and is thus several orders of magnitude smaller

than the corresponding value obtained for exponential growth, Eq. (2.4), because of the small switching rates. This result is consistent with the observation that typically the fraction of persisters in the population is larger in stationary phase than in exponential growth phase (e.g., a 100-fold effect in *E. coli*) [75].

2.3 Dynamics in constant environment

In the following we will discuss the time evolution of the two subpopulation in more detail. We start by considering a constant environment. To solve the time-dependence of the coupled equations in Eqs. (2.1), we make once more use of the approximation for small switching rates ($\Delta_m^2 \gg ab$).

If the constant environment is one of unstressed growth (with $\Delta_m > 0$), the fixed points can be approximated by $f^{'} \approx 0$ and $f^* \approx \frac{\Delta_g}{a}$. The differential equation for the subpopulation ratio (f) is thereby reduced to a logistic equation,

$$\frac{df}{dt} = \Delta_g f \left(1 - \frac{af}{\Delta_g}\right), \tag{2.10}$$

where $\Delta_g = (\mu_n^g - a) - (\mu_p^g - b)$. Its solution has the following form:

$$f(t) = \frac{\Delta_g}{a + (\Delta_g/f_0 - a)e^{-\Delta_g t}}, \tag{2.11}$$

where f_0 is the initial ratio of normal to persister cells.

For $\Delta_m < 0$, i.e. in stress conditions, a similar differential equation like Eq. (2.2) is obtained for the time evolution of ratio of the persister subpopulation to the normal subpopulation, $\phi = p/n$. The differential equation of ϕ has two fixed points $\phi^* \approx -\Delta_m/b$ and $\phi^{'} \approx a/\Delta_m$, of which $\phi^* = 1/f^*$ is stable. In this case, using the approximation $\phi^{'} \approx 0$, we obtain

$$\frac{d\phi}{dt} = \Delta_s \phi \left(1 - \frac{b\phi}{\Delta_s}\right) \tag{2.12}$$

with $\Delta_s = (\mu_p^s - b) - (\mu_n^s - a)$. With an initial ratio ϕ_0, the solution has the form

$$\phi(t) = \frac{\Delta_s}{b + (\Delta_s/\phi_0 - b)e^{-\Delta_s t}}. \tag{2.13}$$

For large times, these expression approach the steady state results derived previously and given in Eq. (2.4) and Eq. (2.6), respectively. As a consequence, under unstressed growth conditions, the effective growth rate of the persister subpopulation approaches the growth rate of the normal subpopulation in a logistic fashion and vice versa.

The functional form of $f(t)$ and $\phi(t)$ derived here will be used as the basis for our further analysis. Because of the symmetry between the two cases, we will calculate quantities in only one condition (growth or stress). The results for the other condition are obtained by simultaneously exchanging symbols and indices according to the rules $g \leftrightarrow s$, $f_0 \leftrightarrow \phi_0$, $a \leftrightarrow b$, and $p \leftrightarrow n$.

2.4 Response to environment shift

2.4.1 Characteristic time scales of the population dynamics

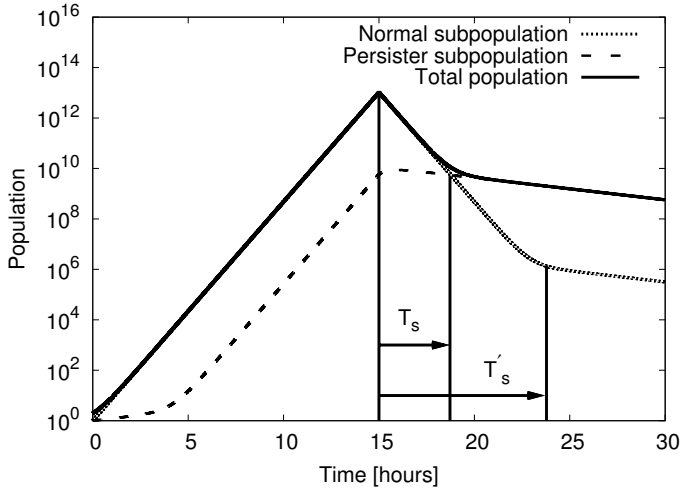

FIGURE 2.2: **Biphasic killing kinetics**: Numerical integration of Eqs. (2.1) over a growth period of 15 hours (with $\mu_n^g = 2\ \mathrm{hr}^{-1}, \mu_p^g = 0.2\ \mathrm{hr}^{-1}$) followed by a stress period (with $\mu_n^s = -2\ \mathrm{hr}^{-1}, \mu_p^s = -0.2\ \mathrm{hr}^{-1}$) of another 15 hours. The switching rates were chosen to be $a = 0.001\ \mathrm{hr}^{-1}$ and $b = 0.001\ \mathrm{hr}^{-1}$. The killing curve of total population show two distinct phases, a fast-decaying phase and a slow-decaying phase. The dynamics is characterized by two time scales T_s and T_s' (see text).

Next we turn to the dynamics after an environmental shift. Experimentally, one typically considers two situations [4, 19, 72]: (i) a population that has been growing under unstressed conditions for a sufficiently long time is exposed to an antibiotic or (ii) a population that has been exposed to an antibiotic for some time is shifted back to a medium without the antibiotic. In both cases, one typically observes a biphasic dynamics. For instance, a population exposed to an antibiotic typically shows biphasic decay.

Such kinetics is obtained as a consequence of the coexistence of the two phenotypes and the time at which the global decay rate changes provides an easily observable signature of phenotype switching that allows to infer its microscopic parameters.

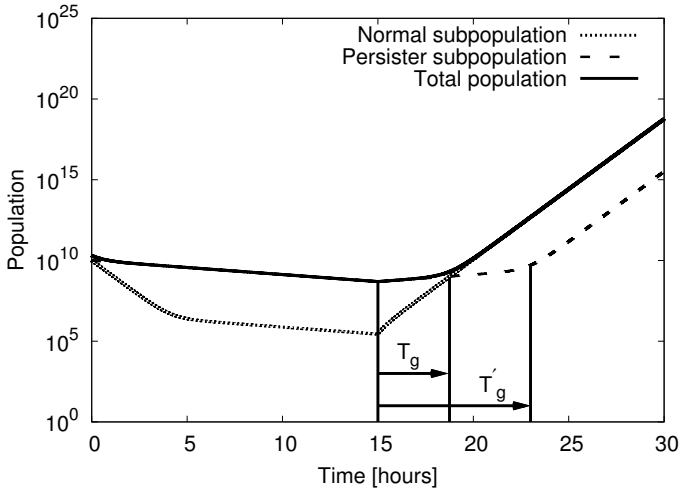

FIGURE 2.3: **Biphasic growth kinetics**: Numerical integration of Eqs. (2.1) over a stress period of 15 hours followed by a regrowth period of another 15 hours. The regrowth curve of the total population shows two distinct phases, a slow-growing phase followed by a fast-growing phase. The parameters are the same as in Fig. 2.2.

Fig. 2.2 shows a numerical example of such dynamics: Here Eqs. (2.1) have been integrated to reach a steady population ratio under growth conditions with a small persister fraction. At time $t = 15$ hours, the parameters were changed to those for stress condition. After the shift to stress conditions (by the addition of an antibiotic), the total population displays the biphasic decay behavior. In the fast-decaying phase, the decay of the total population is dominated by the death of normal cells, while in the second, slower-decaying phase, the total population consists predominantly of persister cells and the decay rate is governed by the death rate of the persisters. The transition between the two different phases occurs when both subpopulation becomes equal in size, i.e. at a time T_s for which $\phi(T_s) = 1$. Therefore, the transition time (T_s) from the fast-decay phase to the slow-decay phase after the shift to stress conditions or to antibiotic-containing medium is given by

$$T_s = \frac{1}{\Delta_s} \ln \frac{\Delta_s/\phi_0 - b}{\Delta_s - b}, \tag{2.14}$$

where $1/\phi_0$ is the initial ratio of normal cells to persister cells at the time antibiotic treatment. During the growth phase, the normal cells make up the majority of the population and persister cells account for only a small fraction of the total population, which means $1/\phi_0 \gg b$. In the limit $\Delta_s \gg b$, i.e. if the growth rate difference is larger

compared to switching rate, the exit time can approximated by

$$T_s \approx \frac{1}{\Delta_s} \ln \frac{n_0}{p_0}. \tag{2.15}$$

The expression for T_s shows that the population will exit sooner from the fast-decaying phase if it has a large ratio of persister cells initially. It shows that the longer survival or persistence of the bacterial populations in antibiotic treatment depends on the fraction of persister cells that the population has formed beforehand as its survival strategy against unpredictable bad conditions.

It is worth mentioning that the time T_s, which characterizes the transition between the two phases of the decay of the total population, is not the characteristic time for reaching the new steady-state population ratio. The latter occurs later and is characterized by a time T_s' that can be determined as the inflection point of the time-dependent decay rate of the normal subpopulation (calculated below), which leads to

$$T_s' = \frac{1}{\Delta_s} \ln \left(\frac{\Delta_s}{b\phi_0} + 1 \right) \approx \frac{1}{\Delta_s} \ln \left(\frac{\Delta_s}{b} \frac{n_0}{p_0} \right) = T_s + \frac{1}{\Delta_s} \ln \left(\frac{\Delta_s}{b} \right). \tag{2.16}$$

The last expression here shows directly that equilibration of the population structure occurs later than the transition in the growth rate. The delay between the two time scales is determined by a balance between the two effects that dominate the population structure under stress conditions [as in Eq. (2.6)], persisters taking over the population by outlasting the normal cells and switching of persisters to the normal state.

The re-growth of a population after the removal of the antibiotic is also biphasic with an initial slow-growth phase followed by a phase of rapid growth (Fig. 2.3). The transition between the two phases can be analyzed in the same way. The transition time from the slow-growing phase to fast growing phase is given by

$$T_g \approx \frac{1}{\Delta_g} \ln \frac{p_0}{n_0} \tag{2.17}$$

and depends on the initial persister subpopulation. Therefore, a larger persister fraction under stress conditions (e.g. due to longer exposure to the antibiotic) results in a delay in resuming the maximum growth rate after the shift to conditions of unstressed growth. As above, the steady state population ratio is reached at the later time T_g', given by

$$T_g' \approx \frac{1}{\Delta_g} \ln \left(\frac{\Delta_g}{a} \frac{p_0}{n_0} \right) = T_g + \frac{1}{\Delta_g} \ln \left(\frac{\Delta_g}{a} \right). \tag{2.18}$$

In both types of experiments, both times scales can be determined experimentally, but

T_s and T_g are much more easily accessible than T_s' and T_g', as they only require measurements of the total population size, e.g. by colony counting, while measuring T_s' or T_g' requires to determine the time-dependent persister fraction. We note that the transition time T_g or T_s are closely related to the "delay times" defined in Ref. [68]. In fact these delay times are obtained from T_g or T_s by further approximating $\Delta_g \approx \mu_n$ and $\Delta_s \approx \mu_p$. The underlying picture of Ref. [68] is that after an environmental shift, the population growth (or decays) exponentially with a new growth rate after a delay during which the population structure adjusts to the new environment. In contrast, our analysis indicates that the new steady state of the population structure is reached later than the macroscopically observable delay or transition time.

If the subpopulation ratio has reached the steady state before the shift from one environmental condition to the other, the expressions for the time scales T_s and T_g can be further simplified using Eqs. (2.15) and (2.17). As a result the transition times of total population growth or decay can be expressed in terms of the switching rates as

$$T_s \approx \frac{1}{\Delta_s} \ln \frac{\Delta_g}{a} \qquad \text{and} \qquad T_g \approx \frac{1}{\Delta_g} \ln \frac{\Delta_s}{b}. \tag{2.19}$$

With the exception of the switching rates a and b, all quantities entering these equations are directly accessible though the time-dependence of the total population size (as shown in Figs. 2.2 and 2.3) and discussed below in more detail). Thus, the phenotype switching rates can be determined from time courses of the total population size in a set of two shift experiments: (i) a sufficiently long period of of unstressed growth long followed by stress (addition of the antibiotic) and (ii) a sufficiently long stress period followed by a growth period (via shift to medium without the antibiotic). Then, the switching rates a and b can be calculated from the parameters of the growth (or decay) curves by inverting the two equations above,

$$b \approx \Delta_s \, e^{-\Delta_g T_g} \qquad \text{and} \qquad a \approx \Delta_g \, e^{-\Delta_s T_s}. \tag{2.20}$$

2.4.2 Time-dependent growth rates

The numerical integration of the population dynamics as plotted in Figs. 2.2 and 2.3 show that the growth of normal subpopulation under unstressed growth conditions is exponential with growth rate approximately given by $(\mu_n^g - a)$, as obtained from our approximation for small switching rates above. By contrast, the growth of the persister subpopulation is biphasic and can be characterized by a time-dependent effective growth rate $\dot{p}(t)/p(t)$. Note that this effective growth rate describes the overall growth

of the persister subpopulation and includes the effects of persister proliferation and of phenotype switching.

Alternatively, it can be characterized by the average of that effective growth rate up to time t,

$$\langle \mu_p^g \rangle = \frac{1}{t} \int_{t_0}^{t_0+t} \frac{\dot{p}(\tau)}{p(\tau)} d\tau. \tag{2.21}$$

The latter quantity has the disadvantage to depend on a somewhat arbitrary initial time t_0, but can easily be determined experimentally from the overall increase of the persister subpopulation. The growth rate can be calculated from Eqs. (2.1) by substituting $n(t) = p(t)f(t)$, where $f(t)$ is the time-dependent subpopulation ratio that we have already calculated in Eq. (2.11). Therefore, the average growth rate of the normal (n) and persister (p) subpopulation over a growth period t_g is

$$\begin{aligned} \langle \mu_n^g \rangle &= (\mu_n^g - a) \\ \langle \mu_p^s \rangle &= (\mu_n^g - a) + \frac{1}{t_g} \ln \frac{a f_0 + (\Delta_g - a f_0) e^{-\Delta_g t_g}}{\Delta_g}. \end{aligned} \tag{2.22}$$

Likewise, the average growth rate for the normal (n) and persister (p) subpopulation over a stress period t_s is given by

$$\begin{aligned} \langle \mu_p^s \rangle &= (\mu_p^s - b) \\ \langle \mu_n^s \rangle &= (\mu_p^s - b) + \frac{1}{t_s} \ln \frac{b\phi_0 + (\Delta_s - b\phi_0) e^{-\Delta_s t_s}}{\Delta_s}. \end{aligned} \tag{2.23}$$

Note that in both cases the effective growth rates growth rate of both subpopulation approach the same value for large times t_s or t_g.

2.4.3 Growth of the total population

Explicit expression for the effective growth rate and the time evolution of the total population can also be computed using the the results of analytical approach. The time evolution equation of total population $P(t) = n + p$ under unstressed growth conditions can be expressed in terms of subpopulation ratio $f(t)$ as

$$\frac{d}{dt} P = \left(\mu_n + (\mu_p - \mu_n) \frac{1}{1 + f(t)} \right) P. \tag{2.24}$$

The time dependent average growth rate of the total population in a growth period t_g is given by

$$\begin{aligned}\langle \mu_P^g \rangle &= \mu_n^g + (\mu_p^g - \mu_n^g)\frac{1}{t_g}\int_{t_0}^{t_0+tg}\frac{1}{1+f(\tau)}d\tau \\ &= \mu_p^g + \frac{(\mu_n^g - \mu_p^g)}{(\Delta_g + a)t_g}\ln\frac{(\Delta_g + a)e^{\Delta_g t_g} + (\Delta_g/f_0 - a)}{\Delta_g(1/f_0 + 1)},\end{aligned} \tag{2.25}$$

where the last expression has been obtained by substituting the explicit functional form of $f(t)$.

Similarly, the average growth rate of the total population during stress conditions is given by

$$\langle \mu_P^s \rangle = \mu_n^s + \frac{(\mu_p^s - \mu_n^s)}{(\Delta_s + b)t_s}\ln\frac{(\Delta_s + b)e^{\Delta_s t_s} + (\Delta_s/\phi_0 - b)}{\Delta_s(1/\phi_0 + 1)}. \tag{2.26}$$

The above expression can be further simplified using again an approximation for small switching rates (compared to Δ_g and Δ_s). As a consequence $f_0 \gg 1$, $\phi_0 \gg 1$. Within this approximation, the total population follows a double exponential dynamics both during unstressed growth,

$$P(t) \approx p(t=0)[e^{\mu_p^g t} + f_0\, e^{\mu_n^g t}] \tag{2.27}$$

and under stress,

$$P(t) \approx n(t=0)[e^{\mu_n^s t} + \phi_0\, e^{\mu_p^s t}]. \tag{2.28}$$

The dynamics of the total population is accessible to direct experimental observations. These expressions can therefore be used for the quantitative analysis of experimental killing curves or regrowth experiments. By fitting such data with these expressions, the growth (or death) rates and the initial fractions of the subpopulation can be obtained [72].

2.5 Dynamics in periodically switching environment

Finally, we consider an environment that switches periodically between growth and stress conditions. The duration of the conditions are denoted by t_g and t_s. To address the evolutionary consequence of phenotype switching in varying environmental conditions, we calculate the average growth of the population over one environmental cycle. The average growth rate of the subpopulation over one environmental cycle of duration $t_g + t_s$

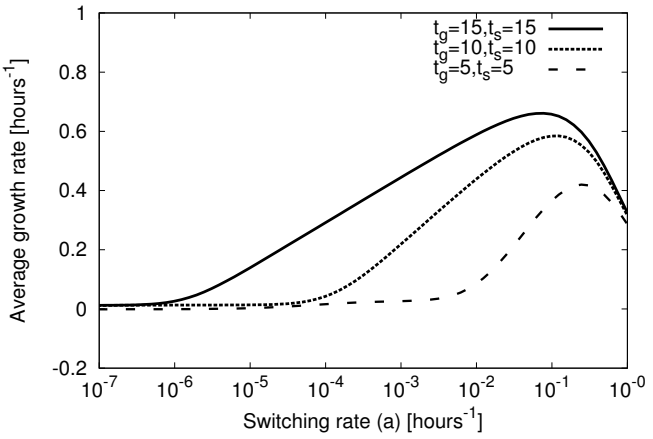

FIGURE 2.4: **Optimal switching rate**: The average growth rate over an environmental cycle is plotted as a function of the phenotype switching rate ($a = b$) for different environmental durations ($t_g = t_s = T$). The figure shows the existence of an optimal switching rate for a given cycle duration ($t_g + t_s$). The growth rates are the same as in Fig. 2.2.

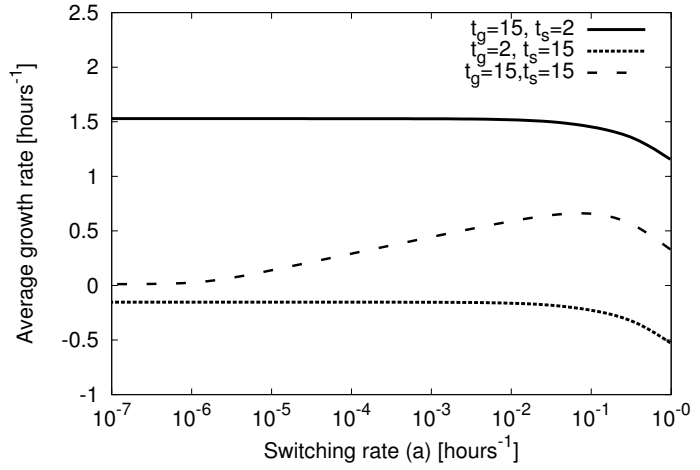

FIGURE 2.5: **Existence of an optimal switching rate**: Average growth rate as function of the switching rate ($a = b$). An optimal switching rate is seen for slowly varying environment, but not if one environmental duration is short. The growth rates are the same as in Fig. 2.2.

are given by

$$\langle \mu_n \rangle = \frac{\langle \mu_n^g \rangle t_g + \langle \mu_n^s \rangle t_s}{(t_g + t_s)} \tag{2.29}$$

$$\langle \mu_p \rangle = \frac{\langle \mu_p^g \rangle t_g + \langle \mu_p^s \rangle t_s}{(t_g + t_s)}. \tag{2.30}$$

In general, these expressions depend on the initial subpopulation ratio during growth and stress. Here we are most interested in the long-time behaviour, where the initial subpopulation ratio of a cycle is given by those subpopulation ratio at the end of a cycle. In that case, the effective growth rates of both subpopulations are equal. Expressions for the growth rates for several cases are given in the 2.7.1.

Here we focus on the case, where both phases of the environmental cycle are sufficiently long such that a steady state of the population structure is reached in each condition. In that case, the average growth rate is given by

$$\langle \mu \rangle = \frac{(\mu_n^g - a)t_g}{t_g + t_s} + \frac{(\mu_p^s - b)t_s}{t_g + t_s} + \frac{\ln(\frac{ab}{\Delta_s \Delta_g})}{t_g + t_s}. \tag{2.31}$$

Evolution will adapt the control of persistence to such cycling conditions in order to maximize the average growth rate under such repeated conditions. The growth and killing rates of the normal and persister cells are environment-dependent but the switching rates can be tuned to maximize the average growth rate for a given environmental periodicity (which in reality will be the typical duration of a cycle defined by a stochastically varying environment) [67, 69]. The optimal values for a and b can be calculated by maximizing above expression, which leads to

$$\begin{aligned} \frac{1}{a_{opt}} &= t_g + \frac{1}{\Delta_s} - \frac{1}{\Delta_g} \\ \frac{1}{b_{opt}} &= t_s - \frac{1}{\Delta_s} + \frac{1}{\Delta_g}. \end{aligned} \tag{2.32}$$

The dominant term in the expression for the optimal switching rates (2.32) are the environmental durations t_g and t_s.The correction terms are in principle dependent on the switching rates. As these expressions are valid for long environmental durations, and thus small switching rates, this dependence can be neglected. So the correction terms in this expression should therefore be taken at zero switching rates. Alternatively, Eqs. (2.32) can be interpreted as implicit equations and solved for the switching rates. These expressions in Eq. (2.32) are similar to the expression given by Kussel et al. [67], which indicates the consistency between different theoretical approaches. Similar results on the existence of such optimal switching have also been obtained in a number of other previous studies [68, 69, 121].

It is worth noting that a maximum of the growth rate and thus optimal switching rates are found only when the environment changes very slowly, as shown in Fig. 2.5. This is different from the behaviour described in previous studies [67, 68], which focused on the limit of long environmental durations. Approximations for this limit cannot predict the

growth rates for cases, where one of the environmental durations is short (e.g., for very brief exposures to antibiotics). Within our approximation this case can be addressed. We find that if one of the environmental duration is short, the growth rate decreases with the increasing phenotype switching rate, which suggests that phenotype switching is unprofitable under such conditions (see the expressions for cases 2 and 3 given in the 2.7.1).

In our analysis, we have focused on exponentially growing cells, but as mentioned already, in natural environments, growth is usually limited by the carrying capacity of the environment, so we want to briefly mention how the dynamics is affected by such carrying capacity. We have shown above that, under constant conditions promoting growth, the total population will eventually reach the carrying capacity and that in this steady state the subpopulation ratio is determined by the phenotype switching rates, $p/n = b/a$. In stress conditions, the dynamics is unaffected by the environmental carrying capacity. The dynamics in periodically switching environments depends on whether the average growth rate (in the absence of a carrying capacity) is positive or negative. In the case of net decay, our analysis remains valid, as the carrying capacity is irrelevant. But if there is net growth per environmental cycle, the population will eventually grow to the carrying capacity during a growth period. From then on, the population will oscillate between decaying away from the maximal population size during the stress period and growing back to it in the growth period. The long term growth rate is zero in this case.

2.6 Concluding remarks

One way bacterial population cope with environmental stresses is by setting aside a small fraction of the total population, the persister cells, in a slow-growing, but stress-tolerant phenotypic state. These persisters provide a pool of cells from which the population can recover via a phenotypic switch to the normal growth state after the environmental conditions have improved. Here we have analyzed a simple mathematical model to understand the dynamics of phenotype switching. Typically, the fitness cost associated with the switching of few normal cells to the persister phenotype under growth-permissible conditions is small compared to the fitness benefit of the presence of persister cells under stress conditions. We have used an approximation valid for small switching rates that allows us to obtain explicit analytical expression for many quantities that are directly accessible to experiments. Within this approximation, the population dynamics is mapped to a logistic equation for the ratio of the population fractions corresponding to the two phenotypes. For constant environmental conditions, stable coexistence of the two subpopulations that grow with different growth rates is achieved by a balance

between fast-growing cells outgrowing the slow-growing ones and phenotype switching, by which the slow-growing subpopulation is replenished.

We have then considered shifts between environmental conditions as well as periodically switching environments. Specifically, we have identified several characteristic time scales for changes in the overall population growth or decay and for the approach to a constant ratio between the two subpopulations. Simple analytical expressions for these time scales provide a window into the phenotype switching process and more specifically allow to determine the switching rates from population-scale shift experiments [72], which are typically governed by double-exponential population growth or decay. Finally, we determined the average growth rates for a periodically switching environment. If growth and stress periods have long durations, the phenotype switching rates can be tuned for optimal growth of the total population.

The results derived are based on the assumption that phenotype switching is a stochastic process, independent of the environment. This assumption may not always be valid, as in some cases, persistence may also involve an adaptive response to the stress conditions. One case, where this has been demonstrated is persistence of *E. coli* cells upon treatment with the antibiotic Ciprofloxacin, where persistence is actively induced via the SOS response [21, 22]. Analysis of such cases with our model would lead to condition-dependent apparent switching rates. In such cases, the model may be used as a 'null model' to identify deviations from the simple dynamics discussed here.

Finally, we want to emphasize that the analysis we have developed here, can also be applied to other cases of 'growth bistability', i.e. cases of phenotypic heterogeneity, where genetically identical subpopulations grow with different growth rates. One interesting case is bacterial competence, a program for genetic transformation (quasi-sexual exchange of genetic material), which is typically activated in only a subpoulation [25]. In this case, it has been proposed that phenotypic heterogeneity provides a evolutionary advantage in a homogeneous environment [134]. Recent studies of growth effects on various genetic circuits suggest that growth bistability may be a rather generic consequence of the coupling of gene expression and cell growth [59, 60, 109, 119].

2.7 Supporting information

2.7.1 Average growth rate in periodic environmental conditions

In this appendix, we give expression for the average growth rate of the total population for several different cases beyond the case of slow environmental variation discussed in

the main text.

Case 1: $t_g > T'_g$ and $t_s > T'_s$. For slow variation of the environment, i.e. for long durations of the growth and stress periods, the average growth rate is given by

$$\langle\mu\rangle = \frac{(\mu_n^g - a)t_g}{t_g + t_s} + \frac{(\mu_p^s - b)t_s}{t_g + t_s} + \frac{\ln(\frac{ab}{\Delta_s \Delta_g})}{t_g + t_s} \tag{2.33}$$

Case 2: $t_g > T'_g$ and t_s is very small. For short duration of the stress period and long duration of the growth period, the average growth rate is given by

$$\langle\mu\rangle = \frac{(\mu_n^g - a)t_g}{t_g + t_s} + \frac{(\mu_p^s - b)t_s}{t_g + t_s} + \frac{\ln(\frac{ab+(\Delta_s\Delta_g - ab)e^{-\Delta_s t_s}}{\Delta_s \Delta_g})}{t_g + t_s}. \tag{2.34}$$

The average growth rate decreases as the switching rate increases as shown in Fig. 2.5. The maximal growth rate for infinitesimally small switching rates ($a \to 0$ and $b \to 0$) is given by

$$\langle\mu\rangle_{max} = \frac{(\mu_n^g - a)t_g}{t_g + t_s} + \frac{(\mu_n^s - a)t_s}{t_g + t_s}. \tag{2.35}$$

Case 3: $t_s > T'_s$ and t_g is very small. Likewise, for short duration of the growth period and long duration of the stress period, the average growth rate is given by

$$\langle\mu\rangle = \frac{(\mu_p^s - b)t_s}{t_g + t_s} + \frac{(\mu_n^g - a)t_g}{t_g + t_s} + \frac{\ln(\frac{ab+(\Delta_s\Delta_g - ab)e^{-\Delta_g t_g}}{\Delta_s \Delta_g})}{t_g + t_s}. \tag{2.36}$$

Again, the average growth rate decreases as the switching rate increases as shown in Fig. 2.5. The maximum growth rate for small switching rates ($a \to 0$ and $b \to 0$) is given by

$$\langle\mu\rangle_{max} = \frac{(\mu_p^g - b)t_g}{t_g + t_s} + \frac{(\mu_p^s - b)t_s}{t_g + t_s}. \tag{2.37}$$

2.7.2 Steady state ratio of sub populations

In this paper, we make extensive use of approximations based on the observation that the switching rates a and b are typically very small (Table 2.1). As a numerical test of this approximation, we consider the subpopulation ratio, which becomes constant over long times of constant growth or decay conditions. In periodically varying environment the ratio of the subpopulations at end of an environmental duration is determined by the environmental periodicity (the durations of the two phases, t_g and t_s). The exact steady state ratio of the subpopulations can be determined numerically by integrating the dynamical equations Eqs. (2.1) over a long time under a given environmental condition.

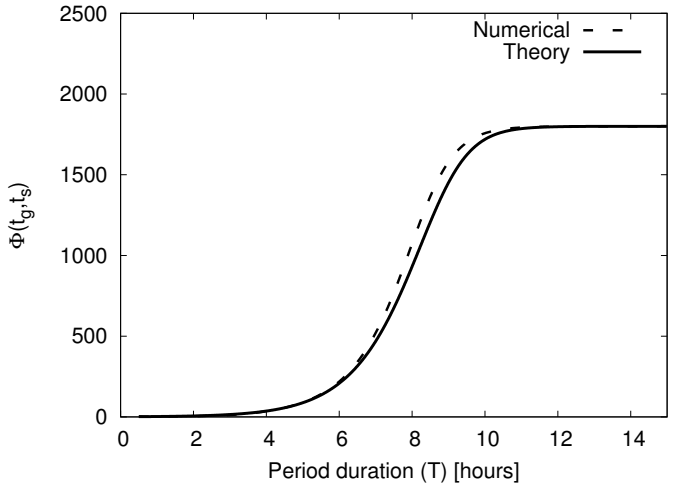

FIGURE 2.6: **Comparison of the approximation for small switching rates with the exact numerical result**: Steady-state ratio of the normal to the persister subpopulation at the end of an environmental cycle ($T = t_g = t_s$). The parameters are the same as in Fig. 2.2

Here, we compare the value of the subpopulation ratio $\phi(t_g, t_s)$ at the end of a stress phase as obtained from our analytical approximation with the corresponding numerical result. The analytical result is obtained by iterating the following recursion

$$\begin{aligned} f(t_g, t_s) &= \frac{\Delta_g}{a + [\Delta_s \phi(t_g, t_s) - a]\, e^{-\Delta_g t_g}} \\ \phi(t_g, t_s) &= \frac{\Delta_s}{b + [\Delta_g f(t_g, t_s) - b]\, e^{-\Delta_s t_s}}. \end{aligned} \tag{2.38}$$

The comparison between the numerical and analytical results are plotted in Fig. 2.6, which shows good agreement between the two methods.

Chapter 3

Phenotypically heterogeneous populations in spatially heterogeneous environments

A version of this chapter is submitted to Physical Review Letters as: P. Patra and S. Klumpp, Phenotypically heterogeneous populations in spatially heterogeneous environments (2013).

Abstract

The spatial expansion of a population in a non-uniform environment may benefit from phenotypic heterogeneity with interconverting subpopulations using different survival strategies. We analyze the crossing of an antibiotic-containing environment by a bacterial population consisting of rapidly growing normal cells and slow-growing, but antibiotic-tolerant persister cells. The dynamics of crossing is characterized by mean first arrival times and is found to be surprisingly complex. It displays three distinct regimes with different scaling behavior that can be understood based on an analytical approximation. Our results suggest that a phenotypically heterogeneous population has a fitness advantage in non-uniform environments and can spread more rapidly than a homogeneous population.

3.1 Introduction

The development of populations of cells or organisms depends not only on these organisms themselves, but also on their interactions with competing populations and with their environment. Specifically, the spatial structure of the environment can play an important role, for example by separating populations or providing barriers to the spreading of a species [14, 123]. Recently, experimental techniques such as microfluidic habitats [56, 137] and range expansion of microbial populations on plates [38, 41, 64] and complex interactions between multiple species [104] have been used to study the influence of spatial structures in a quantitative fashion using microbes (bacteria or yeast) as model organisms. For example, it has been shown that spatial heterogeneity (different drug concentrations in different organs or concentration gradients for locally administered drugs [6, 12, 92]) can both speed up and slow down the emergence of antibiotic resistance in bacteria [35, 42, 43, 52].

Another aspect of microbial survival under stressful conditions is phenotypic heterogeneity [19, 113], i.e. different behaviors (e.g. normal growth, sporulation, competence, persistence) exhibited by genetically identical cells under identical conditions, a feature usually attributed to multistability in the underlying genetic circuitry. A prime example of phenotypic heterogeneity is bacterial persistence, phenotypic tolerance to antibiotics [4, 19, 71, 72, 75]. A subpopulation of cells is tolerant against antibiotics or other stresses and allows prolonged survival of the population under such conditions. The cells switch stochastically between the normal and the persistent phenotype, thus after the stress is removed, the population can grow back from the surviving persisters (in contrast to resistant mutants, the re-grown population remains susceptible to the antibiotic). Persistence has thus been characterized as a bet-hedging strategy, optimal for survival in fluctuating environments [67–69].

In this letter, we address a related problem, namely the role of persisters in the spatial expansion of a bacterial population. The basic idea is that just as persisters allow a population to live through times of stress, they also allow the population to cross regions in space in which the conditions are stressful. Specifically, we consider the case of a population of bacteria expanding from a growth-sustaining environment into another one that is separated from the first by an environment with a high antibiotic concentration (Figure 3.1). We calculate the average time it takes for the cells to reach the third environment and determine the conditions under which the presence of persister cells is beneficial by speeding up the arrival. This dynamics is surprisingly complex with several distinct regimes, which we identify by a combination of simulations and an analytical theory. We conclude the paper with some remarks concerning possible experiments and an analogy to the crossing of valleys in fitness landscapes.

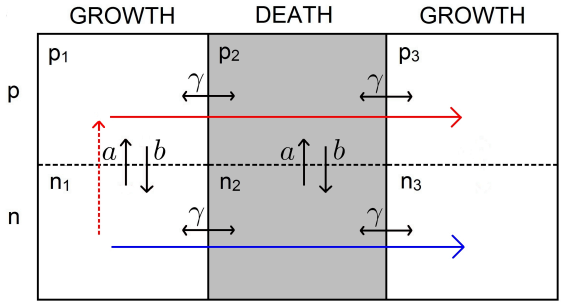

FIGURE 3.1: Model for phenotype switching and migration in three connected micro environments (patches): Bacteria switch between two phenotypic states, normal cells (n_i) and persisters (p_i) with rates a and b and migrate to a neighbouring patch with rate γ. While the first and third patch sustain growth of the population, the second patch contains antibiotics and does not allow for growth. Growth and death rates are phenotype dependent: persisters grow more slowly but survive longer in patch 2. The red and blue arrows shows the two paths via which a cell can arrive in the third patch.

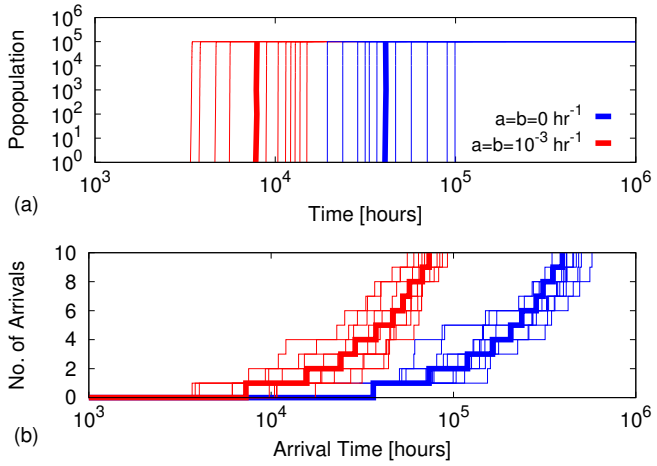

FIGURE 3.2: Population dynamics in the third patch with (red) and without (blue) phenotype switching: (a) Time dependent population size and (b) number of cells that have arrived in the third patch. The rates are $\mu_n = 2$ hr^{-1}, $\mu_p = 0.2$ hr^{-1}, $\delta_n = 4$ hr^{-1}, $\delta_p = 0.4$ hr^{-1} as measured for E. coli cells [4] and $\gamma = 3.2 \times 10^{-5}$ hr^{-1} , $K = 10^5$. The thin lines are individual simulations and the thick lines are averages of several trajectories.

3.2 Model

We consider a population with two phenotypes (normal and persisters) in an environment consisting of three connected patches (Figure 3.1). The numbers of normal cells and persisters in patch $i = 1, 2, 3$ are denoted n_i and p_i. The first and third patch sustain growth, described as logistic growth with rates μ_n and μ_p, respectively, and carrying capacity K. The middle patch contains antibiotics, therefore cells migrating into this patch are killed, with death rates, δ_n and δ_p, and $\delta_p < \delta_n$. Cells migrate between

the patches with rate γ, which we take to be independent of phenotype. Switching between the phenotypes is described by rates a and b (normal to persister and vice versa, respectively). These rates are taken to be independent of the environment.

Simulation results. We simulated this model and determined the time after which the first cell crosses the antibiotic-containing environment and arrives in the third patch. In a competitive situation [64], a population that arrives faster will obviously have a fitness advantage compared to other populations. One may expect that the slowly dying persister cells can cross a region of high antibiotic concentration more easily and hence might speed up the population expansion in such a heterogeneous environment. Figure 3.2 shows results of simulations with realistic growth, death and switching rates that start with a single normal cell in the first patch. Indeed, a population with persisters (red) arrives faster in the third patch than a population without persisters (blue). One also sees that on the time scale on which cells cross the antibiotic barrier, growth in the third patch is very rapid, so it is fully populated by the offspring of the first arriving cell.

For a systematic study, we next vary the migration rate γ. For simplicity, we assume for the moment that only persisters arrive in the third patch ($\delta_p \ll \delta_n$). Surprisingly, the dependence of the mean first arrival time (MFAT) on γ is quite complex (Figure 3a). For small γ, the MFAT decreases as $1/\gamma^2$, as one might guess, because two migration steps are required to reach the third patch; but for intermediate and large γ, it scales as $1/\gamma$ and $1/\gamma^{1/2}$, respectively. In the following, we use an analytical approximation to obtain a better understanding of these observations.

3.3 Growth dynamics in the first patch.

Typically growth in the first patch will be rapid compared to phenotype switching [4] and migration [43]. Therefore, the population in the first patch can be described by the steady state of the deterministic equations,

$$\begin{aligned}\dot{n}_1 &= \mu_n \left(1 - \frac{n_1 + p_1}{K}\right) n_1 - a n_1 + b p_1 - \gamma(n_1 - n_2) \\ \dot{p}_1 &= \mu_p \left(1 - \frac{n_1 + p_1}{K}\right) p_1 + a n_1 - b p_1 - \gamma(p_1 - p_2).\end{aligned} \tag{3.1}$$

The steady state can be solved exactly [98], but here two limiting cases are sufficient. If migration is slow compared to phenotype switching ($\gamma \ll a, b$), the total population in the first patch is given by the carrying capacity K and the subpopulations are determined

by a balance of phenotype switching,

$$n_1 \approx K\frac{b}{a+b}, \quad p_1 \approx K\frac{a}{a+b}. \tag{3.2}$$

For fast migration ($\gamma \gg a, b$), expansion of the exact result leads to

$$n_1 \approx K, \quad p_1 \approx K\frac{a\mu_n}{(\mu_n - \mu_p)\gamma}. \tag{3.3}$$

In this case, the balance of processes increasing and decreasing the population is different. Cells of both phenotypes are lost by emigration. Because normal cells grow more rapidly, the emigrants are quickly replaced by normal cells, while the persister population is replenished by "one-way" phenotype switching (with rate a) from the normal cells. This situation is reminiscent of the population balance in an exponentially growing population [97].

3.4 Migration through the second patch

Next, we consider the dynamics of the number m ($= n_2$ or p_2) of cells in the second patch. This number is typically small, so a stochastic description is necessary. To this end, we neglect phenotype switching in the second patch, so we can consider the migration of normal cells and persisters separately (we therefore drop the indices p and n in that calculation). The MFAT of a cell in the third patch can be calculated by adapting a method that was used recently for the related problem of mutation and migration [42, 43]. We define P_m as the probability that at time t no cell has yet migrated to the third patch and there are m cells in the second. The master equation for this probability is given by

$$\frac{dP_m}{dt} = -(\lambda + \delta' m + \gamma m)P_m + \lambda P_{m-1} + \delta'(m+1)P_{m+1} \tag{3.4}$$

with initial condition $P_0(t = 0) = 1$. Here $\lambda = N\gamma$ is the rate of immigration from the first patch (with population size N, assumed to be constant and specified below), $\delta' = \delta + \gamma$ is an effective death rate, into which we have absorbed backward migration. The master equation can be solved [98] via the moment generating function $G(s,t) = \sum_0^\infty s^m P_m(t)$, which is obtained as

$$G(s,t) = \exp\left[\frac{\lambda}{\delta'+\gamma}\left(s - \frac{\delta'}{\delta'+\gamma}\right)\left(1 - e^{-(\delta'+\gamma)t}\right)\right] \times \exp\left(-\frac{\lambda\gamma}{\delta'+\gamma}t\right). \tag{3.5}$$

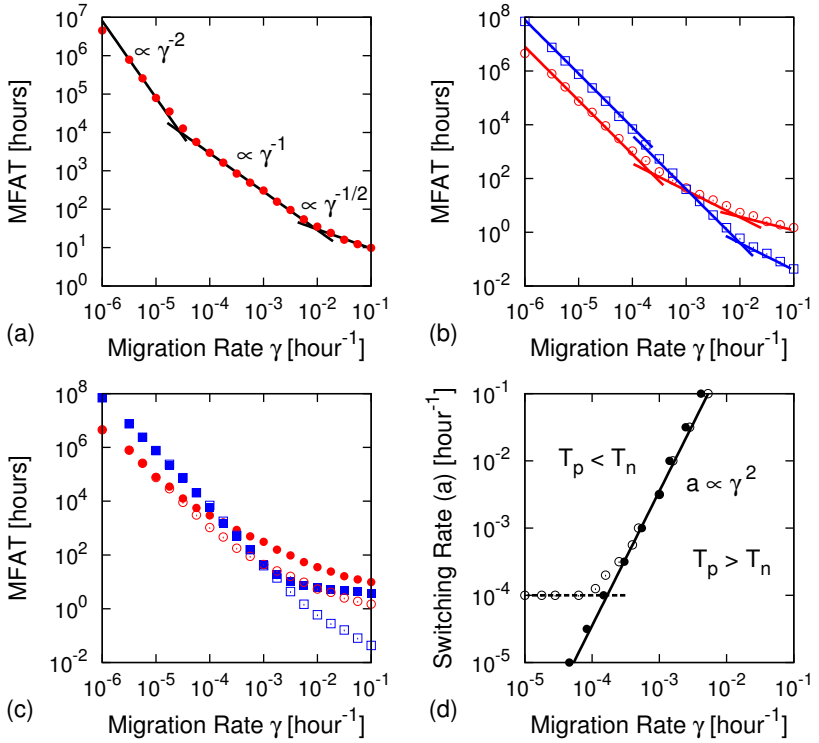

FIGURE 3.3: Mean first arrival time (MFAT) in the third patch: (a) The MFAT of persisters as a function of the migration rate γ displays three different scaling regimes. (b) MFAT for normal cells (blue) and persisters (red) as obtained from simulations (symbols, starting with a fully populated first patch) and our analytical approximations for the three regimes (lines). (c) Comparison of simulations starting with a single cell (filled symbols) and with a fully populated first patch (open symbols). (d) Regions of first arrival of persisters and normal cells in the space of migration and switching rates. The parameters are the same as in Figure 3.2, and $a = b = 10^{-4}\ hr^{-1}$.

The net probability that no cell has migrated yet to the third patch at time t is given by $\sum P_m(t) = G(1,t)$ and the MFAT by $T = \int_0^\infty G(1,t)dt$. There are again two distinct limits, depending on whether migration is fast or slow compared to cell death in the second patch (indicated by indexes 'f' and 's', respectively).

For $\lambda\gamma = N\gamma^2 \ll (\delta' + \gamma)^2$, i.e. slow migration, we obtain

$$T_s \approx \int_0^\infty \exp\left[-\frac{N\gamma^2 t}{(\delta' + \gamma)}\right] dt \approx \frac{\delta' + \gamma}{N\gamma^2} \approx \frac{\delta}{N\gamma^2} \tag{3.6}$$

and for fast migration, $N\gamma^2 \gg (\delta' + \gamma)^2$, the MFAT can be approximated by

$$T_f \approx \int_0^\infty \exp\left[-\frac{N\gamma^2}{2}t^2\right] dt = \frac{1}{\gamma}\sqrt{\frac{\pi}{2\,N}}. \tag{3.7}$$

In this limit, the MFAT T_f is independent of the death rate because the cells move quickly through the second patch.

MFAT of Persister cells. The MFAT for persisters and normal cells can now be obtained by combining, Eqs. (3.7) and (3.6) with the population sizes in the first patch given by Eqs. (3.2) and (3.3). We first consider again the case that only persisters can reach the third patch (δ_n very large). The three regimes seen in Figure 3.3(a) can now be understood as reflecting the three different time scales for phenotype switching, migration, and cell death: In the first regime (T_1), migration is the slowest process, slower than phenotype switching and cell death, $\gamma \ll a, b \ll \delta_p$, so the population size is given by $N = p_1$ with p_1 from Eq. (3.2) and the MFAT by Eq. (3.6). A second regime (T_2) is obtained when migration is rapid compared to phenotype switching, but slow compared to cell death, $a, b \ll \gamma \ll \delta_p$. In this case, T_s from Eq. (3.6) is combined with the persister population size from Eq. (3.3). In the third regime (T_3), migration is rapid compared to both switching and cell death [1]. We thus obtain

$$T_{p,1} \approx \frac{(a+b)\delta_p}{aK\gamma^2}, \quad T_{p,2} \approx \frac{(\mu_n - \mu_p)\delta_p}{a\mu_n K\gamma} \quad \text{and} \quad T_{p,3} \approx \sqrt{\frac{\pi(\mu_n - \mu_p)}{2\,Ka\,\mu_n\gamma}} \tag{3.8}$$

corresponding to the three scaling regimes discussed above.

MFAT of normal cells and of the total population. In general, the death rate δ_n of normal cells is finite, and therefore normal cells also have a chance to reach the third patch. We thus repeat the analysis using the population size expressions for normal cells. Here, the first and second regime both display the same $1/\gamma^2$ scaling, but with different prefactors, $T_{n,1} \approx (a+b)\delta_n/(bK\gamma^2)$ and $T_{n,2} \approx \delta_n/(K\gamma^2)$. In the third regime, our approximation leads to $T_{n,3} \approx \gamma^{-1}\sqrt{\pi/2K}$. Our analytical expressions for both normal cells and persisters are in quantitative agreement with the simulation results if we start our simulations with a fully populated first patch (Figure 3b). If we start simulations with a single cell in patch 1 as above and if γ is large, the first arrival to the third patch can happen before the steady state in the first patch is reached. Thus the MFAT in the third regime is longer than in simulations starting with a fully populated first patch (Figure 3c, open and filled symbols, respectively). In this case, the MFAT is limited by the exponential growth and the γ^{-1} scaling in regime 3 is not seen [2].

The MFAT for the population as a whole is given by the MFAT of the subpopulation that arrives first. In the rapid migration regime, the MFAT is independent of the death rate, so the normal cells arrive faster due to their larger number. In this regime, there is no benefit due to the presence of persisters. For slow migration, however, persisters arrive first, and the MFAT for the whole population is given by $T_{p,1}$. Clearly, if persister cells

[1] In principle, a fourth regime with $\delta_p \ll a, b \ll \gamma$ is possible, but measured parameter values [4, 71] indicate $a, b < \delta_p$.

[2] The MFAT for persisters displays the same scaling with γ, but with a larger prefactor [98].

arrive faster than normal cells, the phenotypic splitting of the population is a beneficial strategy. In this regime, the ratio of the arrival times of persisters and normal cells is $T_{p,1}/T_{n,1} = (\delta_p/\delta_n) \times b/a$. Compared to a population without persisters, the arrival time is reduced f-fold with

$$f \equiv \frac{T_{n,1}(a=0)}{T_{p,1}} \approx \frac{\delta_n}{\delta_p} \times \frac{a}{a+b}. \tag{3.9}$$

Thus the fold-reduction in the arrival time of the population by the presence of persisters is given by the ratio of the death rates of the two subpopulations times the persister fraction in a *stationary-phase* population. We note that while persister fractions are typically very small in exponentially growing populations, they can reach up to 10–50% in stationary phase [71].

Things are more complex in the middle regime, where the crossover between persister-dominated migration and normal-cell dominated migration to the third patch is expected to occur. Because of the different death rates, the two cell types enter this regime at different values of γ, so several different crossover scenarios are possible. In Figure 3.3(d), we plot the regions in the parameter space (a, γ) in which persisters or normal cells arrive first in the third patch, respectively. The boundary separating distinct region is found to be given by $a \propto \gamma^2$ with the assumption that the two switching rates are equal ($a = b$, filled symbols). Persisters are faster and thus beneficial to the population for migration rate smaller than this limiting value. If we take b as constant and vary a (open symbols), there is another limiting condition: For persisters to arrive more rapidly, a/b must not be smaller than the ratio of the death rates δ_p/δ_n.

3.4.1 Dynamics with multiple antibiotic patches.

The competitive advantage of populations with persisters is further enhanced if there are multiple antibiotic patches in between two growth sustaining patches (Figure 4). In the case of M antibiotic-containing patches, the MFAT to patch $(1 + M + 1)$, which supports growth, can be estimated as

$$T_N(M) \approx \frac{\delta'}{\gamma^2} \sum_1^M \frac{1}{N_j} \approx \frac{\delta'}{N_1 \gamma^2} \frac{(\delta'/\gamma)^M - 1}{(\delta'/\gamma) - 1}, \tag{3.10}$$

where N_j $(= p_j, n_j)$ is the average population $(= N_{(j-1)}\gamma/\delta'$, for slow migration) in the jth patch and δ' is the effective death rate in the antibiotic patches.

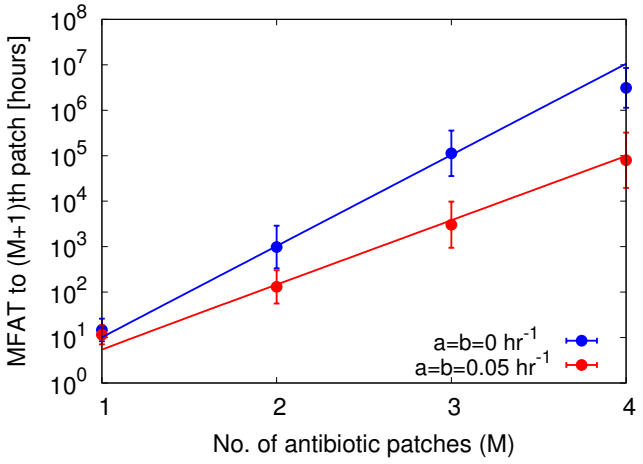

FIGURE 3.4: Multiple antibiotic patches: MFAT of the population with and without phenotype switching for different numbers (M) of antibiotic patches ($\gamma = 0.01, \mu_n = 2, \mu_p = 0.2, \delta_n = 1, \delta_p = 0.2$ (all in hr^{-1}), K= 10^3). The lines are from Eq. (3.10).

3.5 Concluding remarks

In this letter, we have studied the effect of phenotypic heterogeneity in a population expanding in a spatially heterogeneous environment with regions in which normal cells die rapidly due to the presence of antibiotics. We have calculated mean first arrival time and found that the presence of drug-tolerant persister cells is beneficial for slow migration, as it allows the population to cross regions of high antibiotic concentration. To some extent, this effect can be interpreted as mapping the better-studied scenario where the environment fluctuates in time and the persisters allow the population to survive times of stress to a spatial structure. However, the dynamics is unexpectedly complex with several different regimes.

Our simple model suggests a novel role of phenotypic heterogeneity, the help in spatial expansion of a population in a heterogeneous environment. Such heterogeneous environments with high and low drug concentration are likely present in the body during treatment [6, 12, 92]. In addition, such environments can be realized experimentally using microfluidic devices [56, 137] or growth on plates, which have recently been used to study range expansion of populations [41]. The benefit of persisters could be studied by comparing the expansion of normal strains, with mutants having higher [88] or lower [79] persister fractions.

Finally, we want to mention, that the present problem is closely related to mutational pathways containing so-called 'fitness valleys' [92, 106, 132]. To apply our analysis to that case, migration through real space has to be replaced by migration through genotype

space, and γ is interpreted as the mutation rate. The case studied here corresponds to one in which a single mutation leads to lower fitness, but two mutations increase fitness. In such scenario, a population with persister cells can thus more easily cross a fitness valley, which otherwise would, for example, slow down the emergence of antibiotic resistance [35].

Chapter 4

Interplay between Population Dynamics and Drug Tolerance of *Staphylococcus aureus* Persister Cells

A version of this chapter is published as: S. Lechner, P. Patra, S. Klumpp, and R. Bertram, Interplay between population dynamics and drug tolerance of *Staphylococcus aureus* persister cells, J. Mol. Microbiol. Biotechnol. **22**, 381-391 (2012).

Online version: `http://dx.doi.org/10.1159/000346073`

Abstract

Population dynamics parameters of *Staphylococcus aureus* strain SA113 were quantified based on growth and killing experiments with batch culture cells in rich medium. Eradication kinetics and the concomitant isolation of a subpopulation of drug-tolerant SA113 persisters upon treatment with super-minimal inhibitory concentrations of antibiotics such as ciprofloxacin, daptomycin, and tobramycin served as a basis for mathematical analyses. According to a two-state model for stochastic phenotype switching, levels of persister cells and their eradication rates were influenced by the antibiotics used for isolation, clearly indicating a heterogeneous pool of *S. aureus* persisters. Judging from time-dependent experiments, the persisters' degree of drug tolerance correlated with the duration of antibiotic challenge. Moreover, cross-tolerance experiments with cells consecutively treated with two different antibiotics revealed that multi-drug tolerance is not a necessary trait of *S. aureus* persisters isolated by antibiotic challenge. In some cases, the results depended on the order of the two antibiotic treatments, suggesting that antibiotic tolerance may be achieved by a combination of preexisting persisters and an adaptive response to drug exposure. Counts of live cells which had endured drug treatment increased only after lag phases of at least 3 h after the shift to non-selective conditions. Thus, this study provides quantitative insights into population dynamics of *S. aureus* persisters with regard to antibiotic challenge.

4.1 Introduction

Bacterial persister cells are dormant variants of regular cells that neither grow nor die in the presence of bactericidal compounds. Since persisters make up a small fraction within a culture dominated by isogenic sibling cells, the persister state is a paradigm of bacterial phenotypic heterogeneity [19, 124]. Wiuff et al. [133] noted that a decrease in the overall bacterial mortality of a culture upon antibiotic challenge could be attributed to drug-tolerant persisters. Our present understanding of the heterogeneous response to antibiotics within a genetically uniform population is predicated on studies addressing persistence on two different levels of description. One type of studies asks for the regulatory network motifs that enable the coexistence of persistent and non-persistent cells. Positive feedback loop-mediated bistability and threshold amplification of intracellular regulatory noise were identified as critical for bacterial persistence [2]. Genes associated with altered persister levels clearly point towards toxin- antitoxin systems as a prime instance [15, 55, 79, 88, 110, 127]. On a population scale, a mathematical analysis defined the important parameters that control the dynamics of the normal and persistent subpopulations to calculate switching rates between the two phenotypes [33]. Two types of persisters can be discriminated dependent on whether or not a triggering signal to enter the dormant state is required [2, 4, 19, 33]. Whereas the level of type I persisters increases at the onset of stationary growth phase, type II persisters appear to be formed continuously, irrespective of environmental stimuli [4, 19, 32, 33, 67]. It seems that not one single mechanism is responsible for persister formation, but instead, the activation of different stress modules results in growth arrest, and various different genetic pathways may converge towards persistence [1, 19]. The change between the dormant and the growing state is a hallmark of persister cells [11, 33, 48]. In variable environments, phenotype switching provides a bet-hedging strategy that has been proposed to be superior to sensing as an adaptive mechanism to ensure the population's survival [67, 68]. The exit of bacteria from dormancy may be triggered by extracellular compounds [26, 90] or in a stochastic manner [11] and may be accompanied by specific lag-phases during the resuscitation process [33, 48]. Although the persister state was described for staphylococci more than 65 years ago [7], only few studies addressed persisters in this genus so far [55, 87, 111, 112]. Keren et al.[55] conjectured that a stationary culture might exclusively consist of persisters, whereas we found that the pool of stationary phase *Staphylococcus aureus* cells represents a mixture of persisters and drug-susceptible cells [71]. Upon aminoglycoside treatment, selection of persister and small colony variant (SCV) cells, representing another and possibly related dormant form of bacteria, was observed [133]. *S. aureus* SCVs frequently have genetically manifested defects in their electron transport chain or auxotrophies for hemine, menadione, or thymine (reviewed by [101]). Most SCVs are inherently tolerant to aminoglycosides [130], and are capable

of switching between the normal and the small colony phenotype, even during the course of an infection [82, 125]. Based on our previous work on the identification of conditions for *S. aureus* persister isolation [71], the present study aims at providing parameters of population dynamics for *S. aureus* cells grown in liquid culture and challenged by antibiotics. We analyzed persisters that were isolated by treatment with various antibiotics for cross-tolerance and resuscitation dynamics. Growth, death and switching rates of normal and persister cells were calculated, and subpopulation fractions of these cell types were defined. Our results demonstrate that the choice of antimicrobial compounds applied for isolating drug-tolerant *S. aureus* persisters is critical for the behavior of the population. The observed dependence on the choice of antibiotics suggests that there may be multiple types of persisters with complex patterns of cross-tolerance and that the response of the population to antibiotic challenge may be due to a combination of selection for preexisting persisters and an adaptive response.

4.2 Results and Discussion

To provide a basis for modeling of staphylococcal persister dynamics, we first revisited key results described in our previous study on *S. aureus* persisters [71]. Therein, a number of *S. aureus* strains and mutants had been challenged with various antibiotics applied at different magnitudes of the minimal inhibitory concentration (MIC; 1-fold, 10-fold and 100-fold) at exponential or stationary growth phase, and bacterial killing had been monitored over time.

4.2.1 Mathematical Analysis of Killing Curves Indicates the Existence of Multiple *S. aureus* Persister Types

Antibiotic treatment experiments indicated a variety of dynamic behaviors of *S. aureus* cells of an isogenic inoculum in a common batch culture reflected by different killing kinetics. Eradication of exponential phase cells had frequently been biphasic, as expected in the presence of two different subpopulations, normal cells and persisters [71]. We here analyzed mathematically the killing dynamics observed with the antimicrobials tobramycin, which inhibits translation, ciprofloxacin, which corrupts the function of topoisomerase, or daptomycin, which targets the cell envelope. A model for phenotype switching (defined by Eq. 4.1 in 'Methods') was applied that describes isolation of preexisting persisters by these antibiotics. To that end, killing curves of different experiments using strain SA113 were fitted with a double-exponential expression (Eq. 4.2) to obtain killing rates of the two subpopulations and the initial fraction of persister cells (

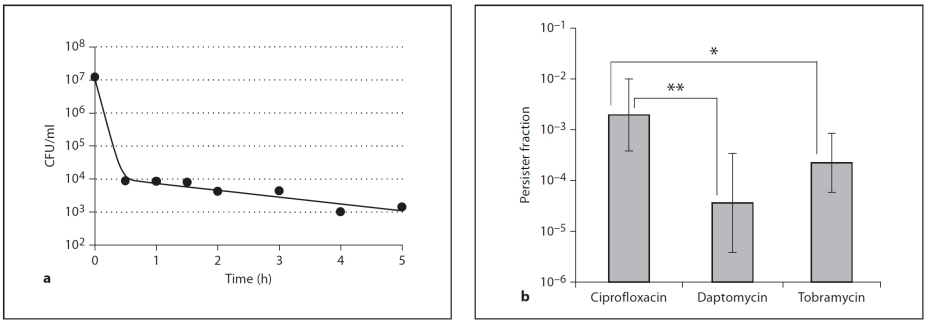

FIGURE 4.1: Fitting of killing curves. (**a**) Example of a measured killing curve (data points, for strain SA113 taken from exponential growth phase and treated with 100-fold MIC of tobramycin) and a double-exponential fit to it (solid line). Fits like this one were performed for individual experiments and the resulting parameters averaged over repeat experiments to obtain the parameters given in Table 4.1. (**b**) Initial persister fractions (i.e. fraction of persisters present in the population at the time of addition of the drug) obtained from the fits based on values obtained with ciprofloxacin (100-fold MIC), tobramycin (100-fold MIC) and daptomycin [10-fold MIC; mean plus standard deviation of $log(p_0/n_0)$, see Table 4.1]. Differences were found to be significant between ciprofloxacin and daptomycin (** p = 0.01) and ciprofloxacin and tobramycin(*p = 0.045).

TABLE 4.1: Parameters obtained from the fitting of killing curves.

Antibiotic	Conc. in MIC	No. of exp.	Death rate of normal cells $\mu_n^{(AB)}(h^{-1})$	Death rate of persister cells $\mu_p^{(AB)}(h^{-1})$	Fraction of persisters $log_{10} f_0$	Switching rate:n→p $a(h^{-1})$
Ciprofloxacin	10	3	-6.96 ± 0.20	-0.55 ± 0.12	-3.22 ± 0.21	7.4×10^{-4}
	100	6	-4.37 ± 1.62	-0.56 ± 0.20	-2.71 ± 0.71	2.4×10^{-4}
Rifampicin	10	3	-7.05 ± 2.47	-0.81 ± 0.36	-2.62 ± 1.13	2.9×10^{-3}
Tobramycin	10	3	-9.87 ± 1.66	-0.14 ± 0.08	-3.83 ± 0.26	1.9×10^{-4}
	100	6	-13.65 ± 4.82	-0.32 ± 0.22	-3.65 ± 0.58	2.8×10^{-4}
Daptomycin	10	6	-9.31 ± 0.81	-0.55 ± 0.55	-4.44 ± 0.98	4.6×10^{-5}
Dapto/Ca^{2+}	1	3	-3.13 ± 2.18	$+0.22 \pm 0.68$	-2.31 ± 0.31	6.0×10^{-3}

All values are for strain SA113, mean ± standard deviation from three(1) or six(2) experiments as indicated. Calculations are based upon results of Lechner et al. [71].

Table 4.1 ; Fig. 4.1). The switching rate from the normal phenotype to the persister phenotype was estimated from the persister fraction. Not surprisingly, the death rates of the two subpopulations depended on the type and concentration of the antibiotic used, as also shown in other bacteria [54, 55, 79]. In addition, considerable variation between the initial persister fractions (and thus the switching rates) was obtained from these fits, which argues against a single preexisting persister subpopulation isolated by the antibiotics, also in agreement with previous reports [1, 133]. In many cases however, the difference between persister levels observed in experiments with two different antibiotics was similar to the variation in persister fraction between repeats of experiments with the same antibiotic. Hence, we tested for the statistical significance of these differences

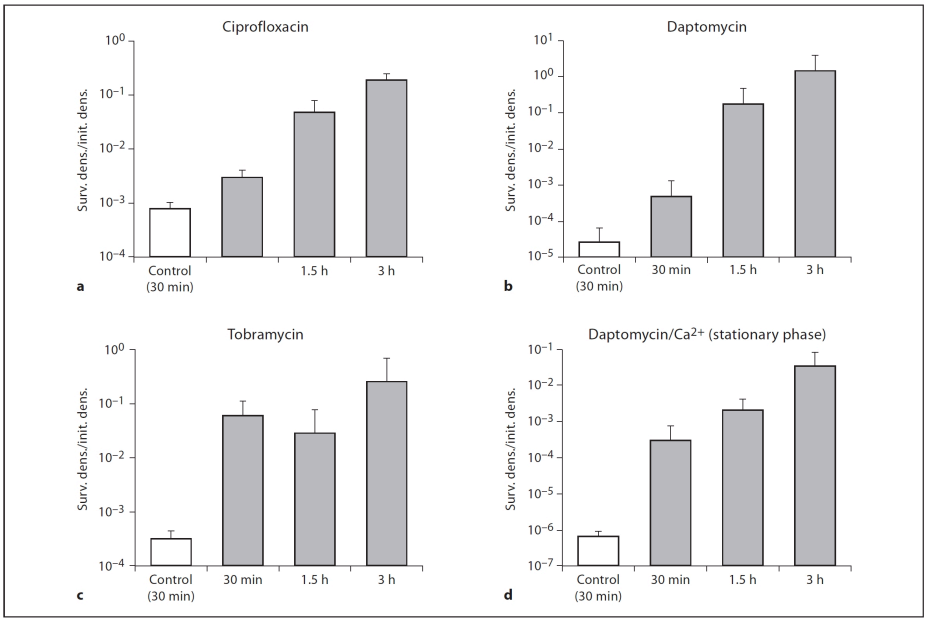

FIGURE 4.2: Recurrent reexposure experiments. Exponential phase SA113 cells were treated with 100-fold MIC of ciprofloxacin (**a**), 10-fold MIC of daptomycin (**b**), or 100-fold MIC of tobramycin (**c**), or stationary phase cells were challenged with 100-fold MIC of daptomycin/Ca^{2+} (**d**). Cells from samples taken after 30 min, 1.5 h, and 3 h were then treated again with the same antibiotic at the same concentration. The values at the y-axis display the log_{10} ratios between CFU counts of surviving cells after 3 h of reexposure and CFU counts of cells prior to reexposure. The values are averages of three replicates, and the error bars indicate standard deviations.

using only experiments that were repeated six times (Fig. 4.1 b). The most striking difference was found between the persister fractions for SA113 cultures that had been treated with ciprofloxacin (100-fold MIC) and daptomycin (10-fold MIC) ($p = 0.01$; Fig. 4.1 b), but the difference between treatment with ciprofloxacin and tobramycin (100-fold MIC) was also found to be significant ($p=0.045$). A dependence of the persister fraction on the drug used to isolate the persisters is not expected for a homogeneous subpopulation of preexisting persisters as assumed in the model of Eq. 4.1. It may however be obtained if the persister subpopulation is heterogeneous with different types of persisters exhibiting tolerance to different antibiotics or if the observed tolerance to the drug involves an adaptive reaction to the drug exposure. The absolute values of the switching rates are in the range of 10^{-5} to 10^{-3} per hour. Previous estimates for the switching rate of *E. coli* upon treatment with ampicillin were in the same range [4], with values for wild-type *E. coli* being slightly lower and values for a high-persistence mutant (hipA7) being slightly higher than in the present study.

4.2.2 Degree of Drug Tolerance of Isolated *S. aureus* Persisters Is Dependent on the Kind and Duration of Antibiotic Treatment

Deduced from our data and from studies in other bacteria [1, 32, 71, 75], an *S. aureus* culture in the logarithmic phase was expected to mainly consist of susceptible cells and a tiny subpopulation of bacteria (that may collectively be classified as type II persisters) which exhibit different degrees of drug tolerance. The addition of an antibiotic should then isolate cells gradually more tolerant over time to yield a population dominated by highly robust persisters. To further corroborate this picture, we performed a test for phenotypic tolerance to antibiotics proposed earlier [133], in which tolerant cells isolated with an antibiotic are reexposed to fresh medium with the same antibiotic. To this end, SA113 cells were treated at exponential growth phase with 100-fold MIC of ciprofloxacin, 10-fold MIC of daptomycin, or 100-fold MIC of tobramycin for 30 min, 1.5 h, and 3 h (primary culture), and the washed pellets were transferred to fresh media supplemented with the identical antibiotics at the same concentration (secondary culture). Cells grown under nonselective conditions in the first culture, but exposed to the respective drugs in the second culture served as controls. The same experiment was also conducted with stationary-phase cells treated with 100-fold MIC of daptomycin/Ca^{2+}. Generally, cells taken from selective primary cultures were more tolerant to the respective antibiotics than naïve cells first grown under antibiotic-free conditions. Killing rates of secondary culture cells exposed to ciprofloxacin or daptomycin were reciprocally correlated with the length of drug exposure in the primary culture (Fig. 4.2 a, b, d), whereas this was not the case for bacteria sampled from tobramycin-containing medium. There, the slower colony-forming unit (CFU) decrease was independent of whether cells in the first culture had been treated with the drug for 30 min or longer (Fig. 4.2 c). Comparable findings were described by Wiuff et al.[133] for *E. coli*. In line with data of our first study [71], killing kinetics of secondary culture cells corroborate the assumption that a highly tobramycin-tolerant pool of persisters was rapidly isolated by 100-fold MIC of the drug. In contrast, sorting of robust persister cells appears to occur rather slowly (within 3 h) after addition of 100-fold MIC of ciprofloxacin or 10-fold MIC of daptomycin. Cells with a lower degree of drug tolerance thus seem to be reprieved from killing at earlier time points. A comparison with the model using the parameters obtained from Table 4.1 indicates that the reexposure experiments led to population sizes that were very similar to what was obtained with continued exposure to that antibiotic (correlation coefficients $R \geq 0.9$). This observation provides further quantitative support for the phenotypic tolerance model used to describe the killing assay above. Within the model, the difference between the antibiotics in the kinetics of persister isolation were mostly due to the death rate of the susceptible cells, which was significantly higher for tobramycin at 100-fold MIC than for the other two conditions (Table 4.1).

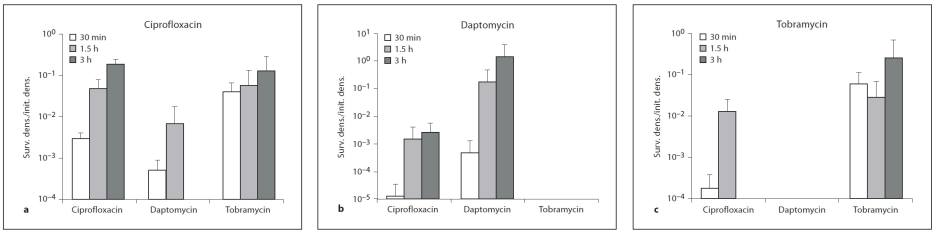

FIGURE 4.3: Cross-tolerance experiments. Exponential phase SA113 cells pretreated with one antibiotic for different periods of time (30 min, 1.5 h, and 3 h, as indicated at abscissa) were reexposed to a different kind of drug: 100-fold MIC of ciprofloxacin (**a**), 10-fold MIC of daptomycin (**b**), and 100-fold MIC of tobramycin (**c**). The values at the ordinate display the log 10 ratios between CFU counts of surviving cells after 3 h of reexposure and CFU counts of cells prior to reexposure. Values given for identical antibiotic treatments at first and second exposures resemble those in Fig. 4.2. Note that no colonies were observed when cells were treated consecutively with tobramycin and daptomycin in either order. The values are averages of three to four replicates, and the error bars indicate standard deviations.

4.2.3 Mono- and Multi-Drug Tolerance Is Not Necessarily Correlated in *S. aureus* Persisters

The analysis of the eradication experiments suggested that there may not be one single persister phenotype, but several types of dormant cells in different physiological states and with different patterns of drug tolerance, consistent with the model of Allison et al. [1]. To shed further light on possible differences in drug tolerance among a pool of persisters, cultures were again exposed to one antibiotic for 0.5-3 h, but now cells were subsequently challenged by a different drug for an additional 3 h. Cross-tolerance was assumed when a similar or greater number of bacteria recovered after treatment with the second antibiotic compared to recurrent reexposure to the same drug. Results shown in figure 3 demonstrate that cross-tolerance was usually not observed, with the exception of cells treated first with tobramycin and second with ciprofloxacin (Fig. 4.3 a). For a quantitative analysis, the two-phenotype model of persisters was extended towards including multiple persister phenotypes, falling into three categories: (1) tolerant to the first antibiotic but not to the second; (2) tolerant to the second but not to the first, and (3) tolerant to both antibiotics. To account for the biphasic nature of the observed killing curves for single antibiotics (as compared to more complex dynamical behavior that would be possible in models with several types of persisters), all cells susceptible to an antibiotic were assumed to be killed with the same rate as the normal cells. This assumption fixed all parameters of the model except the relative frequencies of the different types of persisters in the population. Figure 4 shows killing curves predicted from the extended model for the combination of three antibiotics and several scenarios. In case of full cross-tolerance (solid lines), as expected for a single type of persisters, the killing rate is abruptly switched upon exchange of the antibiotic to that of persisters

under the influence of the second antibiotic. In the complete absence of cross-tolerance, which is obtained if there are two mutually disjunct persister populations for the two antibiotics, rapid eradication with a rate similar to killing of susceptible cells is expected after the exchange of antibiotics (dotted lines). Finally, partial cross-tolerance with a fraction of persisters tolerant to both antibiotics results in biphasic killing upon antibiotic exchange (dashed lines). The data for daptomycin and tobramycin (Fig. 4.4 e, f) clearly showed no cross-tolerance, as expected for two disjunct subpopulations constituted by persisters tolerant to either tobramycin or daptomycin. This in agreement with our previous observations, when stationary-phase bacteria had been killed completely upon simultaneous addition of both daptomycin and tobramycin at super-MICs [71]. In the cross-tolerance experiments of either antibiotic with ciprofloxacin (Fig. 4.4 a-d), however, the order in which the antibiotics are applied was found to be crucial. This observation suggests that the behavior of the isolated persisters was influenced by the challenge with the first antibiotic and is inconsistent with models that assume preexisting tolerant subpopulations, neglecting any response to the antibiotic challenge. It also indicates that care must be taken to separate cellular responses due to the antibiotic treatment from those characteristic for persisters, which underscores that methods for persister isolation should be as gentle as possible to obtain unstressed (ideally naïve) persisters for further characterization [50, 53, 110].

4.2.4 Delay in Resuscitation and Subsequent CFU Doubling Times Are Dependent on the Kind and Duration of Antibiotic Treatment

How long do *S. aureus* persisters, which have endured antibiotic treatment, require to reassume growth, and what are the CFU doubling times within the first hours after resuscitation? To answer these questions, SA113 cells were challenged by single drugs for 0.5-3 h, and were then transferred to fresh non-selective media. Cells treated with 100-fold MIC of ciprofloxacin exhibited a consistent increase in live counts approximately 4 h after the shift to fresh media (Fig. 4.5 a). Resulting cultures exhibited relatively similar CFU doubling times (calculated on the basis of t = 10 h and t = 5 h values) ranging between 43 and 67 min, irrespective of the duration of the ciprofloxacin pretreatment. CFU values of cells challenged with 10-fold daptomycin also increased rather uniformly (23 - 33 min doubling times) starting approximately 3 h after the shift (Fig. 4.5 b). By contrast, live counts of cultures treated for 30 min or 1.5 h with 100-fold tobramycin rose after about 3 h, whereas those of cultures challenged with the drug for 3 h remained constant for at least 9 h (Fig. 4.5 c). This is reflected by doubling times of 37 min, 67 min or more than 6 h, respectively. Similar behavior as for the 3-hour exposure to

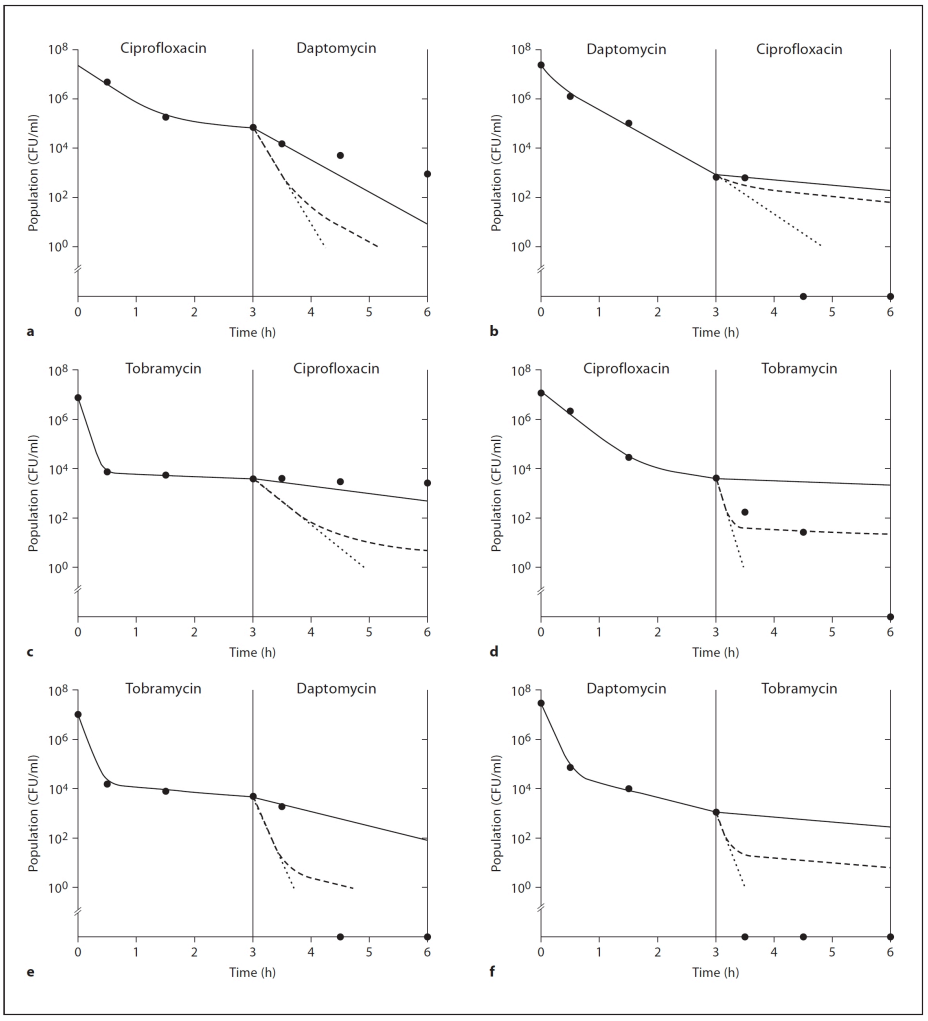

FIGURE 4.4: Model for multiple persister types and cross-tolerance. **a-f** Time course of killing by exposure to one antibiotic for 3 h and to a second antibiotic for the following 3 h. The three lines in each panel indicate model predictions for a case with a single persister phenotype tolerant to both antibiotics (solid line), a case with two types of persisters that are tolerant to one antibiotic each, without any cross-tolerance (dotted line), and a case with partial cross-tolerance or three persister phenotypes (dashed line). In all models, the antibiotics are assumed to select for cells with a preexisting phenotype from a heterogeneous population. The data points indicate measured population sizes (from the experiments of Fig. 4.3).

tobramycin was also observed for stationary-phase cultures treated with 100-fold MIC of daptomycin/Ca^{2+}. As shown in figure 5 d, CFU counts for this case leveled off within 10 h after the cells had been inoculated into fresh medium, but values increased by two to four orders of magnitude after 24 h. Growth resumption in our experiments thus occurred not before 3 h (Fig. 4.5 a-c), in relation to a period of about 1.5 h as deternmined for *E. coli* [33], which, however, depends on the growth medium used [48]. For a quantitative analysis, the results of these experiments were fitted with a double exponential outgrowth model (Eq. 4.3), from which switching rates from the persistent to the regular growing phenotype were obtained (Table 4.2). Consistent with the

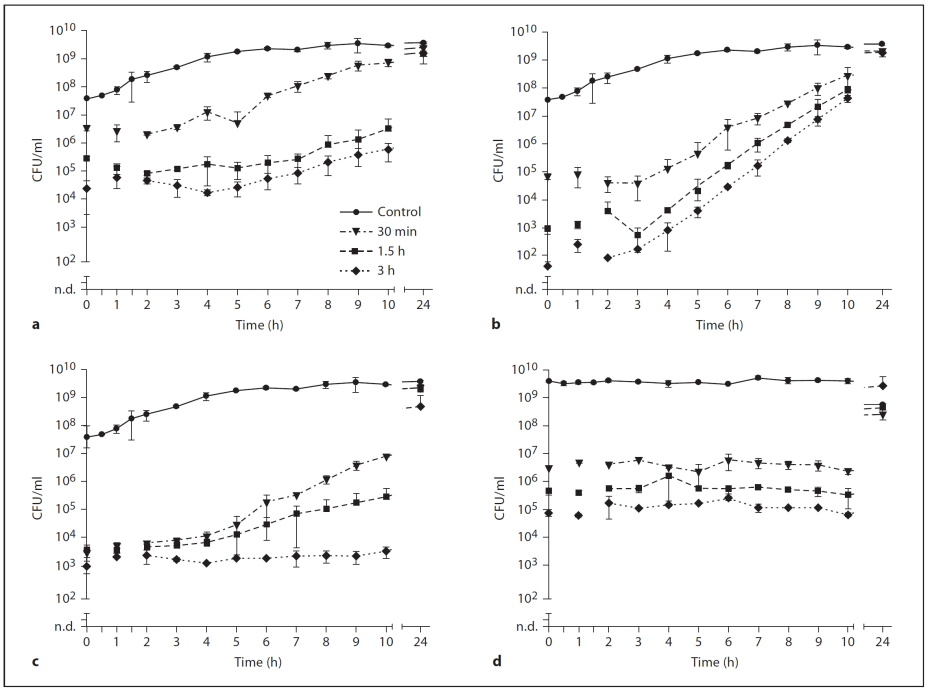

FIGURE 4.5: Resuscitation experiments. Exponential phase SA113 cells were treated with 100-fold MIC of ciprofloxacin (**a**), 10-fold MIC of daptomycin (**b**), or 100-fold MIC of tobramycin (**c**), or stationary phase cells were challenged with 100-fold MIC of daptomycin/Ca^{2+} (**d**). Cells from samples taken after 30 min, 1.5 h, and 3 h were then cultured in fresh medium without antibiotic for 24 h to determine resuscitation times. The values are averages of two replicates, and the error bars indicate standard deviations. The limit of detection was 100 CFU/ml.

observations described above, the parameters obtained for different exposure times to either ciprofloxacin or daptomycin were very similar, while for tobramycin only the two shorter exposure times could be described well with the model. The latter observation suggests that prolonged exposure to tobramycin affects the cells beyond simple random phenotype switching. Instead, it possibly induces a phenotype of 'deep dormancy' (with an as of yet unknown molecular basis) that results in delayed wake-up kinetics. Parameters obtained for the longest exposure time for each antibiotic that is well described by the model are summarized in Table 4.2. For all three antibiotics, the switching rates from the persistent to the regular growing phenotype are in the same range as previously found for *E. coli* persisters [4]. For tobramycin, the switching rate is similar to the killing rate of persisters during antibiotic treatment, consistent with the idea that the observed killing of persisters is due to so-called 'scout' cells, persisters resuming growth stochastically [11]. On the other hand, the switching rates observed using ciprofloxacin and daptomycin are smaller than the killing rates of persisters exposed to these drugs, indicating that these two drugs kill persisters independently of growth resumption. Intriguingly, CFU doubling times of daptomycin-treated cells fell below usual generation times of naive SA113 bacteria (which we determined as approximately 37 min under comparable antibiotic-free conditions) after being shifted to non-selective media (Fig.

4.5 5 b). We attribute this effect to the presence of a fraction of cells that start to proliferate at very late time points on the agar plates (whereas most cells initiate multiplication already in liquid medium). If such cells are missed at early time CFU counts, the population is given an apparent growth boost. It should be noted that the observed results in these resuscitation experiments show striking parallels to the 'post-antibiotic effect' phenomenon. Well established in pharmacodynamics, it describes delayed growth of bacteria after antibiotic treatment [24]. The post-antibiotic effect of *S. aureus* cultures treated with different antibiotics has extensively been studied before. For ciprofloxacin, a delay of 1.5-2.5 h was determined [17]. Cells after tobramycin treatment resumed growth after 6.6-12 h [47]. For daptomycin-treated *S. aureus* cells, Hanberger et al. [39] observed a PAE of 1-6.3 h. Obviously, differences among the studies with regard to different antibiotic concentrations, growth phase, media, strains backgrounds and other variables impede direct comparisons, but we note that time delays in our resuscitation experiments fit well into the window of previously described PAE values for the three drugs. Future studies may more precisely define the possible role of persisters in the PAE.

TABLE 4.2: Parameters obtained from the fitting of resuscitation curves.

Antibiotic	Conc.(MIC) & exposure time[1]	Growth rate of normal cells,$\mu_n(h^{-1})$	Growth rate of persister cells,$\mu_p(h^{-1})$	Fraction of normal cells,$log_{10}f_1$	Switching rate[2]:p→n $b(h^{-1})$
Ciprofloxacin	100, 3h	0.88 ± 0.16	-0.15 ± 0.11	-2.02 ± 0.04	2.1×10^{-2}
Daptomycin	10, 3h	1.84 ± 0.17	-0.57 ± 0.51	-2.7 ± 0.52	1.6×10^{-2}
Tobramycin	10, 1.5h	0.74 ± 0.01	-0.06 ± 0.11	-1.63 ± 0.16	4.0×10^{-1}

All data are for strain SA113, mean ± standard deviation from three repeats.
Calculations are based on results graphically shown in Fig. 4.5 a-c.
[1]Very similar results were obtained for shorter exposure times; 3-hour exposure to tobramycin resulted in different dynamics (Fig. 4.5 c).
[2] Estimated via $f_1 = b/[\mu_p^{(AB)} - \mu_n^{(AB)}]$ using the killing rates measured with the same culture.

4.3 Conclusion

Exploiting rich nutrient media conditions in vitro, we here define switching rates of *S. aureus* cells between growth and the dormant persister state. Upon isolation of persisters by super-MICs of antibiotics, it was observed that the choice of the drug influenced population dynamics of staphylococcal cultures with regard to cross-tolerance to another antibiotic and the behavior of growth resumption. The complex patterns of cross-tolerance indicate the existence of multiple types of persisters and suggest (via the observed dependence on the order of treatment) that adaptive responses to drugs

as well as preformation of dormant subpopulations are involved in persister formation. The quantitative data gathered here provide a basis for more comprehensive studies in the future and for a more refined, molecular-level modeling of *S. aureus* population dynamics in relation to antibiotic challenge. A quantitative understanding of *S. aureus* susceptibility to antibiotics incorporating information about physiologic downshift phenomena such as SCV and persister cells as well as strain background and mutations will help develop tailored antibiotic therapies to treat staphylococcal infections.

4.4 Experimental Procedures

4.4.1 Bacterial Strains, Media, and Culture Conditions

Throughout this study, *S. aureus* SA113 was used [46]. Bacteria were grown at 37°C with aeration in baffle flasks containing tryptic soy broth (Sigma) at a 1:6 culture-to-flask ratio or on tryptic soy agar. Liquid cultures were shaken at 150 rpm. To prepare exponential phase cultures, cells grown overnight were transferred to 16 ml of fresh media to an initial OD_{578} of 0.07 and were shaken for about 1.5 h until an OD_{578} of approximately 0.5 was reached. Overnight cultures were used to work with stationary phase cells. Numbers of viable cells were determined in retrospect by CFU analysis. Therefore, cells from respective cultures were collected, washed and suspended in 1% saline and spotted as 10 μl aliquots of serial dilutions on tryptic soy agar as described [71].

4.4.2 Antibiotics

Daptomycin analytic grade powder (designated 'Cubicin') was purchased from Novartis Pharma. Facultatively, Ca^{2+} cations (50 μg/ml final concentration), provided as $CaCl_2$, were added to daptomycin-treated cultures, to increase antibiotic activity, where indicated. Ciprofloxacin was obtained from Fluka and tobramycin was from Sigma. Solutions of antimicrobials were prepared freshly prior to each application and were sterilized using a filter of 0.2 μm pore size (Whatman).

4.4.3 Reexposure and Resuscitation Experiments

Cells were grown to exponential or stationary phase in baffle flasks under different antibiotic selective conditions (as indicated in the main text and in figure legends) to provide primary cultures. After 30 min, 1.5 h, and 3 h, 2.24 ml samples were withdrawn, cells

were pelleted, washed in 1% saline and transferred to 14-ml tubes which contained 2.24 ml of fresh tryptic soy broth media. The medium of this secondary culture was supplemented with either the same antibiotic at the same concentration as used in the primary culture (in recurrent reexposure experiments), with a different drug to check for cross-tolerance, or antibiotics were omitted to monitor resuscitation. The CFU content was determined 30 min, 1.5 h, and 3 h after addition of the first and second antibiotic, or on an hourly basis for up to 10 h and after 24 h in case of the resuscitation tests. Experiments were conducted at least twice, using two to four biological replicates. Samples from cultures not exposed to antibiotics in the primary culture but subsequently treated in an identical manner in the secondary culture served as controls.

4.4.4 Theoretical Analysis

Killing and resuscitation data were analyzed quantitatively with a model for stochastic phenotype switching by Balaban et al.[4]. It describes a population of cells as consisting of two subpopulations representing persisters (p) and normal cells (n) that exhibit different exponential growth or death rates (μ_n and μ_p). According to this model, cells switch between these two phenotypes with rates a and b, respectively. These rates are assumed to be independent of environmental triggers (type II persisters). The full dynamics of the model is given by

$$\begin{aligned} \frac{d}{dt}n &= \mu_n n - an + bp \\ \frac{d}{dt}p &= \mu_p p + an - bp \end{aligned} \tag{4.1}$$

A shift from a growth medium (with $\mu_n > \mu_p \geq 0$) to a medium containing an antibiotic (for which $\mu_n < \mu_p \leq 0$) is described by a change in the growth/death rate starting from a steady state of Eq. 4.1. It is based on the growth rates from the first medium and results in double-exponential decay of the population:

$$N(t) = n_0 \left[\exp(-\mu_1 t) + f_0 \exp(-\mu_2 t)\right] \tag{4.2}$$

where the three parameters μ_1, μ_2 and f_0 can be identified with the absolute values of the death rates of normal cells and persisters and to the initial fraction of persisters (the fraction of persisters extrapolated to the time of addition of the drug), respectively $[\mu_1 = \mu_n^{(AB)}, \mu_2 = \mu_p^{(AB)}, f_0 = p_0/n_0 \approx p_0/(n_0 + p_0)]$. The latter identification is an approximation for small switching rates between the phenotypes, a condition that is generally valid in our experiments. The three parameters were determined by fitting killing curves with Eq. 4.2. The switching rate from the normal to the persistent phenotype was estimated via $f_0 \approx a/\mu$ (where μ is the growth rate of the population

before the addition of the antibiotic). Each killing experiment was fitted separately, and the resulting parameter values were averaged over three or six repeats (Table 4.1). Fit results for individual experiments were used for the statistical analysis of the difference between experiments with different antibiotics, applying the t test to the logarithm of the persister fraction $\log_{10} f_0$.

For the analysis of cross-tolerance experiments, the model given by Eq. 4.1 was extended to incorporate three types of persisters that are tolerant to only the first, only the second, or both antibiotics, assuming that all non-tolerant cells exhibit the same behavior. Resuscitation curves were also fitted by the same procedure using again a double exponential expression:

$$N(t) = p_0 \left[f_1 \exp(\mu_1^{'} t) + \exp(\mu_2^{'} t) \right] \tag{4.3}$$

The parameters $\mu_1^{'}, \mu_2^{'}$ and $f_1 = n_0/p_0 \approx n_0/(n_0 + p_0)$ correspond to the growth rates of normal and persister cells after the removal of the antibiotic and to the initial fraction of normal cells. The switching rate b from the persistent to the normal phenotype is estimated via $f_1 \approx b/(\mu_p^{AB} - \mu_n^{AB})$. Each resuscitation experiment was fitted separately, and the resulting parameter values were averaged over three repeats (Table 4.2).

4.4.5 Acknowledgements

We thank Tanja Hildebrandt for technical assistance and Friedrich Götz for support. This work was supported by grants within the priority programmes 1316 'Host Adapted Metabolism of Bacterial Pathogens' and 1617 'Phenotypic Heterogeneity and Sociobiology of Bacterial Populations' and by the research training group Graduate College 685 'Infection Biology: Human-and Plant-Pathogenic Bacteria and Fungi' of the Deutsche Forschungsgemeinschaft.

Chapter 5

Role of persisters in antibiotic resistance

Abstract

Bacterial finds numerous ways to survive under adverse environmental conditions which could lead to extinction. Bacterial persistence is one such mechanism where a population generates a fraction of drug-tolerant "persister" cells that survive under antibiotic attacks, and upon removal of antibiotic can switch back to normal cells. Sometimes bacteria also develops antibiotic resistance whereby some cells continue to multiply in the presence of an antibiotic. Emergence of antibiotic resistance from drug tolerant persister cells has not been observed yet. However, several observations point towards this possibility. We observe a biphasic decay behavior, indicating a fast killing and a slow killing phase, in *Staphylococcus aureus* population followed by a growth phase under two antibiotics, rifampicin and tobramycin. To analyze the observations, we extend the two state model for bacterial persistence to a three state model that allows mutations to a resistant state. We find that the probability of mutation is enhanced in presence of persister subpopulation. The time to such mutation first increases then decreases with the increase in persister fraction. In the case when mutants are generated from persister cells, moderate dose of antibiotic will lead to survival and growth, whereas higher dose of will lead to extinction. We observe such dependencies, when the concentration of antibiotic is varied, in a population of *Staphylococcus aureus* cells upon treatment of tobramycin. Our result suggests that persister cell plays a role in the emergence antibiotic resistance, at least, in the case of tobramycin treatment.

5.1 Introduction

Bacterial cells often display diversity in their physiological properties due to variability in cellular processes [19, 25, 69, 74, 121]. Phenotype switching is one such cellular mechanism that generates subpopulations of cells displaying different physiological properties in a constant environment [4, 53]. For example, in *E. coli* population, cells are shown to switch between two phenotypic states, i.e. fast growing 'normal' and slow growing 'persister' state [4]. The slow growing persister cells cause a small fitness cost to a growing population, but ensure longer survival due to their increased tolerance to antibiotics or other environmental stress. During antibiotic treatments, cells often undergo mutations that generate antibiotic resistants and allow growth in the presence of antibiotics [18]. The chance of such mutation is extremely low in a fast dying population as the rate of mutation is usually small. As persister cells survive longer during antibiotic killing, their presence may enhance the probability of resistant mutation.

A requirement for such a scenario is that persisters undergo mutations. In *E. coli* persisters are usually considered as non-replicating cells (or very slowly growing) [75] and thus can undergo mutation in limited ways. However, a recent study on *M. segmentis*, a non pathogenic strain of mycobacteria, showed that the persister cells were dividing as fast as the normal cells before antibiotic treatment and during treatment (but had reduced death rates). The surviving subpopulation during the antibiotic killing was found to be in a dynamic balance between persister subpopulation growth and antibiotic death [131]. The ongoing cell division and DNA replication in the presence of antibiotics may lead to emergence of resistant genetic variants as rate of spontaneous mutation is proportional to the division rate [95]. These results suggest that the persister subpopulation selected by antibiotics which do not affect growth related process in persisters might play a role in the development antibiotic resistance [23, 61, 73, 117]. However, conclusive evidence for this mechanism is still absent.

5.2 Experimental results and motivation

In the systematic experimental characterisation of *Staphylococcus aureus* persister cells, the emergence of antibiotic resistance was observed upon treatment with two different antibiotics (rifampicin and tobramycin [71]). In these cases, the dynamics of the population was triphasic rather than biphasic. In the first two phases, the population decays corresponding to the death of normal cells and persisters, but the population resumes growth in the third phase. The observed triphasic behavior is shown in Figure (5.2,5.1)).

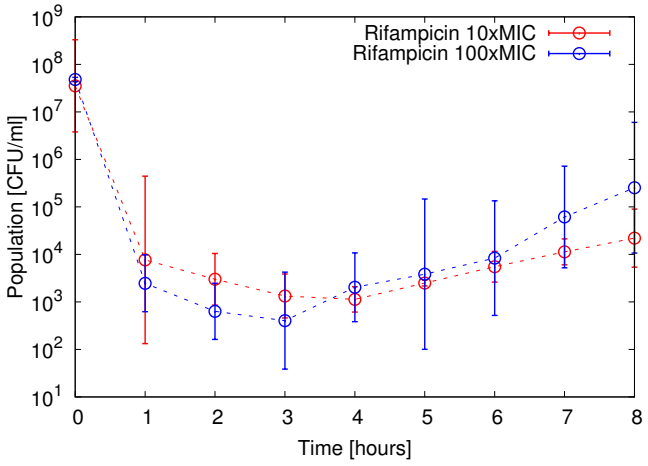

FIGURE 5.1: Antibiotic killing experiment showing three distinct phase: fast decay, slow decay and growth of the pre-existing resistant population.

The data points in the figure are averages of three experimental repeats and the bars gives the standard error in these repeats

In case of rifampicin, the population starts to grow within 3-4 hours of antibiotic treatment and, the growth appears to be independent of concentration of the antibiotic (although higher concentration slightly increases the death rate of the persisters) (Figure 5.1). This suggests that the resistant cell might be existing in the population prior to the antibiotic addition [120, 126]. In case of tobramycin, the population regrowth

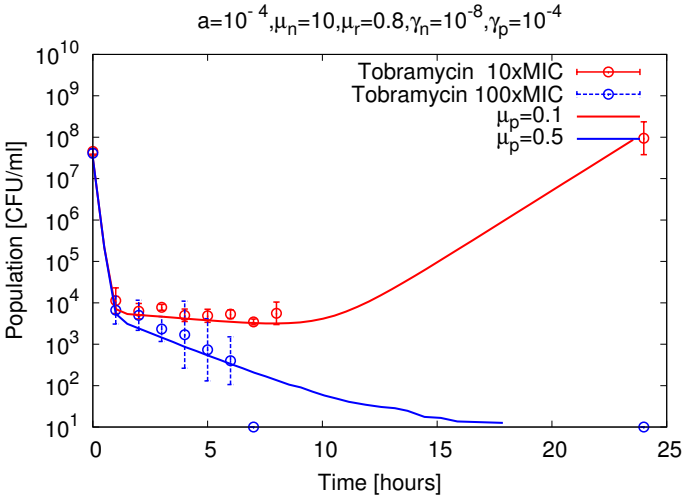

FIGURE 5.2: Antibiotic killing experiment showing three distinct phase: fast decay, slow decay and growth of the resistant population. The solid lines are two stochastic realization of the population dynamics for different values of death rate of persisters.

after few hours of killing in presence of the antibiotics depends on the concentration. At a moderate concentration (10 fold of minimum inhibitory concentration (MIC)) of antibiotic, the population grows after 8 hours, whereas at high concentration (100 fold MIC) the population goes extinct before 8 hours (Figure 5.2). The death rate of the normal cells is equal in both concentrations, whereas the death rate of persister cell increases with increase in antibiotic concentration. The population survival and growth is dependent on the death rate of persister cells, which suggests that the resistant cells are generated after antibiotic treatment due to longer survival. Therefore, we will focus only on the second case, antibiotic resistance against tobramycin, for our further analysis and comparisons. In this study, we investigate, using experimentally observed parameters, the role of surviving persister cells in the emergence of antibiotic resistance during an antibiotic treatment.

To understand the above results, we propose a three state population model consisting of two phenotypic states and one resistant state. We study the deterministic and stochastic dynamics of the population during antibiotic treatment using computer simulations and analytic calculations. The deterministic description is useful in extracting death rates, initial persister fraction and mutation rates from experimental data. The stochastic description is necessary to evaluate the probability of survival and its dependence on various parameters such as death rates, mutation rates and persister fraction. The time to first mutation or extinction can be properly defined only in a stochastic description due to small population numbers.

5.3 Model : Deterministic dynamics

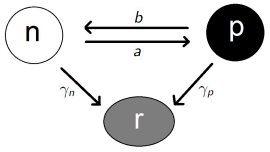

FIGURE 5.3: Model : Two phenotypic (n & p) and a resistant state (r).

We consider a mixed population of normal (n) and persister (p) cells dying with rates μ_n and μ_p, respectively in the presence of an antibiotic. Cells in the normal and the persister state can mutate with rate γ_n and γ_p respectively to the resistant state (r), in which cells can duplicate with rate μ_r (Figure 5.3). The population dynamics can be

represented by the following equations,

$$\begin{aligned} \dot{n}(t) &= -\mu_n n(t) - an(t) + bp(t) - \gamma_n n(t) \\ \dot{p}(t) &= -\mu_p n(t) + an(t) - bp(t) - \gamma_p n(t) \\ \dot{r}(t) &= \mu_r r(t) + \gamma_n n(t) + \gamma_p p(t). \end{aligned} \tag{5.1}$$

If p_0 and n_0 are the initial subpopulation sizes, then

$$\begin{aligned} p(t) &\approx p_0 e^{-(\mu_p+\gamma_p+b)t} \\ n(t) &\approx \frac{bp_0}{\Delta} e^{-(\mu_p+\gamma_p+b)t} + \frac{n_0\Delta - bp_0}{\Delta} e^{-(\mu_n+\gamma_n+a)t} \end{aligned} \tag{5.2}$$

where $\Delta = (\mu_n + \gamma_n + a) - (\mu_p + \gamma_p + b)$.

If the resistant cells are generated after the treatment, we have $r_0 = 0$. Therefore,

$$\begin{aligned} r(t) = \frac{\gamma_p p_0 (e^{\mu_r t} - e^{-(\mu_p+\gamma_p+b)t})}{\mu_r + \mu_p + \gamma_p + b} + \frac{\gamma_n b p_0 (e^{\mu_r t} - e^{-(\mu_p+\gamma_p+b)t})}{\Delta_s(\mu_r + \mu_p + \gamma_p + b)} \\ + \frac{(\gamma_n n_0 \Delta_s - \gamma_n b p_0)(e^{\mu_r t} - e^{-(\mu_n+\gamma_n+a)t})}{\Delta_s(\mu_r + \mu_n + \gamma_n + a)}. \end{aligned} \tag{5.3}$$

In the long time limit, transient term decays and the exponential growth is given by

$$r_\infty(t) = \left(\frac{\gamma_p p_0}{\mu_r + \mu_p + \gamma_p + b} + \frac{\gamma_n b p_0}{\Delta_s(\mu_r + \mu_p + \gamma_p + b)} + \frac{\gamma_n n_0 \Delta_s - \gamma_n b p_0}{\Delta_s(\mu_r + \mu_n + \gamma_n + a)} \right) e^{\mu_r t} \tag{5.4}$$

after neglecting small terms like $\gamma_n b$, we get

$$r_\infty(t) = \left(\frac{\gamma_p p_0}{\mu_r + \mu_p + \gamma_p + b} + \frac{\gamma_n n_0}{\mu_r + \mu_n + \gamma_n + a)} \right) e^{\mu_r t}. \tag{5.5}$$

The growth of the resistant population depends weakly on the phenotype switching rate. In the deterministic description, resistant population is generated with $\gamma_p p_0$ or $\gamma_n n_0$ at time $t = 0$ and grows exponentially with growth rate μ_r. When $\gamma_p p_0 \sim 1$ or $\gamma_n n_0 \sim 1$, i.e. for small mutation rates, the population might go extinct if a resistant cell is not generated during its lifetime. Therefore, a stochastic description of the population decay is necessary to quantify the chance of survival or extinction.

5.4 Stochastic simulation

The stochastic dynamics of the model is implemented using the Gillespie algorithm [34], where we consider the following events.

(1) Death of a normal or persister cell.

$\mu_n n$ or $\mu_p p \Rightarrow n \to n-1$ or $p \to p-1$

(2) Switching between the phenotypes.

$a\,n$ or $b\,p \Rightarrow n \to n-1\ ;\ p \to p+1$ or $p \to p-1\ ;\ n \to n+1$

(3) Mutation from the phenotypes.

$\gamma_n n$ or $\gamma_p p \Rightarrow n \to n-1\ ;\ r \to r+1$ or $p \to p-1\ ;\ r \to r+1$

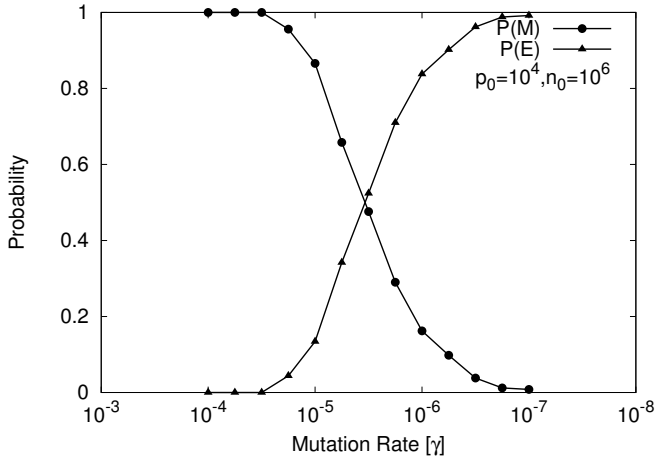

FIGURE 5.4: Probability of extinction and first mutation of the total population.

We start with a mixed population of normal and persister cells, and allow the population to perform the above listed processes. The population, over a long duration, might go extinct because of antibiotic death or survive by undergoing a mutation. We denote the extinction probability of the total population by $P(E)$ and the mutation (or survival) probability by $P(M)$. Fig. 5.4 show that the extinction probability $P(E)$ decreases with the increase in mutation rate and as consequence the mutation probability $P(M)$ increases. The probabilities $P(M)$ and $P(E)$ for different values of the switching rate (a=b) are is shown in Fig. 5.5. The figure shows that these probabilities are nearly independent of the phenotype switching rates. However, the initial persister fraction that is determined by phenotype switching rates, affects the probability of extinction and mutation.

5.5 Model : Stochastic dynamics

To analytically calculate expressions for probabilities and first passage times for extinction and mutation processes, we assume the subpopulation dynamics during the antibiotic killing to be independent of each other (i.e. assuming the switching rates to be approximately zero). Therefore, we will first calculate the probability distribution

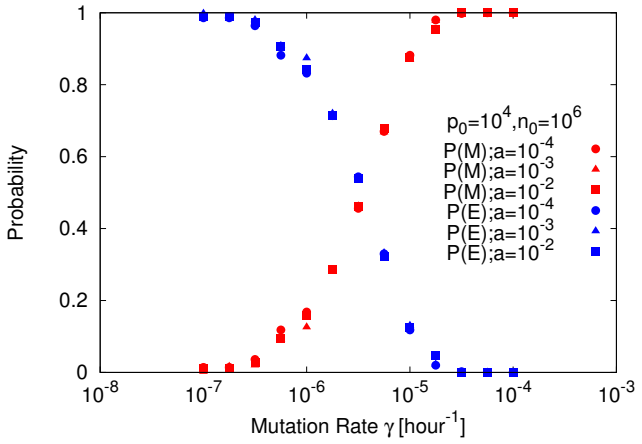

FIGURE 5.5: Extinction and survival probability as a function of the mutation rates for different values of phenotype switching rate (with $a = b$).

function for a single population and afterwards, we will use it to evaluate the joint distribution function the extinction and mutation process with two subpopulations.

5.5.1 Single population

We consider a population of size N where individuals die with rate μ and mutate with rate γ. The probability P_k that the population size is k at given time $'t'$ before any mutation has occurred is given by

$$\frac{dP_k}{dt} = -(\mu k + \gamma k)P_k + \mu(k+1)P_{k+1} \tag{5.6}$$

$$\frac{dP_N}{dt} = -(\mu N + \gamma N)P_N \tag{5.7}$$

with $P_N(0) = 1$ as initial condition.

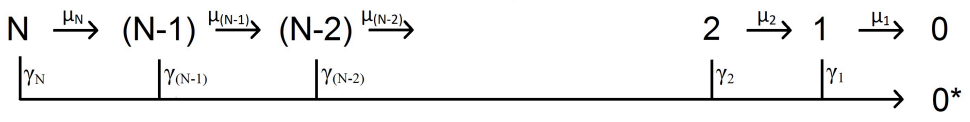

FIGURE 5.6: Network representation: State space for a population of N individual which is decreasing either due to death with rate μ or due to mutation with rate γ. The population extinction state is represented by (0) and, the first mutation state by (0^*).

The probability P_k can be calculated iteratively starting with $P_N = e^{-(\mu+\gamma)Nt}$. The probability of having a population size k before any mutation is

$$P_k(t) = \left(\frac{\mu}{\mu+\gamma}\right)^{N-k} \frac{N!}{k!(N-k)!} \left(1 - e^{-(\mu+\gamma)t}\right)^{N-k} e^{-(\mu+\gamma)k\,t}. \tag{5.8}$$

The extinction probability of the population is

$$P_0(t \to \infty) = P(E) = \left(\frac{\mu}{\mu+\gamma}\right)^N \tag{5.9}$$

and consequently, the survival probability of the population is

$$P(M) = 1 - \left(\frac{\mu}{\mu+\gamma}\right)^N. \tag{5.10}$$

The distribution function of the first passage time to extinction is defined as follows,

$$F_E(t) = \mu P_1(t) = \mu N \left(\frac{\mu}{\mu+\gamma}\right)^{N-1} \left(1 - e^{-(\mu+\gamma)t}\right)^{N-1} e^{-(\mu+\gamma)t}. \tag{5.11}$$

Hence, the mean time to extinction is given by

$$T_E = \frac{1}{\Pi_E} \int_0^\infty t F_E(t) dt \tag{5.12}$$

where $\Pi_E = \int_0^\infty F_E(t)dt = \left(\frac{\mu}{\mu+\gamma}\right)^N$ is the total probability for extinction. Solving, we get

$$T_E = \frac{1}{\mu+\gamma} \sum_{i=1}^{N} \frac{1}{i} \approx \frac{1}{\mu+\gamma} \log N. \tag{5.13}$$

For $\gamma = 0$, T_E reduces to the average extinction time for a population of size N.

Likewise, the first passage distribution function for mutation is defined as

$$F_M(t) = \sum_{k=1}^{N} \gamma_k P_k(t) = \gamma N \left(\frac{\mu}{\mu+\gamma}\right)^{N-1} \left(1 + \frac{\gamma}{\mu} e^{-(\mu+\gamma)t}\right)^{N-1} e^{-(\mu+\gamma)t}. \tag{5.14}$$

The mean time of mutation is given by

$$T_M = \frac{1}{\Pi_M} \int_0^\infty t F_M(t) dt \tag{5.15}$$

where $\Pi_M = 1 - \left(\frac{\mu}{\mu+\gamma}\right)^N$ is total probability of first mutation. Solving, we get

$$T_M = \frac{1}{\mu+\gamma}\sum_{i=1}^{N}\frac{1}{i}\frac{(1+\gamma/\mu)^i - 1}{(1+\gamma/\mu)^N - 1}. \tag{5.16}$$

5.5.2 Subpopulation of normal cells and persisters

Now, we consider two independent subpopulations, the normal and persister subpopulation of sizes n and p respectively. The probability at given time t that any normal cell from a population of size (n) has not yet arrived at the first mutation state (0^*) is

$$S_n(t) = \sum_{0}^{n} P_k(\mu_n, \gamma_n, t) = \left(\frac{\mu_n}{\mu_n+\gamma_n}\right)^n \left[1 + \frac{\gamma_n}{\mu_n}e^{-(\mu_n+\gamma_n)t}\right]^n. \tag{5.17}$$

The probability that any persister cell has not arrived at the first mutation state is

$$S_p(t) = \sum_{0}^{p} P_k(\mu_p, \gamma_p, t) = \left(\frac{\mu_p}{\mu_p+\gamma_p}\right)^p \left[1 + \frac{\gamma_p}{\mu_p}e^{-(\mu_p+\gamma_p)t}\right]^p. \tag{5.18}$$

The total probability that no cell from a mixed population of size $(N = n + p)$ has undergone mutation is $S_n \times S_p$.

Therefore, the joint first passage distribution function for mutation process is given by

$$F_{n+p} = \frac{d(1 - S_p S_n)}{dt} = F_n S_p + F_p S_n \tag{5.19}$$

where $F_n = -\frac{dS_n}{dt}$ and $F_p = -\frac{dS_p}{dt}$ are the respective first passage distribution function for the normal and persister subpopulation.

To simplify further, we consider the case $(\mu_n >> \mu_p)$, when normal cells are killed at much higher rate than persister cells. In this limit

$$S_n \approx \left(\frac{\mu_n}{\mu_n+\gamma_n}\right)^n \tag{5.20}$$

$$F_n \approx 0. \tag{5.21}$$

The joint first passage distribution reduces to $F_{n+p} \approx F_p S_n$ and, the mean first passage time to mutation is given by

$$T_M = \frac{\int_0^\infty tF_{n+p}\,dt}{\int_0^\infty F_{n+p}\,dt} = \frac{S_n \int_0^\infty tF_p\,dt}{[S_p\,S_n]_0^\infty} \tag{5.22}$$

$$T_M = \frac{\left(\frac{\mu_n}{\mu_n+\gamma_n}\right)^n}{1-\left(\frac{\mu_n}{\mu_n+\gamma_n}\right)^n\left(\frac{\mu_p}{\mu_p+\gamma_p}\right)^p} \int_0^\infty tF_p\,dt. \tag{5.23}$$

Solving, we get

$$T_M = \left[\left(1+\frac{\gamma_n}{\mu}\right)^n\left(1+\frac{\gamma_p}{\mu_p}\right)^p - 1\right]^{-1}\left(\frac{1}{\mu_p+\gamma_p}\right)\sum_i^p \frac{1}{i}\left[\left(1+\frac{\gamma_p}{\mu_p}\right)^i - 1\right]. \tag{5.24}$$

Similary, the first passage time to extinction

$$T_E = \frac{1}{\mu_p+\gamma_p}\sum_{i=1}^{p}\frac{1}{i}. \tag{5.25}$$

The expression is same as before because of the assumption $\mu_n >> \mu_p$.

5.6 Simulation Results & Comparisons

In this section, we will compare the results from stochastic simulations of the complete system with results of the theoretical approximation.

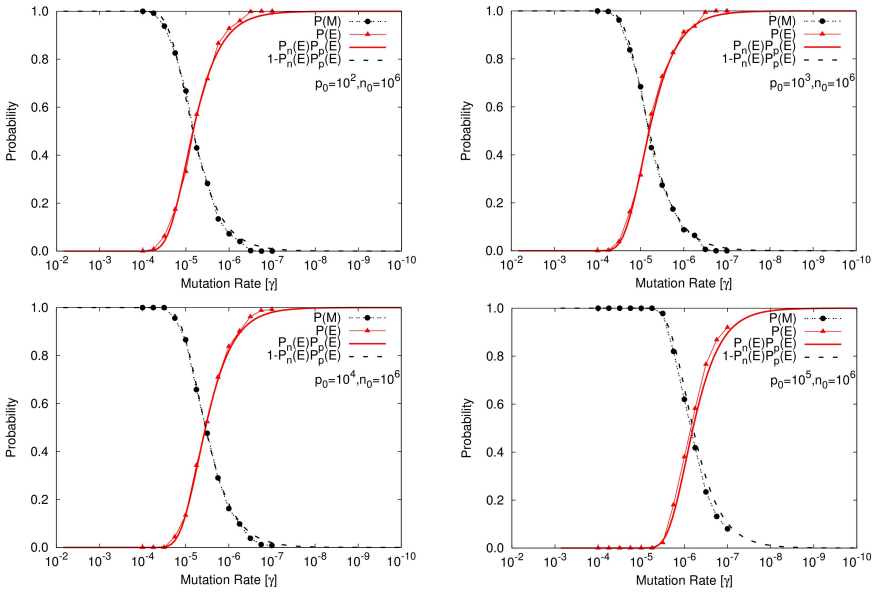

FIGURE 5.7: Comparison of simulation results with theoretical approximations.

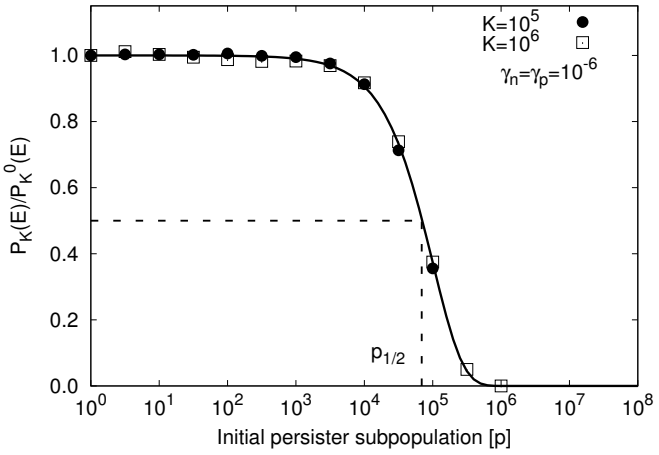

FIGURE 5.8: Fold change in extinction probability with the increase of persister subpopulation

The total extinction probability of a mixed population of normal (n) and persister (p) cells is given by

$$P_K(E) = \left(\frac{\mu_n}{\mu_n + \gamma_n}\right)^n \left(\frac{\mu_p}{\mu_p + \gamma_p}\right)^p \tag{5.26}$$

where $K = n + p$ is the initial population size. Then, the total probability of first mutation is $P_K(M) = 1 - P_K(E)$. The analytical expression for both the probabilities agree with simulation results as shown in Figure 5.7.

The extinction probability can be written as

$$P_K(E) = \left(\frac{\mu_n}{\mu_n + \gamma_n}\right)^{(K-p)} \left(\frac{\mu_p}{\mu_p + \gamma_p}\right)^p = P_K^0(E) \frac{\left(1 + \frac{\gamma_n}{\mu_n}\right)^p}{\left(1 + \frac{\gamma_p}{\mu_p}\right)^p} \tag{5.27}$$

where $P_K^0(E) = \left(\frac{\mu_n}{\mu_n+\gamma_n}\right)^K$ is the extinction probability with no persisters. Thus, the presence of persisters reduces the probability for extinction. Figure 5.8 shows that the extinction probability from simulations with different initial total population size (K) normalized to the probability with no persisters follows the analytical expression of Eq.(5.27). The fold change $P_K(E)/P_K^0(E)$ extinction probability is half at persister subpopulation size of

$$p_{1/2} = \frac{\log(2)}{\log\left(\frac{\mu_n(\mu_p+\gamma_p)}{\mu_p(\mu_n+\gamma_n)}\right)}. \tag{5.28}$$

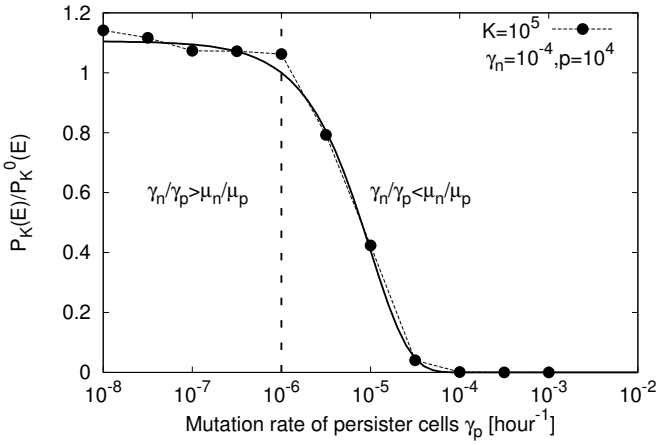

FIGURE 5.9: Fold change in extinction probability with the increase of mutation rate of persisters.

The extinction probabilty of the total population will be reduced only if

$$\frac{\gamma_n}{\gamma_p} < \frac{\mu_n}{\mu_p}. \tag{5.29}$$

If mutation rate rate of persisters is decreased below the above limits, the probability of extinction increases as shown in Figure 5.9. This increase in extinction probability is due to lower rate of mutation from persister cells in the total population. In this case the presence of persisters might increase the lifetime of the population but does not help in developing resistance.

Now, we could understand the dependence of the emergence antibiotic resistance on the antibiotic concentration. Figure 5.1 shows that the increase in the concentration of tobramycin increase the death rate of persisters while death rate of normal cells remain unaffected. This increase in death rate of persisters increases the probability of extinction of the population (Eq. 5.27), which leads to population extinction.

5.6.1 First passage time

The first passage events to mutational state (0^*) and extinction state (0) defines the time of first mutation (CMTM) before the normal and persister subpopulation goes extinct and, the time of extinction (CMTE) of normal and persister subpopulation before mutation.

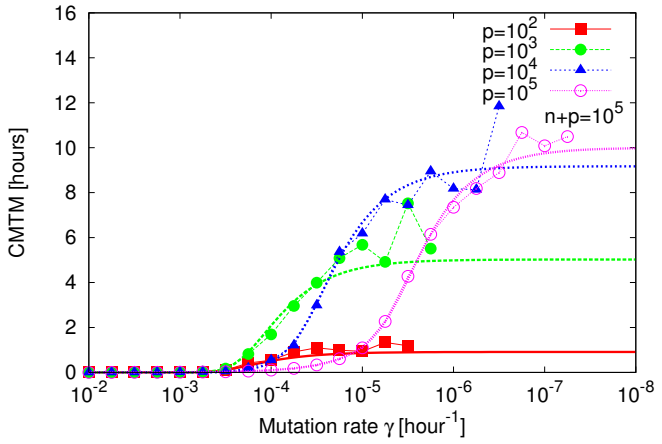

FIGURE 5.10: Conditional mean time to first mutation of the total population. The points are from stochastic simulation and the solid curves are the analytic expression (Eq. 5.30).

The conditional first passage time to mutation is

$$T_M = \left[\left(1+\frac{\gamma_n}{\mu}\right)^n \left(1+\frac{\gamma_p}{\mu_p}\right)^p - 1\right]^{-1} \frac{1}{\mu_p+\gamma_p} \sum_i^p \frac{1}{i}\left[\left(1+\frac{\gamma_p}{\mu_p}\right)^i - 1\right]. \qquad (5.30)$$

Figure 5.10 shows, for high mutation rates, the CMTM is very low and as the mutation rate decreases, the CMTM increases until a saturation value. The probability of mutation is reduced with the decrease in mutation rates, which is evident from the lack of data points for very low mutation rate or in the saturation regime.

The CMTM curve for different initial persister subpopulation (p) sizes cross each other at certain mutation rate (let say γ_c). For example, the CMTM is longer for $p = 10^4$ (blue) than $p = 10^3$ (green) for mutation rate $\gamma < \gamma_c (\approx 10^{-4.7})$, whereas it is shorter for mutation rate $\gamma > \gamma^c$. This behavior can be understood by looking at the dependence of CMTM on the persister subpopulation while keeping the mutation rate fixed. For a fixed value of γ, CMTM show a maximum (Figure 5.11) when the initial persister subpopulation is changed, which keeping the initial total population size fixed.

To the left of the maximum, the probability of mutation by persister subpopulation $P_p(M)$ increases compared to the probability of mutation by normal subpopulation $P_n(M)$, but the mean time to mutation by normal cells is much shorter than persisters because of the large population size. Hence, an increase in $'p'$ increases the probability of mutation by persisters which therefore increases the CMTM as persister cells take a longer time to first mutation. To the right of the maximum, the probability of mutation by persister subpopulation is larger than normal subpopulation and mean time to

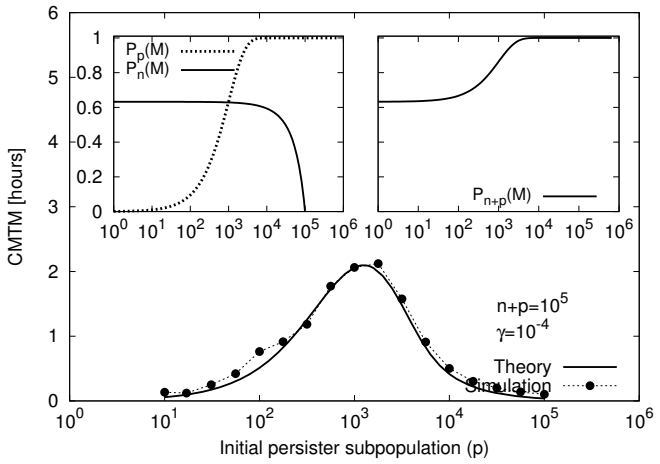

FIGURE 5.11: Conditional mean time to first mutation of total population shows a maxima as persister subpopulation is varied.

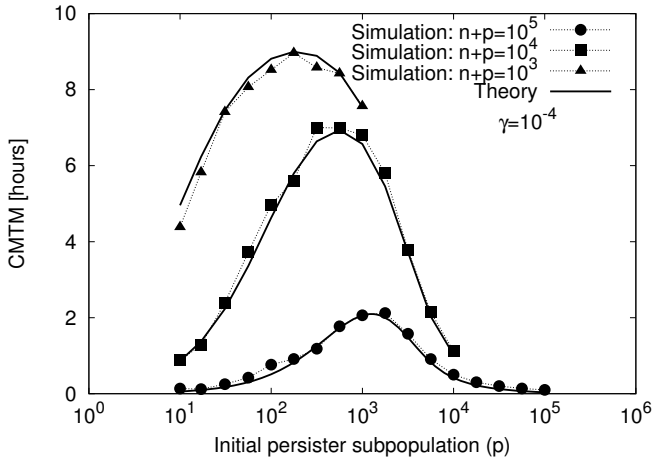

FIGURE 5.12: Conditional mean time to first mutation of total population for different initial population size.

mutation decreases as the population size increases. The maximum arises due to the interplay of subpopulation size and individual mutation probabilities. The total probability of mutation always increases with the increase in persister subpopulation size as shown right inset of Figure 5.11.

Figure 5.12 shows the effect of the total population size on the maximum. As we decrease the initial total population size, the probability of mutation by persister subpopulation becomes higher than normal subpopulation at lower values of persister subpopulation size, hence the maximum shifts leftwards. Since the subpopulation sizes are reduced, the CMTM becomes even higher.

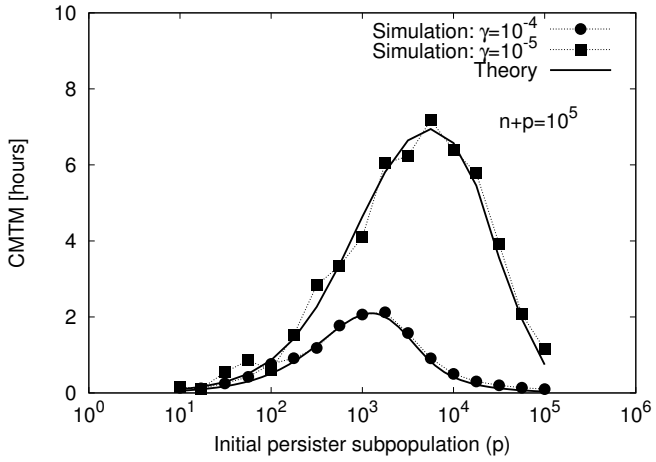

FIGURE 5.13: Conditional mean time to first mutation of total population for different mutation rates.

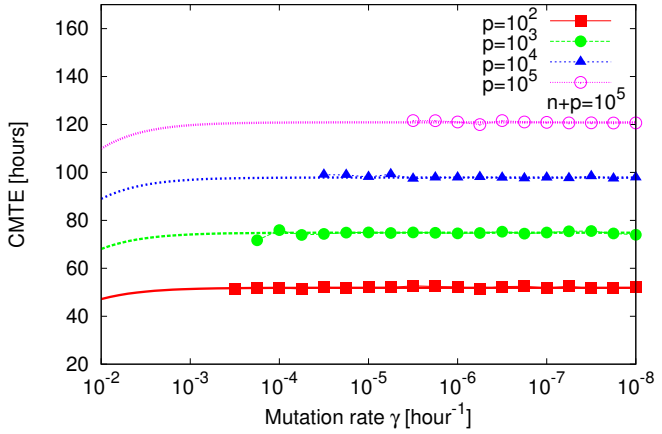

FIGURE 5.14: Conditional mean time to extinction for different fractions of persisters in a fixed total population.

Figure 5.13 shows the effect of mutation rate on the maxima, as the mutation rate is reduced the probability of mutation of by persister subpopulation requires higher $'p'$ to become large than normal subpopulation, hence the maximum shifts rightwards. And, the reduction in mutation rate also increases the CMTM.

Similarly, the conditional first passage time to extinction follows the following analytical expression

$$T_E = \frac{1}{\mu_p + \gamma_p} \sum_{i=1}^{p} \frac{1}{i}. \tag{5.31}$$

5.7 Conclusion

Bacterial persistence is well known survival strategy exhibited by bacterial population to survive under antibiotic treatment [67]. It is a cause of treatment failure and recalcitrance of several infectious disease, which is turning into a serious threat to medical treatments [19, 28, 75, 91, 115]. In this phenomenon a fraction of population survives upon antibiotic treatment which allows the population to regrow once the antibiotic treatment is removed. The surviving population during the antibiotic treatment might also provide a long lived pool of bacteria which can undergo resistance mutations. Observations displaying persistence together with antibiotic resistance are very rare in the literature. However, several experiments point towards this possibility. The role of persistence in antibiotic resistance is an emerging field of study which will gain importance in the future.

This study shows one such example where the longer survival of population leads to antibiotic resistance and this longer survival is mediated through persister cells. We extend the current two state model of bacterial persistence into a three state model including the resistant population which can be generated during the course of antibiotic treatment. We explain two different possibilities through which one could observe a resistant population. Using stochastic modeling we show that when *Staphylococcus aureus* population is treated with tobramycin antibiotic, the generation of resistant is not a simple selection of preexisting resistant population. Rather, it is a consequence of longer survival of persister subpopulation at moderate antibiotic concentrations. We further study the physical properties of the three state model and analytically calculate different probabilities and time to mutation or extinction. We find that the presence of persister subpopulation always increase the probability of mutation, but the time to acquire such mutation is longer due to small number of persister cells. This study will provide a tool to understand role of persistence in antibiotic resistance and to design suitable experiments considering all the possibilities arising from simple model.

Chapter 6

Discussion & Summary

In the preceding chapters, we have presented some theoretical and experimental results that identify several aspects of bacterial persistence in different environmental conditions [72, 96, 97]. The first notion about the presence of drug tolerant persisters, the culprit behind persistence against antibiotics, in a population was made 60 years ago [7], nonetheless the present understanding about the physiology of persisters and, the mechanism of their emergence is limited [3]. The main window into persistence is the study of survival of populations over time upon antibiotic treatment [4, 53, 55, 71]. The results from such studies are explained and interpreted using a model for stochastic phenotype switching between two cellular states, namely the normal state and the persister state. However, the existing analysis of this model does not provide an explicit relation among experimental observations and model parameters. We analyzed an existing model using a simple approximation method to answer this issue, and calculated analytic expressions for measuring model parameters for persistence in time-shift experiments [97]. To illustrate our analysis, we computed model parameters for *S. aureus* populations under multiple drugs at different concentrations. Further, we extended our analysis to understand qualitatively the outcome of cross-drug treatment on a bacterial population.

The previous theoretical studies have identified bacterial persistence as a survival mechanism that population has developed to deal with temporally fluctuating environments [29, 66–68]. We showed that bacterial persistence also plays a significant role in several other realistic situations, such as help in spatial expansion, emergence of antibiotic resistance and development of multidrug tolerance in bacterial populations [72, 96, 97]. Thus, our results extend the current knowledge of bacterial persistence and, furthermore, provide a toolbox for designing and analyzing experiments.

In the following sections, we will summarize the main results of the manuscripts included in this thesis and give an outlook.

6.1 Overview of the main results

Bacterial persistence in temporally varying environments. Bacterial populations tackle sudden environmental stresses by keeping a small fraction of the total population, the persister cells, in a slow-growing but stress-tolerant phenotype state [67]. The persister cells cause a small fitness cost to the total population under growth supporting conditions, but provide a large benefit by withstanding antibiotic attacks. Once the growth conditions are restored, the population can recover from surviving persister cells via a phenotypic switch to normal growing state. The underlying population dynamics is well described by a two state model, which considers exponential growth of the subpopulations coupled with phenotype switching between the subpopulations [4]. We analyzed this mathematical model using a simple approximation valid for small phenotype switching rates that allows to map the dynamics of subpopulation ratio to a logistic equation [97]. This indicates that under constant conditions, the effective growth rate of the persister (slow-growing) subpopulation approaches the growth rate of the normal (fast-growing) subpopulation in a logistic fashion. The steady state in the subpopulation ratio is achieved by a balance between fast-growing cells outgrowing the slow-growing ones and phenotype switching, by which the slow-growing cells are replenished from the fast growing cells. Therefore, a primary determinant of the persister fraction in a population is the switching rate from the normal to the persister state. A recent study, characterizing persistence in three strains (SC552, SC649, MG1655) of *E. coli* against three antibiotics (ampicilin, ciprofloxacin and nalidixic acid), observed this dependence. The study showed that the fractions of persisters in a population and the rate of switching from the normal to the persister state are strongly correlated across both strains and antibiotics [45].

We then investigated the population dynamics during environment shifts from growth to stress and vice-versa. We calculated analytical expression of the characteristic time scale for changes in the total population growth or decay and for approaching a constant ratio in subpopulations. These analytical expressions can be used to extract switching rates by following the population dynamics in environment shift experiments. Moreover, using our simple theoretical approach, we could also show that under periodically fluctuating environment, when the growth and stress periods have long duration, the phenotype switching rates can be tuned for optimal growth of the total population, confirming results from previous studies [67–69]. Additionally, we showed that, in case when one of

the environmental duration (growth or stress) is brief, the phenotype switching cannot be optimally tuned and the increase in phenotype switching progressively reduces the growth rate of the total population [97]. In summary, using the basic model we could look at various aspects of bacterial persistence mechanism which have not been considered before.

Dynamics of phenotype switching in non-uniform spatial environments. Spatially structured environments are often used to study evolution in bacterial populations, they play, e.g., an important role in the emergence of drug resistance [41, 56, 70, 102, 103, 137]. In the highly compartmentalized human body, different organs and tissues usually have different pharmacokinetic parameters that often lead to non-uniform distribution of antibiotics [6, 12, 92]. Persister cells being less sensitive to antibiotics, could assist a population to cross a region of high antibiotic concentrations or other stressful environments that otherwise might act as a bottleneck to population expansion in non-uniform spatial environments. Therefore, to investigate the role of persister cells in population expansion, we studied the expansion of a phenotypically heterogeneous population in a spatial environment consisting of two growth sustaining patches separated by an antibiotic patch [96].

We have calculated the mean first arrival time (MFAT) of a cell to the third patch (i.e. the growth supporting patch) in a population with and without persisters. We found that the time to cross an antibiotic patch is reduced in the presence of drug tolerant persisters in a population. Specifically, we observed that the MFAT of the subpopulations depends on the phenotype switching and migration rates, and show three distinct scaling regimes as the migration rate is varied. We explained these different regimes by means of an analytical approximation. Furthermore, we identified regions in the parameter space (of phenotype switching and migration rate), where phenotype switching is beneficial to the population expansion. This basic model can be applied to several situations where a population encounters adverse environmental conditions while expanding into other growth permitting regions. For example, hospital acquired infections occur in a similar fashion, where bacterial infection is transmitted from an infected individual to an uninfected individual through several routes such as physical contacts, airborne transmission, common equipment usage [20, 77], etc.

Multidrug-tolerance in *Staphylococcus aureus*. In Chapter 4 of the thesis, we analyzed results from an experiment using the theoretical expressions obtained in Chapter 2. We used the data from antibiotic killing and resuscitation experiments performed on *Staphylococcus aureus* population under different antibiotics, to obtain important parameters such as persister fraction, switching rates, death rates, etc. We found that different antibiotics select different fraction of persisters. To test the importance of the

results, we performed a statistical hypothesis test (t-test) that quantifies how significant is the difference between the survival persister fraction against different antibiotics compared to the measurement error within the repeats of an experiment.

The survival of different fractions of populations indicates that the persisters selected might have a different physiology. A test to determine the physiology was performed by our collaborators through a cross-drug treatment experiment, where survivors from one antibiotic treatment were exposed to another antibiotic. We extended our analysis to predict the outcome of this cross-drug tolerance experiment. Specifically, we proposed three possible outcomes, i.e., zero cross tolerance, full cross tolerance and partial cross tolerance. We found that the persister cells selected by one antibiotic either show full tolerance or zero tolerance to the second antibiotic. Surprisingly, the fate of the population was found out to be dependent on the order of antibiotic treatment, under one order the population could survive and in another the population went extinct. This suggests that persisters selected with some antibiotics may develop full tolerance to other antibiotics. We also reported model parameters for several strains of *S. aureus* (*menD, hemB, HG's*) under different antibiotics (appendix A.2).

Role of persisters in the emergence of antibiotic resistance. Bacteria have developed, over the years, mechanisms to survive attack from antibiotics designed to eliminate them, one such mechanism is antibiotic resistance [61, 94, 117]. Most of the earlier developed drugs against infectious diseases have lost potency because the targeted pathogens became resistant against them [18]. Several studies have suggested that the longer survival of a population due to the persister cells may help in the emergence of antibiotic resistance [73, 117, 131]. Our collaborators observed the emergence of antibiotic resistant cells in *Staphylococcus aureus* populations upon treatment with antibiotics rifampicin and tobramycin. In case of rifampicin treatment, the population started to grow within 3-4 hours of treatment and the dynamics was unperturbed with the increase in antibiotic concentration. This implies that the resistant cells might be pre-existing in the population and, were selected upon antibiotic treatment [120, 126]. In case of tobramycin, the population started to grow after 8 hours of antibiotic treatment and the emergence of resistance was found to be dependent on the concentration of antibiotic. This suggests that the resistant cells might have emerged from the population during antibiotic treatment. To explain the experimental results, we extended the two state model to a three state model consisting two phenotypic states and one resistant state. We found that stochastic trajectories predicted by the model agree with the experimental results. We further performed a theoretical analysis of this model, and found that the probability of mutation to the resistant state is enhanced in the presence of persister subpopulation. We also observed that the time to mutation first increases, with the increase in persister subpopulation, to a maximum and then decrease afterwards. Our

theoretical analysis presents a tool to develop further experiments to understand the role of persister cells in emergence of antibiotic resistance.

6.2 Outlook

The present study on bacterial persistence can be extended in several directions. For instance, the spatial structure that we have used to study spatial expansion of a heterogeneous population can be easily realized in experiments [70]. The benefit of having persisters can be quantified, first by separately using different strains displaying either lower [79] or higher [88] persister fraction to measure the arrival time and then competing them against each other [56]. Similarly, the theoretical analysis presented in chapter 5 can be used for further systematic studies to understand the role of persisters in the emergence of antibiotic resistance. For example, one could study the effect of the change in concentration of antibiotics, in a killing experiments, on the emergence time of the resistant population and compare with the theoretical expressions.

The processes or conditions responsible for the evolution of persistence are unclear. Most theoretical studies suggest that phenotype switching rates might evolve towards an optimal value in periodically fluctuating conditions [29, 66–68]. Also, the fraction of persisters is found to increase under repeated exposure of antibiotics [88, 91]. However, a proper realization of this evolutionary process has not been achieved. Such a study would provide the rate at which persister frequency evolves in a population, which could help to control the dosage and duration of the antibiotics for efficient treatments.

The existing theoretical models for bacterial persistence considers phenotype switching rates to be independent of environmental conditions. However, certain antibiotics are known to induce the persister phenotype [21, 22], and growth limiting conditions, such as nutrient depletion or entry to stationary phase, are also shown to increase persister fraction [53]. These environmental effects must be considered while studying population dynamics or understanding experimental results. The environmental effects such as induced persistence and stress responses, in addition to selection pressure might influence the evolutionary dynamics of a population. Therefore, a systematic study including all these environmental interactions must be performed to understand the emergence of persistence.

6.3 Summary

In this thesis, we studied a survival mechanism termed 'bacterial persistence' exhibited by most bacterial populations. This mechanism finds implication in antibiotic therapy failures and emergence of drug resistance in several pathogenic bacteria such as *Mycobacterium tuberculosis, Staphylococcus aureus, Pseudomonas aeruginosa, Escherichia coli* etc. We studied a known two state phenotype switching model for bacterial persistence with a new theoretical approach valid only for small switching rate, which is usually the case. Using our approximation method, we expressed the parameters of the model in terms of experimentally observed time scales and recapitulated known results that show the existence of an optimal switching which maximizes the population growth rate in periodic fluctuating environments. Additionally, using this approach, we showed that if one of the environmental duration is short in a periodic fluctuating environment, the increase in phenotype switching decreases the overall growth rate and serves as a harmful strategy for the population. Using our theoretical analysis we characterize the dynamics of multidrug tolerance in *S. aureus* populations. We found that the population dynamics in a cross antibiotic treatment is complex and, indicates that drug tolerance in *S. aureus* populations is a combination of population selection and adaptive response to antibiotics. Next, we considered the expansion of a population exhibiting phenotype switching in an environment with non-uniform antibiotic distribution and found that the presence of persister cells can accelerate the population expansion rate by helping the population to a cross region of high concentration faster. Further, we considered another important aspect of bacterial persistence, i.e. the emergence of antibiotic resistance from persister cells. We explained the experimental observations showing antibiotic resistance in *S. aureus* against anitbiotic tobramycin, using stochastic analysis of an extended model of bacterial persistence that allows mutation of cells to resistant state. In summary, in this thesis we have analyzed several aspects of bacterial persistence mechanism under changing environments, such as multidrug tolerance, population expansion and antibiotic resistance.

Appendix A

Appendix

A.1 Phenotypically heterogeneous population in spatially heterogeneous environments

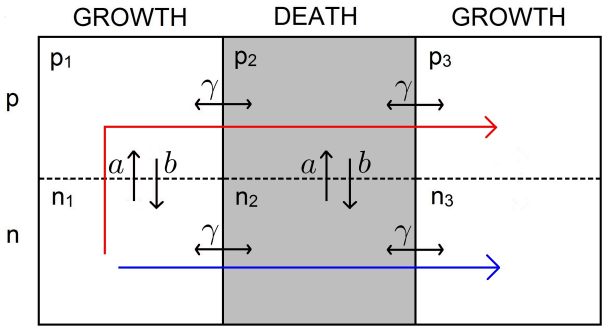

FIGURE A.1: Model for phenotype switching and migration in three connected micro environments (patches): Bacteria switch between two phenotypic states, normal cells (n_i) and persisters (p_i) with rates a and b and migrate to a neighbouring patch with rate γ. While the first and third patch sustain growth of the population, the second patch contains antibiotics and does not allow for growth.

Deterministic dynamics in the first patch. In Chapter 3, we have presented only the main results for the case of population expansion in a heterogeneous environment. In this section, we provide detailed the calculation for some results that were used in the Chapter 3. In the model, we considered expansion of a heterogeneous population from a growth sustaining patch into another, which is separated an antibiotic patch (Figure A.1). The subpopulation sizes in the first patch follows the following equations,

$$\begin{aligned} \dot{n_1} &= \mu_n \left(1 - \frac{n_1 + p_1}{K}\right) n_1 - a n_1 + b p_1 - \gamma n_1 \\ \dot{p_1} &= \mu_p \left(1 - \frac{n_1 + p_1}{K}\right) p_1 + a n_1 - b p_1 - \gamma p_1, \end{aligned} \tag{A.1}$$

where backward migration from the second patch has been neglected. The above non-linear coupled differential equations have three fixed points (F_0, F_1, F_2). The find the feasible solution (i.e. the stable fixed points), we inspect the population total $(n_1 + p_1)$ and the subpopulation ratio (n_1/p_1) for the two fixed points other than $F_0 \equiv (n_1 = 0, p_1 = 0)$, as below

$$F_1 : (n_1 + p_1, n_1/p_1) = \left(\frac{\mu_n(2\mu_p - b - \gamma) - \mu_p(a + \gamma) + \sqrt{B^2 + C}}{2\mu_n\mu_p} K, \frac{B + \sqrt{B^2 + C}}{2a\mu_n} \right);$$

$$F_2 : (n_1 + p_1, n_1/p_1) = \left(\frac{\mu_n(2\mu_p - b - \gamma) - \mu_p(a + \gamma) - \sqrt{B^2 + C}}{2\mu_n\mu_p} K, \frac{B - \sqrt{B^2 + C}}{2a\mu_n} \right),$$

where $B = \mu_n(b + \gamma) - \mu_p(a + \gamma)$ and $C = 4ab\mu_n\mu_p$.

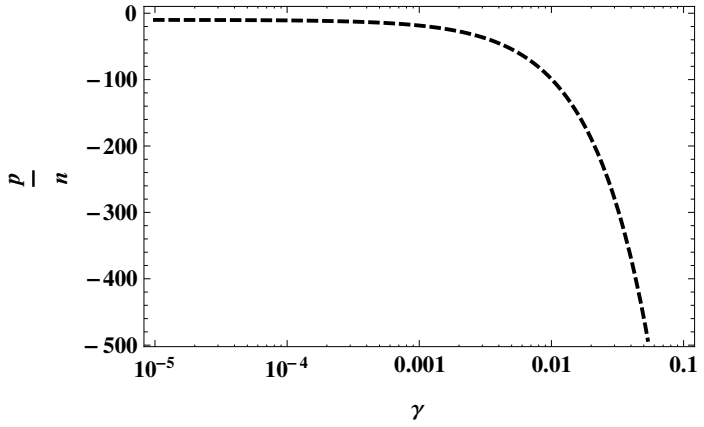

FIGURE A.2: Sub population ratio (p/n) for the unstable fixed point in first patch for K=100,a=0.001,b=0.001,$\mu_n = 2$, $\mu_p = 0.2$.

It is evident from the above expressions that in growth conditions $(C > 0)$, F_2 is not a feasible solution because the ratio of (n_1/p_1) is negative for this fixed point (as shown in Figure A.2). Therefore, F_1 is a stable solution; and the subpopulation sizes are

$$n_1 = \frac{\mu_n(2\mu_p - b - \gamma) - \mu_p(a + \gamma) + \sqrt{B^2 + C}}{2a\mu_n + B + \sqrt{B^2 + C}} \times \frac{K(B + \sqrt{B^2 + C})}{2\mu_n\mu_p} \tag{A.2}$$

$$p_1 = \frac{\mu_n(2\mu_p - b - \gamma) - \mu_p(a + \gamma) + \sqrt{B^2 + C}}{2a\mu_n + B + \sqrt{B^2 + C}} \times \frac{2a\mu_n K}{2\mu_n\mu_p}. \tag{A.3}$$

Next, we evaluate the subpopulation sizes in two important limits, namely fast and slow migration rate, which have been reported in Chapter 3. For fast migration $(\gamma >> a, b)$, we assumed $B^2 >> C$ and $B + \sqrt{B^2 + C} \approx 2B$. Hence, the stable solution is given by

$$n_1/p_1 \approx \frac{B}{a\mu_n} = \frac{(\mu_n - \mu_p)\gamma}{a\mu_n}$$

$$n_1 + p_1 \approx K\left(1 - \frac{\gamma}{\mu_n}\right); \tag{A.4}$$

and the subpopulation sizes are

$$n_1 \approx K\left(1-\frac{\gamma}{\mu_n}\right), \qquad p_1 \approx \frac{a\mu_n}{(\mu_n-\mu_p)\gamma}K\left(1-\frac{\gamma}{\mu_n}\right). \tag{A.5}$$

Here, the normal subpopulation quickly reaches the carrying capacity, i.e. ($n_1 \approx K$), and the persister subpopulation is given by a balance between the population increment due to generation of cells from the normal subpopulation and the population decrement due to migration into antibiotic patch.

Similary, for slow migration ($\gamma << a, b$), we assumed $B \approx \mu_n b - \mu_p a$. Hence, the stable solution is given by $p_1/n_1 = b/a$ and $n_1 + p_1 = K$; and the subpopulation sizes are

$$n_1 \approx \frac{b}{a+b}K, \qquad p_1 \approx \frac{a}{a+b}K. \tag{A.6}$$

In this case, the steady state is result of balance in phenotype switching of subpopulations.

A.1.1 Stochastic dynamics in the second patch

Now, we consider the stochastic dynamics of subpopulation sizes in the second patch, i.e. the antibiotic patch. The population dynamics in second patch is mapped to an emigration, death and migration problem. The emigration (or migration into second patch) of cells from the first patch happens with a rate $\lambda = N\gamma$. The migration rate of cells to third patch is γn and death rate in the second patch due to antibiotics is $\delta' n$ ($\delta' \approx \delta + \gamma$ includes backward migrations) .

We assume N is the average population (i.e. the steady state population) in first patch at any given time. Then, the probability that the population in second patch is m at any given time t, and no cell has yet migrated to the third patch, is given by

$$\frac{dP_m}{dt} = -(\lambda + \delta' m + \gamma m)P_m + \lambda P_{m-1} + \delta'(m+1)P_{m+1}$$
$$\frac{dP_0}{dt} = -\lambda P_0 + \delta' P_1, \tag{A.7}$$

with $P_0(0) = 1$ as the initial condition.

We define $G(s,t) = \sum_0^\infty s^m P_m(t)$, the moment generating function for the above stochastic differential equation. Then, the boundary conditions translates to $G(s,0) = 1$. The above differential equation can be written in terms of generating function as

$$\frac{\partial G}{\partial t} - (\delta' - \delta' s - \gamma s)\frac{\partial G}{\partial s} = \lambda(s-1)G.$$

The auxiliary equation to above differential equation is

$$\frac{dt}{1} = \frac{ds}{s(\delta' + \gamma) - \delta'} = \frac{dG}{\lambda(s-1)f}.$$

Integrating the above equation, we find the moment generating function $G(s,t)$ as

$$G(s,t) = \exp\left[\frac{\lambda}{\delta'+\gamma}\left(s - 1 - \frac{\gamma}{\delta'+\gamma}\ln\left(s - 1 + \frac{\gamma}{\delta'+\gamma}\right)\right)\right]\Phi\left((s\delta' + s\gamma - \delta')e^{-(\delta'+\gamma)t}\right),$$

where Φ is an arbitrary function of variables (δ', γ, s, t) to be determined by initial condition $G(s,0) = 1$. By substituting the the initial condition we find Φ and hence, $G(s,t)$ as given below

$$G(s,t) = \exp\left[\frac{\lambda}{\delta'+\gamma}\left(s - \frac{\delta'}{\delta'+\gamma}\right)\left(1 - e^{-(\delta'+\gamma)t}\right)\right] \times \exp\left(-\frac{\lambda\gamma}{\delta'+\gamma}t\right).$$

A.1.2 Mean first arrival time (MFAT)

The time at which a cell from second patch migrates to third patch for the first time is represented by the mean first passage time for the above emigration,death and migration process. The MFAT is defined as

$$T = \int_0^\infty \left(\sum_0^\infty P_m(t)\right) dt = \int_0^\infty G(1,t)dt. \tag{A.8}$$

Substituting the functional of $G(1,t)$, we get

$$T = \int_0^\infty \exp\left[\frac{N\gamma^2}{(\delta'+\gamma)^2}\left(1 - e^{-(\delta'+\gamma)t}\right)\right]\exp\left[-\frac{N\gamma^2 t}{(\delta'+\gamma)}\right]dt.$$

The complete solution to the above integral is

$$T = \exp\left[N(\frac{\gamma}{\delta'+\gamma})^2\right] \times \frac{1}{\delta'+\gamma}\sum_0^\infty \frac{(-1)^k}{k!}\frac{\left[N(\frac{\gamma}{\delta'+\gamma})^2\right]^k}{\left[k + N(\frac{\gamma}{\delta'+\gamma})^2\right]}$$

Moreover, we consider two important limits of the above integral, first $N\gamma^2 << (\delta'+\gamma)^2$ i.e. slow migration, where

$$T_s \approx \int_0^\infty \exp\left[-\frac{N\gamma^2 t}{(\delta'+\gamma)}\right]dt \approx \frac{\delta'+\gamma}{N\gamma^2} \tag{A.9}$$

and second $N\gamma^2 >> (\delta'+\gamma)^2$ i.e rapid migration.

For $\Lambda \equiv N\gamma^2/(\delta'+\gamma)^2 \gg 1$, the MFAT can be written in the form $T = \int_0^\infty \exp[\Lambda f(t)]dt$, where $f(t) = (1 - e^{(\delta'+\gamma)t} - (\delta' + \gamma)t$ is a decreasing function of t and has a maximum at $t = 0$. Hence, the integral can be calculated approximately using Laplace's method, which leads to

$$T_f \approx \int_0^\infty \exp\left[-\frac{N\gamma^2}{2}t^2\right] dt = \frac{1}{\gamma}\sqrt{\frac{\pi}{2\,N}}. \tag{A.10}$$

Further simplification with the assumption that antibiotic death is much larger than migration rate $\delta >> \gamma$, we get

$$T_s \approx \frac{\delta}{N\gamma^2} \text{ and } T_f \approx \frac{1}{\gamma}\sqrt{\frac{\pi}{2\,N}} \tag{A.11}$$

The MFAT T_f is independent of the antibiotic death due to the fast drift of cells through the second patch when migration is very fast. We use the average subpopulation size n_1 or p_1) from eq.(A.6) and eq.(A.5) to evaluate the mean first passage time for normal and persister cells.

A.2 Measuring persistence

In chapter 4, we reported physiological parameters such as death rate and persister fraction only for SA113 strain of *Staphylococcus aureus*, measured in the presence of different antibiotics. Here, we report these parameters for several strains of *S. aureus* (menD, hemB and HG's) measured against four different antibiotics (ciprofloxacin, rifampicin, tobramycin and daptomycin).

The antibiotic killing curves for each experiment were fitted with the total population decay curve as given below

$$N(t) = n_0\left[\exp(-\mu_1 t) + f_0\exp(-\mu_2 t)\right]. \tag{A.12}$$

Th the parameters μ_1, μ_2 and f_0 corresponds the absolute values of the death rates of normal cells and persisters and to the initial fraction of persisters, respectively ($\mu_1 = \mu_n^{(AB)}, \mu_2 = \mu_p^{(AB)}, f_0 \approx a/\mu$).

TABLE A.1: SA113 (Growth Rate, μ=1.24 h^{-1})

Antibiotic	Concentration	No. of exps.	Death rate of normal cells $\mu_n^{(AB)}(h^{-1})$	Death rate of persister cells $\mu_p^{(AB)}(h^{-1})$	Fraction of persister $log_{10}f_0$	Switching rate n → p $a(h^{-1})$
Ciprofloxacin	10-fold MIC	3	-6.96 ± 0.20	-0.55 ± 0.12	-3.22 ± 0.21	7.4×10^{-4}
	100-fold MIC	6	-4.37 ± 1.62	-0.56 ± 0.20	-2.71 ± 0.71	2.4×10^{-4}
Rifampicin	10-fold MIC	3	-7.05 ± 2.47	-0.81 ± 0.36	-2.62 ± 1.13	2.9×10^{-3}
Tobramycin	10-fold MIC	3	-9.87 ± 1.66	-0.14 ± 0.08	-3.83 ± 0.26	1.9×10^{-4}
	100-fold MIC	6	-13.65 ± 4.82	-0.32 ± 0.22	-3.65 ± 0.58	2.8×10^{-4}
Daptomycin	10-fold MIC	6	-9.31 ± 0.81	-0.55 ± 0.55	-4.44 ± 0.98	4.6×10^{-5}
Daptomycin/Ca^{2+}	1-fold MIC	3	-3.13 ± 2.18	$+0.22 \pm 0.68$	-2.31 ± 0.31	6.0×10^{-3}

TABLE A.2: SA113: HemB (Growth Rate, μ=0.94 h^{-1})

Antibiotic	Concentration	No. of exps.	Death rate of normal cells $\mu_n^{(AB)}(h^{-1})$	Death rate of persister cells $\mu_p^{(AB)}(h^{-1})$	Fraction of persister $log_{10}f_0$	Switching rate n → p $a(h^{-1})$
Ciprofloxacin	10-fold MIC	3	-2.73 ± 0.53	$+0.04 \pm 0.47$	-2.34 ± 0.42	4.28×10^{-3}
	100-fold MIC	3	-2.25 ± 0.30	-0.29 ± 0.14	-2.66 ± 0.35	2.04×10^{-3}
Rifampicin	10-fold MIC	3	-4.47 ± 2.03	-0.45 ± 0.09	-2.31 ± 0.24	4.56×10^{-3}
	100-fold MIC	3	-4.9 ± 0.69	-0.75 ± 0.16	-1.84 ± 0.16	1.35×10^{-2}
Tobramycin	10-fold MIC	6	-9.13 ± 0.76	-0.52 ± 0.32	-3.94 ± 0.26	1.10×10^{-4}
Daptomycin	10-fold MIC	3	-3.87 ± 1.45	-0.51 ± 0.05	-2.77 ± 0.41	1.60×10^{-3}
Daptomycin/Ca^{2+}	10-fold MIC	3	-9.33 ± 0.29	-1.87 ± 0.04	-3.02 ± 0.34	8.90×10^{-4}
Daptomycin/Ca^{2+}	100-fold MIC	3	-9.21 ± 0.49	-0.89 ± 0.07	-3.81 ± 0.15	1.54×10^{-4}

TABLE A.3: SA113: MenD (Growth Rate, μ=0.7 h^{-1})

Antibiotic	Concentration	No. of exps.	Death rate of normal cells $\mu_n^{(AB)}(h^{-1})$	Death rate of persister cells $\mu_p^{(AB)}(h^{-1})$	Fraction of persister $log_{10}f_0$	Switching rate n → p $a(h^{-1})$
Ciprofloxacin	10-fold MIC	3	-1.51 ± 0.29	-0.13 ± 0.35	-1.94 ± 0.32	8.12×10^{-3}
	100-fold MIC	3	-1.61 ± 0.06	-0.36 ± 0.21	-2.13 ± 0.72	5.24×10^{-3}
Rifampicin	10-fold MIC	3	-1.80 ± 0.63	-0.21 ± 0.22	-2.08 ± 0.42	5.86×10^{-3}
	100-fold MIC	3	-2.02 ± 0.20	-0.21 ± 0.20	-2.46 ± 0.59	2.42×10^{-3}
Tobramycin	10-fold MIC	3	-8.96 ± 0.08	-0.97 ± 0.33	-3.59 ± 0.47	1.82×10^{-4}
Daptomycin	10-fold MIC	3	-3.09 ± 1.33	-0.69 ± 0.18	-2.29 ± 0.35	3.64×10^{-3}
	100-fold MIC	3	-10.80 ± 0.70	-1.32 ± 0.49	-3.96 ± 0.35	7.42×10^{-5}
Daptomycin/Ca^{2+}	10-fold MIC	3	-8.05 ± 0.79	-1.34 ± 0.22	-2.93 ± 0.38	8.25×10^{-4}
Daptomycin/Ca^{2+}	100-fold MIC	3	-9.02 ± 0.79	-2.00 ± 1.32	-3.08 ± 0.58	5.90×10^{-4}

TABLE A.4: Strain : HG's (Growth Rate, μ=1.9 h^{-1})

Antibiotic	Concentration	No. of exps. (avg. of 3)	Death rate of normal cells $\mu_n^{(AB)}(h^{-1})$	Death rate of persister cells $\mu_p^{(AB)}(h^{-1})$	Fraction of persister $log_{10}f_0$	Switching rate n $\rightarrow$ p $a(h^{-1})$
Strain: HG001						
Ciprofloxacin	10-fold MIC	1	-8.17	-0.08	-4.34	8.64×10^{-5}
	100-fold MIC	1	-6.74	-0.51	-3.80	2.98×10^{-4}
Rifampicin	10-fold MIC	1	-4.35	-0.41	-2.88	2.47×10^{-3}
	100-fold MIC	1	-4.07	-0.60	-2.77	3.20×10^{-3}
Tobramycin	10-fold MIC	1	-11.29	0.31	-4.41	7.34×10^{-5}
	100-fold MIC	1	-11.29	-1.52	-3.4	7.47×10^{-4}
Strain: HG002						
Ciprofloxacin	10-fold MIC	1	-9.56	-0.96	-2.89	2.40×10^{-3}
	100-fold MIC	1	-6.26	-0.29	-4.21	1.17×10^{-4}
Rifampicin	10-fold MIC	1	-3.77	-0.33	-3.06	1.65×10^{-3}
	100-fold MIC	1	-3.55	-0.05	-3.42	7.06×10^{-4}
Tobramycin	10-fold MIC	1	-10.09	0.53	-5.21	1.16×10^{-5}
	100-fold MIC	1	-12	-1.33	-3.99	1.92×10^{-4}
Strain: HG003						
Ciprofloxacin	10-fold MIC	1	-7.48	-0.55	-3.38	7.78×10^{-4}
	100-fold MIC	1	-7.53	-0.64	-3.59	4.86×10^{-4}
Rifampicin	10-fold MIC	1	-3.72	-0.29	-3.09	1.52×10^{-3}
	100-fold MIC	1	-4.46	-0.69	-2.59	4.81×10^{-3}
Tobramycin	10-fold MIC	1	-11	0.32	-4.83	2.77×10^{-5}
	100-fold MIC	1	-12	-0.21	-5.06	1.65×10^{-5}

Acknowledgements

First and foremost, I would like to thank my supervisor Dr. Stefan Klumpp for giving me the opportunity to do research in his group and giving me the freedom to pursue my own ideas. I thank him for the continuous support, suggestions and encouragement throughout these years.

I am grateful to our collaborators from University of Tübingen, Dr. Ralph Bertram and Sabrina Lechner, for providing experimental data that provided some ideas for my work.

I am grateful to my group members Mamata, Marco, Michael, Rahul, David and Veronica for always making life more enjoyable in the institute. Special thanks to Florian Berger and Thomas Niedermeyer for giving their time for proofreading the thesis.

Finally, I thank my family for their strength and support throughout the years.

Bibliography

[1] Kyle R Allison, Mark P Brynildsen, and James J Collins. Heterogeneous bacterial persisters and engineering approaches to eliminate them. *Curr. Opin. Microbiol.*, 14(5):593–8, October 2011.

[2] N Q Balaban. Persistence: mechanisms for triggering and enhancing phenotypic variability. *Curr. Opin. Genet. Dev.*, 21(6):768–75, December 2011.

[3] Nathalie Q Balaban, Kenn Gerdes, Kim Lewis, and John D McKinney. A problem of persistence: still more questions than answers? *Nat. Rev. Microbiol.*, 11(8):587–91, July 2013.

[4] Nathalie Q. Balaban, Jack Merrin, Remy Chait, Lukasz Kowalik, and Stanislas Leibler. Bacterial Persistence as a Phenotypic Switch. *Science*, 305(5690):1622–1625, 2004.

[5] Frederick K Balagaddé, Hao Song, Jun Ozaki, Cynthia H Collins, Matthew Barnet, Frances H Arnold, Stephen R Quake, and Lingchong You. A synthetic Escherichia coli predator-prey ecosystem. *Mol. Syst. Biol.*, 4:187, 2008.

[6] F Baquero and M C Negri. Selective compartments for resistant microorganisms in antibiotic gradients. *Bioessays*, 19(8):731–6, August 1997.

[7] JosephW Bigger. Treatment of staphylococcal infections with penicillin by intermittent sterilisation. *The Lancet*, 244(6320):497–500, 1944.

[8] Matthew G Blango and Matthew A Mulvey. Persistence of uropathogenic Escherichia coli in the face of multiple antibiotics. *Antimicrob. Agents Chemother.*, 54(5):1855–63, May 2010.

[9] A Brooun, S Liu, and K Lewis. A dose-response study of antibiotic resistance in Pseudomonas aeruginosa biofilms. *Antimicrob. Agents Chemother.*, 44(3):640–6, March 2000.

[10] M R Brown, D G Allison, and P Gilbert. Resistance of bacterial biofilms to antibiotics: a growth-rate related effect? *J. Antimicrob. Chemother.*, 22(6):777–80, December 1988.

[11] S Buerger, A Spoering, E Gavrish, C Leslin, L Ling, and S S Epstein. Microbial scout hypothesis, stochastic exit from dormancy, and the nature of slow growers. *Appl. Environ. Microbiol.*, 78(9):3221–8, May 2012.

[12] Evan J Burkala, Jun He, John T West, Charles Wood, and Carol K Petito. Compartmentalization of HIV-1 in the central nervous system: role of the choroid plexus. *AIDS*, 19(7):675–84, April 2005.

[13] Dino Di Carlo and Luke P Lee. Dynamic single-cell analysis for quantitative biology. *Anal. Chem.*, 78(23):7918–25, December 2006.

[14] Ted J Case, Mark L Taper, et al. Interspecific competition, environmental gradients, gene flow, and the coevolution of species' borders. *The American Naturalist*, 155(5):583–605, 2000.

[15] Ilaria Cataudella, Ala Trusina, Kim Sneppen, Kenn Gerdes, and Namiko Mitarai. Conditional cooperativity in toxin-antitoxin regulation prevents random toxin activation and promotes fast translational recovery. *Nucleic Acids Res.*, 40(14):6424–34, August 2012.

[16] Ryan T Cirz, Bryan M O'Neill, Jennifer A Hammond, Steven R Head, and Floyd E Romesberg. Defining the Pseudomonas aeruginosa SOS response and its role in the global response to the antibiotic ciprofloxacin. *J. Bacteriol.*, 188(20):7101–10, October 2006.

[17] R J Davidson, G G Zhanel, R Phillips, and D J Hoban. Human serum enhances the postantibiotic effect of fluoroquinolones against Staphylococcus aureus. *Antimicrob. Agents Chemother.*, 35(6):1261–3, June 1991.

[18] Julian Davies and Dorothy Davies. Origins and evolution of antibiotic resistance. *Microbiol. Mol. Biol. Rev.*, 74(3):417–33, September 2010.

[19] Neeraj Dhar and John D McKinney. Microbial phenotypic heterogeneity and antibiotic tolerance. *Curr. Opin. Microbiol.*, 10(1):30–8, February 2007.

[20] L G Donowitz, R P Wenzel, and J W Hoyt. High risk of hospital-acquired infection in the ICU patient. *Crit. Care Med.*, 10(6):355–7, June 1982.

[21] Tobias Dörr, Kim Lewis, and Marin Vulić. SOS response induces persistence to fluoroquinolones in Escherichia coli. *PLoS Genet.*, 5(12):e1000760, December 2009.

[22] Tobias Dörr, Marin Vulić, and Kim Lewis. Ciprofloxacin causes persister formation by inducing the TisB toxin in Escherichia coli. *PLoS Biol.*, 8(2):e1000317, February 2010.

[23] Eliana Drenkard and Frederick M Ausubel. Pseudomonas biofilm formation and antibiotic resistance are linked to phenotypic variation. *Nature*, 416(6882):740–3, April 2002.

[24] George L Drusano. Antimicrobial pharmacodynamics: critical interactions of 'bug and drug'. *Nat. Rev. Microbiol.*, 2(4):289–300, April 2004.

[25] David Dubnau and Richard Losick. Bistability in bacteria. *Mol. Microbiol.*, 61(3):564–72, August 2006.

[26] Jonathan Dworkin and Ishita M Shah. Exit from dormancy in microbial organisms. *Nat. Rev. Microbiol.*, 8(12):890–6, December 2010.

[27] Michael B Elowitz, Arnold J Levine, Eric D Siggia, and Peter S Swain. Stochastic gene expression in a single cell. *Science*, 297(5584):1183–6, August 2002.

[28] Maarten Fauvart, Valerie N De Groote, and Jan Michiels. Role of persister cells in chronic infections: clinical relevance and perspectives on anti-persister therapies. *J. Med. Microbiol.*, 60(Pt 6):699–709, June 2011.

[29] Bernadett Gaál, Jonathan W Pitchford, and A Jamie Wood. Exact results for the evolution of stochastic switching in variable asymmetric environments. *Genetics*, 184(4):1113–9, April 2010.

[30] T S Gardner, C R Cantor, and J J Collins. Construction of a genetic toggle switch in Escherichia coli. *Nature*, 403(6767):339–42, January 2000.

[31] Christian Garzoni and William L Kelley. Staphylococcus aureus: new evidence for intracellular persistence. *Trends Microbiol.*, 17(2):59–65, February 2009.

[32] Orit Gefen and Nathalie Q Balaban. The importance of being persistent: heterogeneity of bacterial populations under antibiotic stress. *FEMS Microbiol. Rev.*, 33(4):704–17, July 2009.

[33] Orit Gefen, Chana Gabay, Michael Mumcuoglu, Giora Engel, and Nathalie Q Balaban. Single-cell protein induction dynamics reveals a period of vulnerability to antibiotics in persister bacteria. *Proc. Natl. Acad. Sci. U.S.A.*, 105(16):6145–9, April 2008.

[34] Daniel T. Gillespie. A General Method for Numerically Simulating the Stochastic Time Evolution of Coupled Chemical Reactions. *J. Comput. Phys.*, 22:403, 1976.

[35] Philip Greulich, Bartłomiej Waclaw, and Rosalind J Allen. Mutational pathway determines whether drug gradients accelerate evolution of drug-resistant cells. *Phys. Rev. Lett.*, 109(8):088101, August 2012.

[36] Ashleigh S. Griffin, Stuart A. West, and Angus Buckling. Cooperation and competition in pathogenic bacteria. *Nature*, 430(7003):1024–1027, 2004.

[37] A Gutierrez, L Laureti, S Crussard, H Abida, A Rodríguez-Rojas, J Blázquez, Z Baharoglu, D Mazel, F Darfeuille, J Vogel, and I Matic. Beta-lactam antibiotics promote bacterial mutagenesis via an RpoS-mediated reduction in replication fidelity. *Nat Commun*, 4:1610, 2013.

[38] Oskar Hallatschek, Pascal Hersen, Sharad Ramanathan, and David R. Nelson. Genetic drift at expanding frontiers promotes gene segregation. *PNAS 2007 104:19926-19930*, December 2008.

[39] H Hanberger, L E Nilsson, R Maller, and B Isaksson. Pharmacodynamics of daptomycin and vancomycin on Enterococcus faecalis and Staphylococcus aureus demonstrated by studies of initial killing and postantibiotic effect and influence of Ca2+ and albumin on these drugs. *Antimicrob. Agents Chemother.*, 35(9):1710–6, September 1991.

[40] Jeff Hasty, David McMillen, and J J Collins. Engineered gene circuits. *Nature*, 420(6912):224–30, November 2002.

[41] Matthew Hegreness, Noam Shoresh, Doris Damian, Daniel Hartl, and Roy Kishony. Accelerated evolution of resistance in multidrug environments. *Proc. Natl. Acad. Sci. U.S.A.*, 105(37):13977–81, September 2008.

[42] Rutger Hermsen, J Barrett Deris, and Terence Hwa. On the rapidity of antibiotic resistance evolution facilitated by a concentration gradient. *Proc. Natl. Acad. Sci. U.S.A.*, 109(27):10775–80, July 2012.

[43] Rutger Hermsen and Terence Hwa. Sources and sinks: a stochastic model of evolution in heterogeneous environments. *Phys. Rev. Lett.*, 105(24):248104, December 2010.

[44] Michael E Hibbing, Clay Fuqua, Matthew R Parsek, and S Brook Peterson. Bacterial competition: surviving and thriving in the microbial jungle. *Nat. Rev. Microbiol.*, 8(1):15–25, January 2010.

[45] Niels Hofsteenge, Erik van Nimwegen, and Olin K Silander. Quantitative analysis of persister fractions suggests different mechanisms of formation among environmental isolates of E. coli. *BMC Microbiol.*, 13(1):25, February 2013.

[46] S Iordanescu and M Surdeanu. Two restriction and modification systems in Staphylococcus aureus NCTC8325. *J. Gen. Microbiol.*, 96(2):277–81, October 1976.

[47] B Isaksson, R Maller, L E Nilsson, and M Nilsson. Postantibiotic effect of aminoglycosides on staphylococci. *J. Antimicrob. Chemother.*, 32(2):215–22, August 1993.

[48] Arvi Jõers, Niilo Kaldalu, and Tanel Tenson. The frequency of persisters in Escherichia coli reflects the kinetics of awakening from dormancy. *J. Bacteriol.*, 192(13):3379–84, July 2010.

[49] B Kahl, M Herrmann, A S Everding, H G Koch, K Becker, E Harms, R A Proctor, and G Peters. Persistent infection with small colony variant strains of Staphylococcus aureus in patients with cystic fibrosis. *J. Infect. Dis.*, 177(4):1023–9, April 1998.

[50] Niilo Kaldalu, Rui Mei, and Kim Lewis. Killing by ampicillin and ofloxacin induces overlapping changes in Escherichia coli transcription profile. *Antimicrob. Agents Chemother.*, 48(3):890–6, March 2004.

[51] J B Kaplan. Biofilm dispersal: mechanisms, clinical implications, and potential therapeutic uses. *J. Dent. Res.*, 89(3):205–18, March 2010.

[52] T B Kepler and A S Perelson. Drug concentration heterogeneity facilitates the evolution of drug resistance. *Proc. Natl. Acad. Sci. U.S.A.*, 95(20):11514–9, September 1998.

[53] Iris Keren, Niilo Kaldalu, Amy Spoering, Yipeng Wang, and Kim Lewis. Persister cells and tolerance to antimicrobials. *FEMS Microbiol. Lett.*, 230(1):13–8, January 2004.

[54] Iris Keren, Shoko Minami, Eric Rubin, and Kim Lewis. Characterization and transcriptome analysis of Mycobacterium tuberculosis persisters. *MBio*, 2(3):e00100–11, 2011.

[55] Iris Keren, Devang Shah, Amy Spoering, Niilo Kaldalu, and Kim Lewis. Specialized persister cells and the mechanism of multidrug tolerance in Escherichia coli. *J. Bacteriol.*, 186(24):8172–80, December 2004.

[56] Juan E Keymer, Peter Galajda, Guillaume Lambert, David Liao, and Robert H Austin. Computation of mutual fitness by competing bacteria. *Proc. Natl. Acad. Sci. U.S.A.*, 105(51):20269–73, December 2008.

[57] Jongmin Kim, Kristin S White, and Erik Winfree. Construction of an in vitro bistable circuit from synthetic transcriptional switches. *Mol. Syst. Biol.*, 2:68, 2006.

[58] Cyrielle I Kint, Natalie Verstraeten, Maarten Fauvart, and Jan Michiels. New-found fundamentals of bacterial persistence. *Trends Microbiol.*, 20(12):577–85, December 2012.

[59] S Klumpp. Growth-rate dependence reveals design principles of plasmid copy number control. *PLoS One*, 6(5):e20403, 2011.

[60] Stefan Klumpp, Zhongge Zhang, and Terence Hwa. Growth Rate-Dependent Global Effects on Gene Expression in Bacteria. *Cell*, 139(7):1366–1375, December 2009.

[61] M H Kollef and V J Fraser. Antibiotic resistance in the intensive care unit. *Ann. Intern. Med.*, 134(4):298–314, February 2001.

[62] S B Korch, T A Henderson, and T M Hill. Characterization of the *hipA*7 allele of *Escherichia coli* and evidence that high persistence is governed by (p)ppGpp synthesis. *Mol Microbiol*, 50(4):1199–1213, November 2003.

[63] Shaleen B Korch and Thomas M Hill. Ectopic overexpression of wild-type and mutant hipA genes in Escherichia coli: effects on macromolecular synthesis and persister formation. *J. Bacteriol.*, 188(11):3826–36, June 2006.

[64] Kirill S Korolev, Melanie J I Müller, Nilay Karahan, Andrew W Murray, Oskar Hallatschek, and David R Nelson. Selective sweeps in growing microbial colonies. *Phys Biol*, 9(2):026008, 2012.

[65] Maria Kostakioti, Maria Hadjifrangiskou, and Scott J Hultgren. Bacterial biofilms: development, dispersal, and therapeutic strategies in the dawn of the postantibiotic era. *Cold Spring Harb Perspect Med*, 3(4), 2013.

[66] Edo Kussell. Evolution in microbes. *Annu Rev Biophys*, 42:493–514, May 2013.

[67] Edo Kussell, Roy Kishony, Nathalie Q Balaban, and Stanislas Leibler. Bacterial persistence: a model of survival in changing environments. *Genetics*, 169(4):1807–14, April 2005.

[68] Edo Kussell and Stanislas Leibler. Phenotypic diversity, population growth, and information in fluctuating environments. *Science*, 309(5743):2075–8, September 2005.

[69] M Lachmann and E Jablonka. The inheritance of phenotypes: an adaptation to fluctuating environments. *J. Theor. Biol.*, 181(1):1–9, July 1996.

[70] Guillaume Lambert, David Liao, Saurabh Vyawahare, and Robert H Austin. Anomalous spatial redistribution of competing bacteria under starvation conditions. *J. Bacteriol.*, 193(8):1878–83, April 2011.

[71] Sabrina Lechner, Kim Lewis, and Ralph Bertram. Staphylococcus aureus persisters tolerant to bactericidal antibiotics. *J. Mol. Microbiol. Biotechnol.*, 22(4):235–44, 2012.

[72] Sabrina Lechner, Pintu Patra, Stefan Klumpp, and Ralph Bertram. Interplay between Population Dynamics and Drug Tolerance of Staphylococcus aureus Persister Cells. *J. Mol. Microbiol. Biotechnol.*, 22(6):381–91, 2012.

[73] Bruce R Levin and Daniel E Rozen. Non-inherited antibiotic resistance. *Nat. Rev. Microbiol.*, 4(7):556–62, July 2006.

[74] Richard Levins. Theory of fitness in a heterogeneous environment. I. The fitness set and adaptive function. *American Naturalist*, pages 361–373, 1962.

[75] Kim Lewis. Persister cells, dormancy and infectious disease. *Nature Reviews Microbiology*, 5(1):48–56, January 2007.

[76] Kim Lewis. Persister cells. *Annu. Rev. Microbiol.*, 64:357–72, 2010.

[77] L L Livornese, S Dias, C Samel, B Romanowski, S Taylor, P May, P Pitsakis, G Woods, D Kaye, and M E Levison. Hospital-acquired infection with vancomycin-resistant Enterococcus faecium transmitted by electronic thermometers. *Ann. Intern. Med.*, 117(2):112–6, July 1992.

[78] Chunbo Lou, Zhengyan Li, and Qi Ouyang. A molecular model for persister in E. coli. *J. Theor. Biol.*, 255(2):205–9, November 2008.

[79] Etienne Maisonneuve, Lana J. Shakespeare, Mikkel Girke Jørgensen, and Kenn Gerdes. Bacterial persistence by RNA endonucleases. *Proceedings of the National Academy of Sciences*, 108(32):13206–13211, 2011.

[80] T.R. Malthus. *An Essay on the Principle of Population.* J. Johnson, London, 1798.

[81] Abu Amar M Al Mamun, Mary-Jane Lombardo, Chandan Shee, Andreas M Lisewski, Caleb Gonzalez, Dongxu Lin, Ralf B Nehring, Claude Saint-Ruf, Janet L Gibson, Ryan L Frisch, Olivier Lichtarge, P J Hastings, and Susan M Rosenberg. Identity and function of a large gene network underlying mutagenic repair of DNA breaks. *Science*, 338(6112):1344–8, December 2012.

[82] R C Massey, A Buckling, and S J Peacock. Phenotypic switching of antibiotic resistance circumvents permanent costs in Staphylococcus aureus. *Curr. Biol.*, 11(22):1810–4, November 2001.

[83] Anna Melbinger, Jonas Cremer, and Erwin Frey. Evolutionary game theory in growing populations. *Phys. Rev. Lett. 105, 178101 (2010)*, October 2010.

[84] J A Metz, R M Nisbet, and S A Geritz. How should we define 'fitness' for general ecological scenarios? *Trends Ecol. Evol. (Amst.)*, 7(6):198–202, June 1992.

[85] M B Miller and B L Bassler. Quorum sensing in bacteria. *Annu. Rev. Microbiol.*, 55:165–99, 2001.

[86] P Mitchell. Microfluidics–downsizing large-scale biology. *Nat. Biotechnol.*, 19(8):717–21, August 2001.

[87] Nina Möker, Charles R Dean, and Jianshi Tao. Pseudomonas aeruginosa increases formation of multidrug-tolerant persister cells in response to quorum-sensing signaling molecules. *J. Bacteriol.*, 192(7):1946–55, April 2010.

[88] H S Moyed and K P Bertrand. hipA, a newly recognized gene of Escherichia coli K-12 that affects frequency of persistence after inhibition of murein synthesis. *J. Bacteriol.*, 155(2):768–75, August 1983.

[89] H S Moyed and S H Broderick. Molecular cloning and expression of hipA, a gene of *Escherichia coli* K-12 that affects frequency of persistence after inhibition of murein synthesis. *J Bacteriol*, 166(2):399–403, May 1986.

[90] G V Mukamolova, A S Kaprelyants, D I Young, M Young, and D B Kell. A bacterial cytokine. *Proc. Natl. Acad. Sci. U.S.A.*, 95(15):8916–21, July 1998.

[91] Lawrence R Mulcahy, Jane L Burns, Stephen Lory, and Kim Lewis. Emergence of Pseudomonas aeruginosa strains producing high levels of persister cells in patients with cystic fibrosis. *J. Bacteriol.*, 192(23):6191–9, December 2010.

[92] Markus Müller, Amparo dela Peña, and Hartmut Derendorf. Issues in pharmacokinetics and pharmacodynamics of anti-infective agents: distribution in tissue. *Antimicrob. Agents Chemother.*, 48(5):1441–53, May 2004.

[93] F C Neidhardt, J L Ingraham, and M Schaechter. Physiology of the bacterial cell: A molecular approach. *Sinauer, Sunderland MA*, May 1990.

[94] H C Neu. The crisis in antibiotic resistance. *Science*, 257(5073):1064–73, August 1992.

[95] Mehmet A Orman and Mark P Brynildsen. Dormancy is not necessary or sufficient for bacterial persistence. *Antimicrob. Agents Chemother.*, 57(7):3230–9, July 2013.

[96] Pintu Patra and Stefan Klumpp. Phenotypically heterogeneous populations in spatially heterogeneous environments. *Submitted*.

[97] Pintu Patra and Stefan Klumpp. Population dynamics of bacterial persistence. *PLoS ONE*, 8(5):e62814, 2013.

[98] Pintu Patra and Stefan Klumpp. unpublished data. *to be published*, xxxx.

[99] S Pearl, C Gabay, R Kishony, A Oppenheim, and N Q Balaban. Nongenetic individuality in the host-phage interaction. *PLoS Biol*, 6(5):e120, May 2008.

[100] Joseph F Petrosino, Rodrigo S Galhardo, Liza D Morales, and Susan M Rosenberg. Stress-induced beta-lactam antibiotic resistance mutation and sequences of stationary-phase mutations in the Escherichia coli chromosome. *J. Bacteriol.*, 191(19):5881–9, October 2009.

[101] Richard A Proctor, Christof von Eiff, Barbara C Kahl, Karsten Becker, Peter McNamara, Mathias Herrmann, and Georg Peters. Small colony variants: a pathogenic form of bacteria that facilitates persistent and recurrent infections. *Nat. Rev. Microbiol.*, 4(4):295–305, April 2006.

[102] P Rainey and K Rainey. Evolution of cooperation and conflict in experimental bacterial populations. *Nature*, 425:72–74, 2003.

[103] P B Rainey and M Travisano. Adaptive radiation in a heterogeneous environment. *Nature*, 394(6688):69–72, July 1998.

[104] Tobias Reichenbach, Mauro Mobilia, and Erwin Frey. Mobility promotes and jeopardizes biodiversity in rock-paper-scissors games. *Nature 448, 1046-1049 (2007)*, April 2008.

[105] Eitan Rotem, Adiel Loinger, Irine Ronin, Irit Levin-Reisman, Chana Gabay, Noam Shoresh, Ofer Biham, and Nathalie Q Balaban. Regulation of phenotypic variability by a threshold-based mechanism underlies bacterial persistence. *Proc. Natl. Acad. Sci. U.S.A.*, 107(28):12541–6, July 2010.

[106] S J Schrag and V Perrot. Reducing antibiotic resistance. *Nature*, 381(6578):120–1, May 1996.

[107] Maria A Schumacher, Kevin M Piro, Weijun Xu, Sonja Hansen, Kim Lewis, and Richard G Brennan. Molecular mechanisms of HipA-mediated multidrug tolerance and its neutralization by HipB. *Science*, 323(5912):396–401, January 2009.

[108] Peter Schuster and Karl Sigmund. Replicator dynamics. *Journal of Theoretical Biology*, 100(3):533–538, 1983.

[109] M Scott, C W Gunderson, E M Mateescu, Z Zhang, and T Hwa. Interdependence of cell growth and gene expression: origins and consequences. *Science*, 330(6007):1099–102, November 2010.

[110] Devang Shah, Zhigang Zhang, Arkady Khodursky, Niilo Kaldalu, Kristi Kurg, and Kim Lewis. Persisters: a distinct physiological state of E. coli. *BMC Microbiol.*, 6:53, 2006.

[111] Julie A Shapiro, Valerie L Nguyen, and Neal R Chamberlain. Evidence for persisters in Staphylococcus epidermidis RP62a planktonic cultures and biofilms. *J. Med. Microbiol.*, 60(Pt 7):950–60, July 2011.

[112] Rachna Singh, Pallab Ray, Anindita Das, and Meera Sharma. Role of persisters and small-colony variants in antibiotic resistance of planktonic and biofilm-associated Staphylococcus aureus: an in vitro study. *J. Med. Microbiol.*, 58(Pt 8):1067–73, August 2009.

[113] Wiep Klaas Smits, Oscar P Kuipers, and Jan-Willem Veening. Phenotypic variation in bacteria: the role of feedback regulation. *Nat. Rev. Microbiol.*, 4(4):259–71, April 2006.

[114] A L Spoering and K Lewis. Biofilms and planktonic cells of Pseudomonas aeruginosa have similar resistance to killing by antimicrobials. *J. Bacteriol.*, 183(23):6746–51, December 2001.

[115] Graham R Stewart, Brian D Robertson, and Douglas B Young. Tuberculosis: a problem with persistence. *Nat. Rev. Microbiol.*, 1(2):97–105, November 2003.

[116] P S Stewart and J W Costerton. Antibiotic resistance of bacteria in biofilms. *Lancet*, 358(9276):135–8, July 2001.

[117] Philip S Stewart. Mechanisms of antibiotic resistance in bacterial biofilms. *Int. J. Med. Microbiol.*, 292(2):107–13, July 2002.

[118] Peter S Swain, Michael B Elowitz, and Eric D Siggia. Intrinsic and extrinsic contributions to stochasticity in gene expression. *Proc. Natl. Acad. Sci. U.S.A.*, 99(20):12795–800, October 2002.

[119] C Tan, P Marguet, and L You. Emergent bistability by a growth-modulating positive feedback circuit. *Nat Chem Biol*, 5(11):842–848, November 2009.

[120] A Telenti, P Imboden, F Marchesi, D Lowrie, S Cole, M J Colston, L Matter, K Schopfer, and T Bodmer. Detection of rifampicin-resistance mutations in Mycobacterium tuberculosis. *Lancet*, 341(8846):647–50, March 1993.

[121] Mukund Thattai and Alexander van Oudenaarden. Stochastic gene expression in fluctuating environments. *Genetics*, 167(1):523–30, May 2004.

[122] J.M. Thoday. Components of fitness. *Symp. Soc. Exp. Bio.*, (VII):96–113, 1953.

[123] David Tilman and Peter Kareiva. *Spatial ecology.* Princeton University Press, 1997.

[124] Tsz-Leung To and Narendra Maheshri. Noise can induce bimodality in positive transcriptional feedback loops without bistability. *Science*, 327(5969):1142–5, February 2010.

[125] Lorena Tuchscherr, Eva Medina, Muzaffar Hussain, Wolfgang Völker, Vanessa Heitmann, Silke Niemann, Dirk Holzinger, Johannes Roth, Richard A Proctor, Karsten Becker, Georg Peters, and Bettina Löffler. Staphylococcus aureus phenotype switching: an effective bacterial strategy to escape host immune response and establish a chronic infection. *EMBO Mol Med*, 3(3):129–41, March 2011.

[126] Audrey Tupin, Maxime Gualtieri, Françoise Roquet-Banères, Zakia Morichaud, Konstantin Brodolin, and Jean-Paul Leonetti. Resistance to rifampicin: at the crossroads between ecological, genomic and medical concerns. *Int. J. Antimicrob. Agents*, 35(6):519–23, June 2010.

[127] Nora Vázquez-Laslop, Hyunwoo Lee, and Alexander A Neyfakh. Increased persistence in Escherichia coli caused by controlled expression of toxins or other unrelated proteins. *J. Bacteriol.*, 188(10):3494–7, May 2006.

[128] Jan-Willem Veening, Wiep Klaas Smits, and Oscar P Kuipers. Bistability, epigenetics, and bet-hedging in bacteria. *Annu. Rev. Microbiol.*, 62:193–210, 2008.

[129] Pierre-François Verhulst. Notice sur la loi que la population suit dans son accroissement. Correspondance Mathématique et Physique Publiée par A. *Quételet*, 10:113–121, 1838.

[130] Christof von Eiff. Staphylococcus aureus small colony variants: a challenge to microbiologists and clinicians. *Int. J. Antimicrob. Agents*, 31(6):507–10, June 2008.

[131] Yuichi Wakamoto, Neeraj Dhar, Remy Chait, Katrin Schneider, François Signorino-Gelo, Stanislas Leibler, and John D McKinney. Dynamic persistence of antibiotic-stressed mycobacteria. *Science*, 339(6115):91–5, January 2013.

[132] Daniel B Weissman, Michael M Desai, Daniel S Fisher, and Marcus W Feldman. The rate at which asexual populations cross fitness valleys. *Theor Popul Biol*, 75(4):286–300, June 2009.

[133] C Wiuff, R M Zappala, R R Regoes, K N Garner, F Baquero, and B R Levin. Phenotypic tolerance: antibiotic enrichment of noninherited resistance in bacterial populations. *Antimicrob. Agents Chemother.*, 49(4):1483–94, April 2005.

[134] C S Wylie, A D Trout, D A Kessler, and H Levine. Optimal strategy for competence differentiation in bacteria. *PLoS Genet*, 6(9), September 2010.

[135] Yoshihiro Yamaguchi, Jung-Ho Park, and Masayori Inouye. Toxin-antitoxin systems in bacteria and archaea. *Annu. Rev. Genet.*, 45:61–79, 2011.

[136] Suzan Yilmaz and Anup K Singh. Single cell genome sequencing. *Curr. Opin. Biotechnol.*, 23(3):437–43, June 2012.

[137] Qiucen Zhang, Guillaume Lambert, David Liao, Hyunsung Kim, Kristelle Robin, Chih-kuan Tung, Nader Pourmand, and Robert H Austin. Acceleration of emergence of bacterial antibiotic resistance in connected microenvironments. *Science*, 333(6050):1764–7, September 2011.